2015

Energy performance evaluation and optimisation of ground source heat pump systems

Su Huang
University of Wollongong, sh377@uowmail.edu.au

Energy Performance Evaluation and Optimisation of Ground Source Heat Pump Systems

A thesis submitted in (partial) fulfilment of the
requirements for the award of the degree

Doctor of Philosophy (Engineering)

from

University of Wollongong

by

Su HUANG

BEng

Sustainable Buildings Research Centre

Faculty of Engineering and Information Sciences

April 2015

Abstract

The worldwide energy shortage and globally increasing energy demand have accelerated the application of Ground source heat pump (GSHP) systems in residential and commercial buildings. The main challenges that prevent the widespread deployment of GSHP systems are their high installation costs, system design and control. Although a great deal of research has been carried out over the last several decades to tackle these challenges, previous studies on appropriate design of ground heat exchangers (GHEs) and optimal control of GSHP systems are still far from sufficient to facilitate optimal exploitation of this technology. The thesis therefore aims to develop optimal design strategies for vertical GHEs, which are commonly used in GSHP systems, and optimal control strategies for GSHP systems to maximise the overall system energy efficiency so as to make GSHP systems more attractive and cost effective for building heating and cooling applications.

To better understand the dynamic characteristics and energy performance of GSHP systems, experimental tests based on a ground source-air source combined heat pump system implemented in the Sustainable Buildings Research Centre (SBRC) at the University of Wollongong were carried out to investigate the effects of the operating configurations of GHEs (i.e. series and parallel) and the water flow rate in the GHEs on the overall performance of the GSHP system. Detailed computer simulations were also carried out to examine the effects of the other main design parameters (such as pipe length, thermal conductivity of grout material/soil) of both vertical and horizontal GHEs on the performance of GSHP systems. The experimental results showed that the parallel configuration of the GHEs has better performance than that of the series configuration and that optimisation of the water flow rate in the GHEs is essential to minimise the energy consumption of water-to-water heat pumps and water pumps in the ground loop. The simulation results confirmed that, for both vertical and horizontal GHEs, the length of the GHEs is the main design parameter. The thermal conductivity

of the grout/soil and the borehole/pipe separation spacing also have important effects on the overall energy efficiency of GSHP system.

In addition, a simulation-based feasibility analysis was performed to examine the economic and environmental benefits of using GSHP systems for major Australian climate zones. The results demonstrated that GSHP systems are potentially economically and environmentally feasible for some major Australian climate zones. The use of GSHP systems can reduce net present values and CO_2 emissions by 2.16±1.06% and 33.0±4.0%, respectively, compared to the use of air source heat pump (ASHP) systems.

In order to minimise the high installation costs of GSHP systems with vertical GHEs, a single-objective design optimisation method for vertical GHEs based on entropy generation minimisation was developed. Five design variables were first selected based on a global sensitivity analysis and then optimised using a genetic algorithm optimisation technique. A small scale GSHP system implemented in the Sustainable Buildings Research Centre (SBRC) at University of Wollongong, Australia was used as the case study. The specifications of the installed ground loop system were used as the original design in this study. The original ground loop field consists of three vertical boreholes, and the depth and diameter of each borehole are 91 m and 0.15 m. The results from the case study showed that this optimal design approach can decrease the total system cost (i.e. the upfront cost of vertical GHEs and water-to-water heat pump and the 20-year operation cost of the water-to-water heat pumps) by 3.5%, compared with the original design. From the thermoeconomic point of view, decreasing the upfront cost was found to be more important than decreasing the operational cost for the case study system.

A multi-objective design optimisation strategy to further facilitate the optimisation of the design of vertical GHEs was developed to simultaneously minimise the system upfront cost and entropy generation rate. A set of Pareto optimal solutions, with respect

to the two competing objectives, were searched by using the genetic algorithm optimisation technique. A decision-making strategy was then used to determine a final optimal solution. Two case studies were presented to validate the effectiveness of the proposed strategy. The results based on a small scale GSHP system in Australia showed that, compared to the original design, the use of this proposed strategy can decrease the total system cost (i.e. the upfront cost of vertical GHEs and water-to-water heat pumps and 20-year operation cost of the water-to-water heat pumps) by 9.5%. Compared to a single-objective design optimisation strategy, 6.2% more cost can be saved by using this multi-objective design optimisation strategy. Results from the multi-objective design optimisation strategy applied to a relatively large scale GSHP system implemented in China showed that a 5.2% decrease in the total system cost can be achieved as compared to the original design.

To further offset the high installation cost of GSHP systems, an optimal control strategy for ground source-air source combined heat pump systems was developed for sequence control of heat pumps and optimisation of the water flow rate in the ground heat exchangers. This optimal control strategy was validated based on the ground source-air source combined heat pump system implemented in the SBRC building. The results showed that 12.0% reduction in total power consumption of the heat pumps and water pumps in the source side of the water-to-water heat pumps can be achieved by using this optimal control strategy, as compared to that of using the original control strategy implemented in the Building Management System (BMS) of the building. This optimal control strategy can also be easily extended to control other types of GSHP systems.

It is believed that the findings obtained from this thesis can facilitate the optimal design and control optimisation of GSHP systems to reduce their energy usage and carbon footprint and assist in achieving more widespread use of GSHPs for heating and cooling of buildings.

Acknowledgements

This thesis could not be completed without the help and support of those who are gratefully acknowledged here.

I sincerely express my deepest gratitude and thanks to my principal supervisor, Dr Zhenjun Ma, for his invaluable guidance, support and continuous encouragement throughout my research in Sustainable Buildings Research Centre, University of Wollongong.

My sincere gratitude is devoted to my co-supervisor, Professor Paul Cooper, who kept an eye on the progress of my research work. This thesis owes much to his thoughtful and helpful comments.

My special appreciation also goes to Mr Craig Mclauchlan, who helped me a lot and gave me many instructions in setting up the experimental test system. Thanks also to Dr Duane Robinson, for his help in field measurements and data management. Thanks also to Mr Yale Carden, Managing Director of GeoExchange Australia Pty Ltd for valuable discussions/suggestions and providing the cost data for the installation of the ground source heat pump systems in Australia.

I further express my gratitude to my colleagues in the Sustainable Buildings Research Centre (SBRC) for their company and support throughout the PhD study.

My heartfelt appreciation also goes to my beloved parents, for their endless love and patience in the pursuit of my academic goals.

Finally I want to thank everyone who directly or indirectly offered his/her help and support to my study.

List of Publications

Part of contents in Chapters 4, 6 and 7 of this thesis are based on one conference paper and two journal articles listed below.

Journal Publications

- Huang S, Ma Z, Wang F. 2015. A multi-objective design optimization strategy for vertical ground heat exchangers. Energy and Buildings, vol. 87, pp. 233-242.
- Huang S, Ma Z, Cooper P. 2014. Optimal design of vertical ground heat exchangers by using entropy generation minimization method and genetic algorithms. Energy Conversion and Management, vol. 87, pp. 128-137.

Conference Publication

- Huang S, Ma Z, Cooper P. 2013. Evaluation of a ground source heat pump system in a net-zero energy office building. 12th International Conference on Sustainable Energy Technologies (SET 2013) (pp. 1-9). Hong Kong: Hong Kong Polytechnic University.

Table of Contents

List of Tables

List of Figures

NOMENCLATURE

B	borehole separation distance (m)
C	cost ($)
$C_1 – C_4$	constants in Equations (8.2) and (8.3)
CLR	cooling load ratio
c_p	specific heat (J/kgK)
CF	cash flow ($)
D	half shank space (m)
$E_1(x)$	exponential integral function
EWT	entering water temperature (˚C)
F_{ij}^n	non-dimensional objective function
F_o	Fourier numbe
f	friction factor
g	gravitational acceleration (m/s^2)
G	Temperature response function
h	convective heat transfer coefficients (W/m^{2}K)
h_w	window width parameter
H	borehole depth (m)
H_p	pump head (m)
IC	upfront cost ($)
IR	discount rate
k	thermal conductivity (W/mK)
$K_1 – K_2$	constants in Equations (8.2) and (8.3)
$K(u)$	kernel function
L	depth (m)

m_f	mass flow rate (kg/s)
n	pump speed (rpm)
N	borehole number
Nu	Nusselt number
N_s	dimensionless entropy number
ΔP	pressure drop (Pa)
Q	design load/heat transfer rate (W)
q	heat flux per unit length (W/m)
r	radius (m)
R	thermal resistance (mK/W)
Re	Reynolds number
S_{flow}	flow resistance (s^2/m^5)
S_{gen}	entropy generation rate (W/K)
T	temperature (K)
ΔT	temperature difference (K)
V	volumetric flow rate (m^3/s)
V_b	storage volume (m^3)
W	power consumption (kW)
Y	CO_2 emissions
α	Convective heat transfer
ξ	local resistance coefficient
τ	time (s)
ρ	density (kg/m^3)
χ	load imbalance ratio
μ	dynamic viscosity (kg/m s)
γ_i	accuracy grade

σ	standard deviation of the Gaussian probability density function
σx_i	uncertainty
σRx_i	relatively uncertainty
β_0 - β_3	constants in Equation (3.6)

Subscripts

b	borehole/borehole wall
c	cooling
ele	electricity
p	U-tube pipe
f	fluid
s	soil
0	environmental condition
1	inlet of U-tube pipe
2	outlet of U-tube pipe
h	heating
hori	horizontal ground heat exchanger
i	inner
o	outer
m	average
tot	total
HP	heat pump

GLOSSARY

AWHP	air-to-water heat pump
ASHP	air source heat pump
COP	coefficient of performance
COP_{sys}	overall system coefficient of performance
EER	energy efficiency ratio
EF	indirect emission factor
EGM	entropy generation minimization
EGN	entropy generation number
GHE	ground heat exchanger
GSHP	ground source heat pump
GSA	global sensitivity analysis
NPV	net present value ($)
OC	operating cost ($)
SEER	seasonal energy efficiency ratio
TAC	total annual cost ($)
WWHP	water-to-water heat pump

Chapter 1

Introduction

1.1 Background and motivation

Increasing demands placed on our global energy supply systems, in conjunction with global warming due to greenhouse gas emissions from the use of fossil fuels, has led to the rapid development of low energy technologies for heating and cooling of buildings (Kharseha *et al*. 2014, Zhu *et al*. 2014). Australia's greenhouse gas (GHG) emissions per capita are amongst the highest in the world, and almost a quarter of GHG emissions within Australia are ascribed to the building sector (Group ASBEC Climate Change Task 2007). As shown in Fig 1.1, one of the major energy consumers in buildings is the HVAC (Heating, Ventilation and Air Conditioning) systems, and the building HVAC systems typically consume around 40% of total building energy usage (Council of Australian Governments 2012). Due to the ever growing demand for better indoor thermal comfort, the energy consumption of building HVAC systems is projected to be even higher in future (Wan *et al*. 2012). It is therefore essential to develop energy efficient technologies and systems to promote and enhance system energy efficiency and significantly reduce the carbon footprint of buildings.

Over the last several decades, different techniques such as evaporative cooling, thermal energy storage, renewable energy technologies, heat recovery technologies and advanced heating and cooling systems have been proposed and used to tackle the critical problem (Jiang *et al*. 2010, Yau *et al*. 2012, Vakiloroaya *et al*. 2014). Among them, ground source heat pumps (GSHPs) with high energy efficiency and low greenhouse gas emissions have been recognised as one of the most sustainable and environmentally friendly solutions for heating and cooling of both residential and commercial buildings (Urchuegu á *et al*. 2008, Self *et al*. 2013, Qi *et al*. 2014).

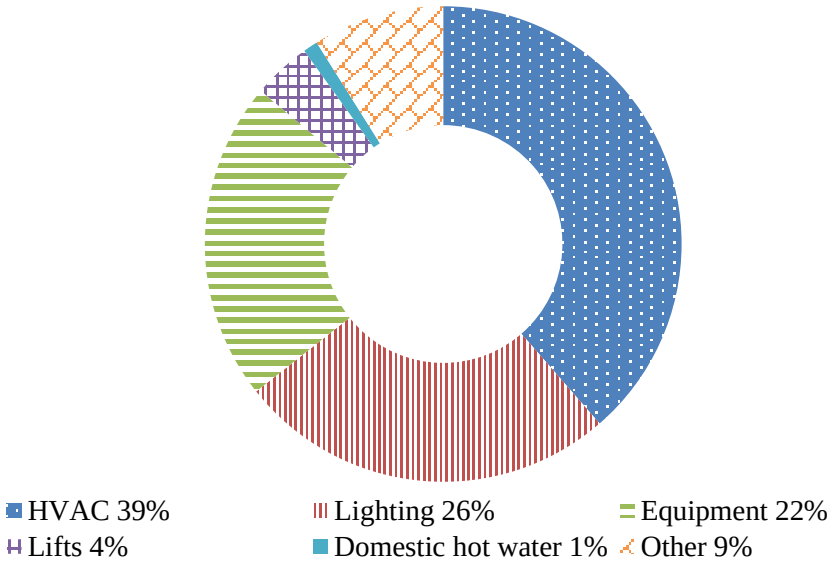

Fig. 1.1 Breakdown of building energy consumption (Council of Australian Governments 2012).

GSHP systems can be grouped into two main types, i.e. open loop and closed loop, in accordance with the installation of ground heat exchangers (GHEs). In an open loop system, GHEs can be installed above the ground surface (e.g. in river, pool or lake), while in a closed loop system, GHEs are installed in either vertical boreholes (i.e. 50-200 m deep in the ground) or horizontal trenches (i.e. 1-2 m below the ground surface) (ASHRAE 2011, Banks 2012). Among the various types of GSHP systems, closed loop GSHP systems have attracted the greatest interest because of their relatively high efficiency and reliability (Chong *et al.* 2013, Sarbu *et al*. 2014). Compared to horizontal GSHP systems, vertical GSHP systems have attracted wide attention, owing to the advantages of the constant deep soil temperature and less land area requirement (Yang *et al*. 2010, Benli *et al*. 2013).

It is reported that reductions in energy consumption of 30-70% in the heating mode and 20-50% in the cooling mode can be achieved through proper use of GSHPs to replace conventional air conditioning systems (Benli *et al*. 2009). Over the past few years, the installations of GSHP system have been continuously growing with an annual rate from 10% to 30%, on a global basis (Yang *et al*. 2010).

Despite their advantages, their high installation cost is one of the main challenges preventing the widespread deployment of GSHP systems in buildings (Lee *et al*. 2008, Goetzler *et al*. 2012, Moon *et al*. 2014). The high investment cost of a GSHP system is mainly due to the installation of GHEs. The drilling cost of vertical GHEs was estimated around 50% - 70% of the overall initial cost of the whole GSHP system depending on the terrain and other local factors (CEC 2011), which is higher than the other types of GHEs. The other key challenges related to the use of GSHP systems are the reported lower-than-expected operating efficiency and the gradual degradation of the long-term performance of the GSHP system due to improper control of some systems (Madani *et al*. 2011, Nguyen *et al*. 2014). High installation costs and improper control features make the short-term economics potentially unattractive. To minimise the implementation costs of vertical GHEs and improve the overall system efficiency, it is essential to develop cost effective strategies to optimise both the design and operation of GSHP systems.

Significant efforts have been made to overcome the barriers associated with the installation of GSHP systems in the past several decades. Various issues related to the use of GSHP systems have been discussed in recent literature. These include but are not limited to:

- The utilisation of building pile foundations as ground heat exchangers to decrease the installation costs of GSHP systems (Fan *et al*. 2013, Moon *et al*. 2014);
- The development and improvement of mathematic models of vertical GHEs to facilitate better system design and control (Capozza *et al*. 2012, Gang *et al*. 2013);
- The investigation of hybrid GSHP systems where GSHP systems are employed to satisfy building base load while traditional systems such as fluid coolers, cooling towers and solar collectors are used for supplementing supply during the

peak demand periods (Kjellsson *et al.* 2010, Park *et al*. 2012, Allaerts *et al.* 2015).

However, limited attention has been given to systematically optimise the key design parameters of vertical GHEs, such as the total length of the GHE, pipe diameter, and borehole diameter. Standard design guidelines for sizing vertical GHEs (ASHRAE 2011) have already existed for many years and a number of researchers have also attempted to optimise the design parameters of vertical GHEs to enhance the thermal performance of GHEs and further reduce the cost of GSHP systems (Alavy *et al*. 2013, Robert *et al*. 2014). However, there is no guarantee that the final design determined based on the design guidelines and strategies developed is optimum or near-optimum. This is because most of the design guidelines and strategies developed were primarily focused on the estimation of the total length of the vertical GHEs and assuming constant values of the other design parameters such as the borehole diameter, pipe diameter, shank space and design fluid flow rate (ASHRAE 2011, Capozza *et al*. 2012). Moreover, most studies did not consider thermal irreversibilities generated within vertical GHEs during the optimisation process and that these irreversibilities will impair the thermal efficiency of vertical GHEs. Therefore, there is a need to develop extensive optimisation strategies which can optimise the main design parameters of vertical GHEs whilst simultaneously reducing the cost of GSHP systems and thermal irreversibilities within vertical GHEs.

Besides system designs, control optimisation of GSHP systems is another effective way to offset the high installation costs of GSHP systems. However, compared with the amount of work devoted on the design of GSHP systems, less effort has been made on the control of GSHP systems. Most of the studies carried out to date were focused on the determining the sequence control of GSHPs and supplementary heating/cooling devices such as cooling tower, fluid cooler and solar collector (Ouyang *et al*. 2012, Yang *et al*. 2014). These supplementary devices commonly employed are restricted to the function of either providing only heating or only cooling. Considering the high

installation cost of GSHP systems, the ground source-air source combined heat pump system has been proposed, in which, the GSHP system can be sized to cover a portion of building heating and cooling load and the rest heating and cooling load can be burdened by the ASHP, and there has been a number of projects employing the ground source-air source combined heat pump systems for air-conditioning buildings (Pardo *et al*. 2010, Nam *et al*. 2010). However, limited work has been performed on the development of optimal control strategies for the ground source-air source combined heat pump systems. It is therefore also important to develop practical, efficient and effective optimal control strategies for this type of combined heat pump systems.

1.2 Research aim and objectives

The overall aim of the project was to provide a better understanding of the dynamic characteristics and energy performance of GSHP systems and to develop optimal design and control optimisation strategies for GSHP systems so as to maximise their overall energy efficiency. The specific objectives of the project were as follows:

I. To investigate the effects of different operating configurations (i.e. series and parallel) of the GHEs and the main design variables on the performance of GSHP systems;

II. To evaluate the financial and environmental feasibility of using GSHP systems in various Australian climatic zones to provide a better understanding of the economic (financial) and environmental benefits of using GSHP systems within Australia;

III. To develop design optimisation methodologies for the vertical ground heat exchangers, which are commonly employed in GSHP systems, based on a second-law of thermodynamic analysis to reduce the high drilling costs while maintaining good thermal performance of vertical GHEs; and

IV. To develop an optimal control strategy for ground source-air source combined

heat pump systems to maximise the overall operating efficiency without sacrificing indoor thermal comfort and violating the operating constraints.

1.3 Research methodology

The research methodology utilised in this study is illustrated in Fig.1.2. Objectives I and II were achieved through combined simulation investigation and experimental tests. The experimental test system was established to examine the effects of the operating configurations of GHEs and the water flow rates within the GHEs on the performance of GSHP systems. A simulation system representing a real ground source-air source combined heat pump system was constructed and used to investigate the effects of different design variables for GHEs on the performance of GSHP systems. A simulation-based feasibility analysis of GSHP systems for major Australian climate zones was then carried out to provide a better understanding of the economic and environmental benefits of using GSHP systems within Australia.

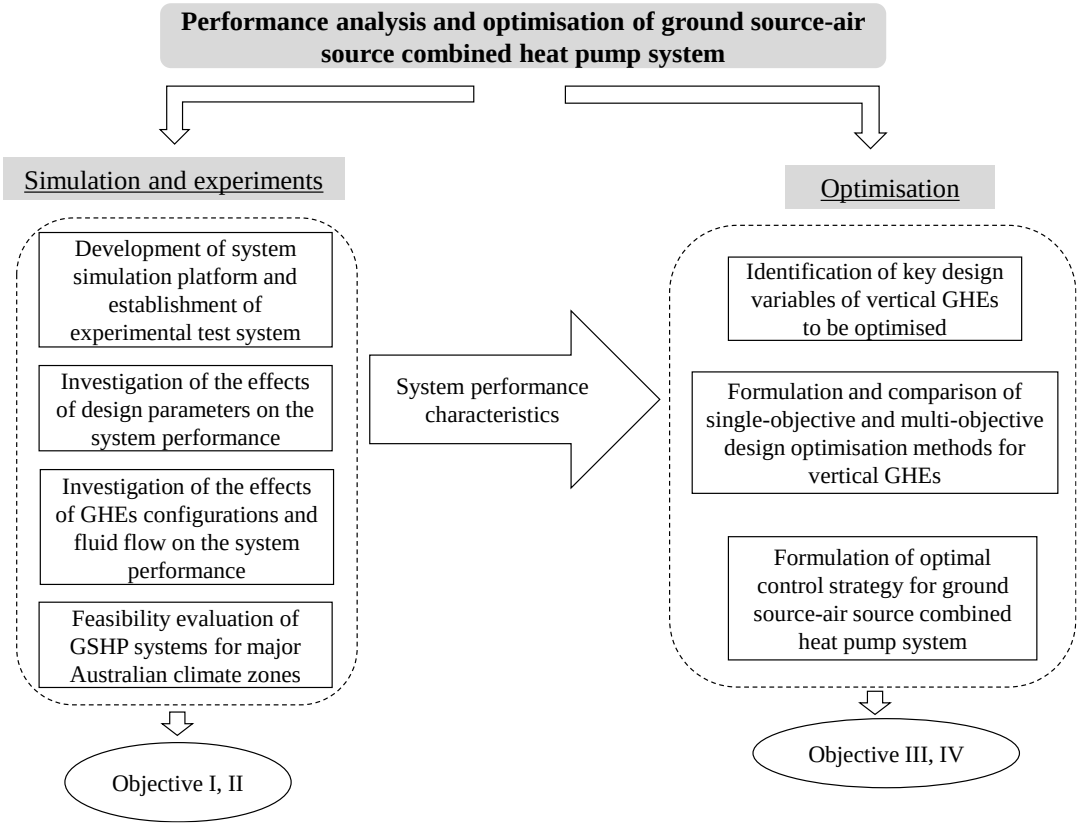

Fig. 1.2 Research methodology employed in this thesis.

The GSHP performance characteristics obtained in the simulation and experimental tests were then used to facilitate the design and control optimisation of GSHP systems through Objectives III and IV. The key design variables of vertical GHEs were first identified through a global sensitivity analysis. The design optimisation methods were then developed to optimise the identified key design variables of vertical GHEs based on thermoeconomic and thermodynamic analysis to reduce the high installation costs of GSHP systems. The development of control optimisation strategies for the ground source-air source combined heat pump system was then investigated to further offset the high installation costs associated with the use of GSHP systems.

1.4 Thesis outline

This chapter outlines the background and motivation of this research by presenting the need of design and control optimisation of ground source heat pump (GSHP) systems. It presents the aim and objectives of this thesis and employed primary research methodology. The subsequent chapters are structured as follows.

Chapter 2 provides a general literature review regarding GSHP systems, with a key focus on design optimisation and control optimisation of the systems. The major mathematical models developed for GHEs and commonly used design methods are also presented.

Chapter 3 describes the design and installation of the GSHP system implemented in a net-zero office building and the experimental investigation of the effects of parallel and series operation of GHEs and different water flow rates circulating through the GHEs on the energy performance of GSHP systems.

Chapter 4 presents the dynamic characterisation and energy performance evaluation of GSHP systems through simulation studies. A parametric analysis is conducted to assess the effects of major design variables of vertical GHEs and horizontal GHEs on the energy performance of GSHP systems.

Chapter 5 presents a financial and environmental feasibility study of using GSHP systems under a range of Australian climatic conditions. The economic evaluation is performed by means of net present value (NPV) while the environmental impact is determined based on the CO_2 emissions related to the system energy usage.

Chapter 6 presents the development and validation of a single-objective design optimisation strategy for vertical ground heat exchangers based on the entropy generation minimisation method. The dimensionless entropy generation number (EGN) is employed as the objective function. Five design variables selected based on a global sensitivity analysis are globally optimised by the genetic algorithm optimisation technique.

Chapter 7 presents a multi-objective design optimisation strategy for vertical ground heat exchangers (GHEs) to minimise the system upfront cost and entropy generation rate simultaneously. A decision-making strategy based on the fuzzy non-dimensionalisation method is used to identify the near-optimal solution among a set of Pareto solutions. The test results based on two different GSHP systems are presented as well.

Chapter 8 presents the development of an optimal control strategy for ground source - air source combined heat pump systems to determine the optimal operational sequence of heat pumps and the optimal water flow rate circulating in the ground loop. The optimal control strategy is also evaluated and the performance test results are also presented.

Chapter 9 summaries the key findings from the thesis and recommendations for future work.

Chapter 2

Literature Review

The main focus of this thesis is on the energy performance evaluation, optimal design and control of GSHP systems. This chapter therefore provides a literature review on recent research and development as well as applications in this field in order to identify some research gaps to assist in developing cost-effective design methodologies and optimal control strategies for GSHP systems.

Section 2.1 highlights the significance of identification of soil thermal properties. Section 2.2 presents several common criteria for performance evaluation of GSHP systems. Section 2.3 overviews the feasibility studies carried out for GSHP systems worldwide. Section 2.4 summarises the current simulation models used for ground heat exchangers (GHEs). Brief reviews on the design optimisation and control optimisation of GSHP systems are presented in Section 2.5 and Section 2.6, respectively. Some key findings from the literature review are summarised in Section 2.7.

2.1 Soil properties

The heat transfer effectiveness between a GHE pipe and the surrounding ground is strongly dependent on the thermodynamic characteristics of the surrounding soil. To improve the design process and energy performance assessment of GSHP systems, the thermal conductivity, density, specific heat, porosity and hydraulic conductivity of soil should be investigated. These thermal properties are generally not easy to measure, in particular for vertical GHEs, as they usually pass through several soil layers and all these layers need to be identified appropriately. The initial mobile test rigs to measure the soil properties were developed in Sweden and USA in 1995 (Gehlin 2002). Since that time, numerous researchers around the world have devoted considerable efforts to developing mobile test facilities for measuring soil properties, for instance, Roth *et al.*

(2004) from Latin America, Marcotte *et al.* (2008) from Canada, Wang *et al.* (2010) from China. Table 2.1 summarises the thermal properties of typical soils identified in the ASHRE handbook (2011).

Table 2.1 Typical thermal properties of selected soils and rocks (ASHRAE 2011)

	Thermal conductivity (W/mK)	Thermal diffusivity (m^2/day)
Soils		
Heavy clay, 15% water	1.4-1.9	0.042-0.061
5% water	1.0-1.4	0.047-0.061
Light clay, 15% water	0.7-1.0	0.047-0.055
5% water	0.5-0.9	0.056
Heavy sand, 15% water	2.8-3.8	0.084-0.11
5% water	2.1-2.3	0.093-0.14
Light sand, 15% water	1.0-2.1	0.047 to 0.093
5% water	0.9 to 1.0	0.055 to 0.12
Rocks		
Granite	2.3 - 3.7	0.084 - 0.13
Limestone	2.4 - 3.8	0.084 - 0.13
Sandstone	2.1 - 3.5	0.11 - 0.65
Shale, wet	1.44 - 2.4	0.065 - 0.084
dry	1.0 - 2.1	0.55 - 0.074

Based on the information provided in table 2.1, soil thermal conductivity varies with the variation of soil moisture content, which indicates the significance of soil moisture in influencing soil thermal properties. When air between soil particles is replaced by water, the contact resistance will be reduced to some extent. The study by Leong *et al.* (1998) showed that soil moisture content strongly influences GSHP system performance. A relatively high soil moisture content is beneficial to the performance of the heat pump.

2.2 Criteria for performance evaluation of GSHP systems

Similar to the performance evaluation of traditional heat pump systems, several performance indicators introduced below can be used to evaluate the performance of GSHPs.

- *Heating Coefficient of Performance* (*COP*): the ratio of the heating energy transfer rate to the energy supply rate.
- *Overall System Coefficient of Performance* (COP_{sys}): the ratio of the total energy transferred to the total energy consumed.
- *Energy efficiency ratio (EER)*: the ratio of output cooling energy in British thermal unit (BTU) to the total input energy in Watt-hour. EER and COP (coefficient of performance) are related to each other, and EER is equal to the product of COP and the conversion factor from BTU/h to Watts. (ANSI/AHRI 2008).
- *Seasonal Energy Efficiency Ratio (SEER)*: the ratio of the total seasonal heating/cooling output during a usage period (in BTU) to the total energy input (in Watt-hour) during the same time frame. It can be used to determine the seasonal energy efficiency of heat pumps during heating and cooling seasons (Florides *et al*. 2013).

The average heating COP and cooling EER for existing GSHPs in the United States were determined as 3.4 and 16 respectively, whereas, the average heating COP and cooling EER of existing air-source heat pump were 2.3 and 13, respectively (Ruan 2012). Self *et al.* (2012) showed great advantages of GSHP systems when compared to traditional heating systems in terms of heating COP, and the detailed results are shown in Table 2.2.

Table 2.2 Performance comparison among different types of heating systems (Self *et al*. 2013)

Types of system	**Heating COP**
Ground source heat pumps	3-5
Air source heat pump	2.3-3.5
Electric baseboard heaters	1
Mild-efficiency natural gas furnace	0.78-0.82
High-efficiency natural gas furnace	0.88-0.97

İnallı *et al.* (2004) used the overall system COP as the evaluation criteria to experimentally evaluate the thermal performance of a horizontal GSHP system. This system was installed in Elazığ, Turkey and the overall system COP for the horizontal GHEs buried at 1 m and 2 m in depth were found to be 2.66 and 2.81, respectively. İnallı *et al.* (2005) further used SEER to evaluate the cooling performance of a ground-coupled heat pump (GCHP) system. The SEER of the GCHP system studied was found to be 10.5. Ozgener *et al.* (2007) evaluated the COP and overall system COP of GSHP systems through detailed energetic and exergetic modelling. The COP of the heat pumps was found to be 3.12-3.64, while the overall system COP varied between 2.72 and 3.43.

Hwang *et al.*(2009) experimentally evaluated the cooling performance of a GCHP system in terms of the average cooling COP of heat pumps and the overall system COP. The results from the experiments showed the heat pump COP and the overall system COP were 8.3 and 5.9 respectively, when the system operated at 65% of partial load conditions. An air source heat pump (ASHP) system with the same capacity as the GSHP system was also experimentally tested and the heat pump COP and the overall ASHP system COP were found to be 3.9 and 3.4, respectively. The comparison between the two systems highlighted the high efficiency of GSHP systems.

Benli *et al.* (2009) evaluated energy performance of a GSHP system integrated with phase change material for heating a greenhouse located in Elazığ, Turkey. The measurements in the heating mode showed that the heat pump heating COP was in the

range of 2.3-3.8 and the overall system COP was in the range 2-3.5, respectively, indicating the feasibility of integrating PCM with GSHP systems for heating purpose.

Bakirci *et al*. (2010) conducted an experimental study to evaluate the performance of vertical GSHP systems installed in Erzurum, Turkey. The experimental apparatus constructed consisted of a number of vertical GHEs, a heat pump unit, water circulating pumps and related measurement equipment. The experimental results from the heating season of 2008-2009 indicated that the average heating COP was approximated at 3.0 and overall system COP was estimated at 2.6 in the coldest months of the heating season, respectively.

Wu *et al.* (2010) evaluated the heat pump COP of a GSHP system with horizontal-coupled slinky ground source heat exchangers by means of experiment and simulation. The experimental results from two-month monitoring showed that the average heat pump COP was 2.5 and it was decreased with the increase of the running time. The results from the validated 3D numerical modelling showed that the heat extraction rate per unit length increased with the increase of the diameter of the coil.

Karabacak *et al.*(2011) experimentally investigated the energy performance of a GSHP system with a vertical single U-tube GHE buried at 110 m depth in cooling operations, in terms of heat pump COP and overall system COP. The heat pump COP was in the range of 3.1-4.8, while the overall system COP was found to be between 2.1 and 3.1. It was concluded that GSHP with vertical GHEs would be more economically feasible if the drilling costs can be further decreased.

Chai *et al.* (2012) used overall system COP as the performance indictor to evaluate a GSHP system for greenhouse heating in northern China. The experimental studies for two greenhouses showed that the overall system COP during the heating period were 3.83 and 3.91, respectively.

Michopoulos *et al.* (2013) investigated the operation characteristics of a GSHP with a vertical GHE by means of SEER. The SEER was found to be between 4.5-5.5 in the

heating mode and 3.6-4.5 in the cooling mode. The GSHP consumed 25.7% less power and emitted 22.7 % lower CO_2 and 99.6% lower NO_x emissions, when compared to traditional air conditioning systems. . The results also showed that the maximum energy load per unit of the total length of the GHEs was found to be 50 W/m in the heating operation, while in the cooling operation, it was determined in the range of 20-210 W/m.

Lee *et al*. (2013) experimentally investigated the heat pump COP of a vertical GCHP system integrated with a prestressed high-strength concrete (PHC) pile, which was integrated with the building foundations. The results showed that the heat pump COP was in the range of 3.9-4.3, which was slightly lower than the GCHP system with normal vertical GHEs. However, in comparison with a conventional vertical GCHP, the 83.7% drilling cost can be reduced.

Luo *et al.* (2015) analysed the accumulated 4-years monitored operation data of a GSHP in Southern Germany to evaluate its heating system COP and cooling system energy efficiency ratio (EER). For a typical winter day, the overall system heating COP was determined at 3.9, and for a typical summer day, the EER was found to be 8.0. For a 4-year operation period, the GSHP system SEER was found to have an annual increase rate at 8.7%, whereas the seasonal system heating COP was decreased by 4.0% by the end of the period.

The above studies on performance evaluations in terms of heat pump COP, overall system COP, EER and SEER showed that GSHP systems are generally more energy efficient than traditional HVAC systems. This is mainly due to the fact that the ground temperature is a more effective condition to operate the heat pump unit in both the cooling and heating modes.

2.3 Feasibility studies of using GSHPs for heating and cooling of buildings

One of the key barriers for wide deployment of GSHPs in buildings is high drilling

costs of vertical GHEs. A feasibility study is therefore necessary for any projects considering using GSHPs to heating and cooling the buildings.

The feasibility of GSHP systems has been investigated by means of economic and environmental analysis in different regions around the world. Chiasson *et al*. (2003) assessed the feasibility of hybridising the solar collectors with GSHP system to air-conditioning the heating- dominated buildings. Three cases were simulated, including: a) GSHP only; b) GSHP and fixed solar collectors; and c) GSHP and an azimuth-tracking solar collector. The results indicated that integration of GSHP system with solar collectors is a practicable alternative applied in heating dominated buildings.

Urchueguía *et al*. (2008) demonstrated that it is technically and economically feasible to use GSHP systems in mixed climate applications. The energy performance of the GSHP system was compared with that of a conventional air-to-water heat pump system by a series of experiments and the results showed that GSHP system saved 43±17% and 37±18%of power consumption in the heating mode and the cooling mode respectively, in comparison with that of the conventional system.

Rice *et al.* (2013) compared the thermal performance of a GSHP system in with that of traditional HVAC systems in five selected American climate zones. The results showed that the GSHP systems tend to be more energy-efficient than the conventional HVAC systems for all five climates studied.

Aste *et al.* (2013) analysed the economic and environmental feasibility of heat pump systems in Italian climate zones. It was shown that both air source and water source heat pump systems were economically and environmentally feasible. Rad *et al*. (2013) performed a study to validate the performance of a hybrid GSHP with solar thermal collectors. Integrating the solar thermal collectors with GSHP systems could reduce a large amount of the length of GHE, which therefore can decrease the initial cost of the GSHP system. A 20-year lifecycle cost analysis showed the limited advantages in comparison with that of conventional GSHP systems.

Based on the literature reviewed above, it can be seen that the feasibility of using GSHP varies with building types, climate conditions and technologies employed. As each building is unique, it is not possible to reach a common conclusion of whether it is feasible to use a GSHP system for each building during its design phrase. Therefore, a detailed feasibility study is necessary before considering GSHPs as an alternative option to provide heating and cooling for buildings. Reference buildings in regional and national scale should be selected and can be used assist the evaluation of the energy performance and economic competitiveness of GSHP systems.

2.4 Modelling and Simulation of Ground Source Heat Pump Systems

Ground heat exchanger (GHE) is one of the most important components of a GSHP system. Appropriate modelling of GHEs is therefore essential to understand dynamic behaviour and characteristics of GSHP systems. Simulation is usually an effective way to evaluate the performance of different GSHP systems, including their design options and control strategies. During the past several decades, many studies have focused on the development of appropriate mathematical models for GHEs to evaluate and predict the heat transfer phenomena in the ground in order to facilitate the design and operation optimisation of GSHP systems. The primary aim of GHE mathematical modelling is to determine the heat carrier fluid temperature circulating between GHEs and heat pump units, under different operating conditions. The following sections will provide a brief review on the GHE models that have been most widely used. More details can be found in several review articles (Florides *et al.* 2007, Yang *et al.* 2010, Lamarche *et al.* 2010, Bertagnolio *et al.* 2012).

2.4.1 Modelling of vertical ground heat exchangers

The heat transfer process of a vertical GHE has usually been analysed in two separate zones. One is the soil or rocks outside the GHE and the other is the zone inside the GHE, including the U-tube pipes, grout and the circulating fluid inside the pipes.

Many mathematic models have been developed for predicting the transient heat transfer in the outside zone of vertical GHEs (Zeng *et al*. 2003, Yang *et al.* 2010). These models can be classified into analytical models and numerical models. The analytical models rely mainly on the infinite line source (ILS) theory (Ingersoll *et al.* 1948) and cylindrical heat source theory (Carslaw *et al.* 1959, Deerman *et al.*1991). The numerical models tend to be more complex and are normally implemented in computer-based simulation tools (Eskilson 1987, Hellstrom 1991). Two models that are widely used in engineering applications, are the line source model (Ingersoll *et al*. 1954) and the cylindrical source model (Carslaw *et al*.(1959) due to their simplicity and acceptable accuracy. The two models share the similarity of assuming infinite length for the vertical GHE and a constant heat source within an infinite homogeneous medium. Several important analytical models are summarised in Table 2.3.

Another important isolated part for analysis is inside zone of the vertical GHE, which includes the grouting materials, the arrangement of pipe channels and circulating fluid. The heat transfer within a borehole depends not only on the arrangement of pipe channels, but also thermal properties of grouting materials and adjacent surrounding soils. Thermal processes between the circulating fluid and the ground are normally classified into three parts, including i) convective heat transfer between the circulating fluid and the pipes; ii) conductive heat transfer through the pipes; and iii) conductive heat transfer through the grouting materials. With the steady state assumption, the above three thermal processes can be characterised by steady thermal resistances, and their sum yields an effective fluid-to-ground thermal resistance R_b, as expressed in Equation (2.1).

$$R_b = R_f + R_p + R_g \tag{2.1}$$

where R_b is the thermal resistance of the borehole, R_f is the convective resistance of the fluid, R_p is the conductive resistance of the pipes, and R_g is the conductive resistance of the grout.

The steady state borehole thermal resistance (R_b) can be calculated as the ratio of the temperature difference between the circulating fluid and the borehole wall with the heat flux, as expressed in Equation (2.2).

$$R_b = \frac{T_f - T_b}{q} \tag{2.2}$$

where q is the heat flux per borehole length, T_f is the average circulating fluid temperature, and T_b is the borehole wall temperature.

A number of models developed to calculate the borehole thermal resistance (Lamarche *et al*. 2010) are listed in Table 2.3 as well.

Table 2.3 Summary of the important expressions of vertical GHEs models

Region	Model type	Expressions of models	References
Outside the vertical GHE	Infinite line source model	$T(r,\tau) - T_o = \frac{q}{4\pi k_s}\int_{\frac{r^2}{4\alpha_s\tau}}^{\infty}\frac{e^{-u}}{u}du = \frac{q_1}{4\pi k_s}E_1(\frac{r^2}{4\alpha_s\tau})$	Carslaw *et al*. 1959, Ingersoll *et al*. 1954.
	Infinite cylindrical model	$T_b - T_o = \frac{q}{k_s}G(F_o, \frac{r_i}{r_o})$; $F_o = \frac{\alpha_s \cdot \tau}{r_i^2}$	Carslaw *et al*. 1959, Ingersoll *et al*. 1954
Inside the vertical GHE	Empirical model	$R_b = \frac{1}{\beta_0 k_b (\frac{r_b}{r_p})^{\beta_1}}$	Paul 1996
	Line source approximation	$R_b = \frac{1}{4\pi k_b}[\ln\frac{r_b}{r_o} + \ln\frac{r_b}{2D} + \frac{k_b - k_s}{k_b + k_s}\ln(\frac{r_b^4}{r_b^4 - D^4})] + \frac{R_p}{2}$	Pahud *et al.* 1996
	Quasi-three dimensional models	$R_b = \frac{L}{\rho_f c_f V_f}(\frac{T_{f,i} - T_b}{T_{f,i} - T_{f,o}}) - \frac{1}{2})$	Diao *et al*. 2004

2.4.2 Modelling of horizontal ground heat exchangers

Compared with vertical ground heat exchangers, there are few theoretic simulation analyses of horizontal GHEs developed to date, probably due to the complexity in the

simulation of horizontal GHEs. Some major difficulties faced are summarised below (Mei 1986, Banks 2012).

1) Lack of knowledge of variations of thermal properties and moisture content in shallow subsoil;
2) The effect of ambient temperature variation on shallow depths of soil;
3) Uncertain thermal resistance due to lack of close contact of GHEs with soil;
4) The geometry of horizontal GHEs (except the most simple ones such as single linear pipe) rapidly becomes mathematically complex to describe.

IGSHPA (1998) provided the thermal response functions for a variety of different horizontal ground loop configurations. Claesson *et al.* (1983) proposed a line-source theory model for horizontal linear ground heat exchangers. Mihalakakou *et al.* (1994) presented a horizontal GHE model by describing the soil surrounding the pipe and the pipe in polar co-ordinates. The model was well validated and incorporated into TRNSYS (a Transit System Simulation Program) simulation platform. Lin *et al.* (2010) developed a plane source heat transfer model to analyse the heat transfer phenomenon of slinky horizontal loop heat exchangers to assist in the design process. A semi-analytical model for serpentine horizontal GHEs was proposed and validated by Philippe *et al.* (2011). Computer-aided simulation tools are also available and the finite-element simulator is among the most commonly used simulation engines to analyse the heat transfer of horizontal loop heat exchangers with various configurations (Congedo *et al*. 2012, Fujii *et al*. 2012, Simms *et al*. 2014).

2.5 Design optimisation of GSHP systems

2.5.1 Identification of optimisation parameters

For a given optimisation problem, the optimisation progress could be realised by analysing the parameters which influence the objective function and finally finding the

optimal values of these parameters to minimise or maximise the objective function. For a GSHP system, its energy performance depends on a variety of parameters such as geological characteristics, geometric variables (i.e. pipe size, borehole size etc.) and operation configurations (Cho *et al.* 2014). Fig. 2.1 illustrates the classification of major design and operating parameters of GSHP systems. Optimisation of these parameters is important to improve energy performance and decrease the upfront and operating costs of GSHP systems (Garber *et al.* 2013).

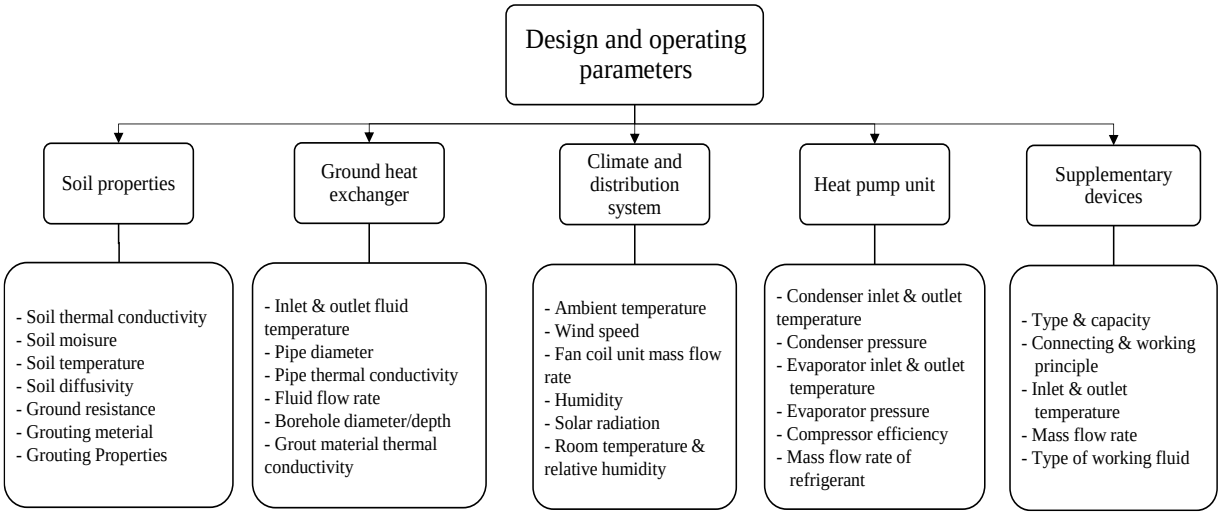

Fig.2.1 Major design and operating parameters relevant to the design of GSHPs.

Some parameters listed in Fig 2.1 can be varied and adjustable, whereas the others may only be regarded as constants. For example, the soil thermal conductivity and undisturbed soil temperature cannot be changed once the construction site is confirmed. It is important to identify the key variables which can be systematically optimised based on the objective function defined by using parametric studies or sensitivity analysis (Russo *et al*. 2012, Casasso *et al.* 2014, Woloszyn *et al*. 2014).

2.5.2 Design approaches of GSHP systems

In a GSHP system, the GHEs can be buried either horizontally or vertically. Horizontal GHEs are normally designed to be buried at a depth of 1-2 m below the ground surface,

while vertical GHEs are normally installed as boreholes which are drilled at a depth of 20-200 m from the ground surface level (Yang *et al*. 2010). Selection of GHE configurations for GSHP system applications is relied on a series of factors, i.e. the availability of the resources of water and land. In general, compared to horizontal GSHP systems, GSHP users tend to believe that vertical GSHP systems are more energy efficient, as the ambient temperature variations will have less influence on vertical GHEs which are buried at a deep depth (Chong *et al.* 2013, Sarbu *et al*. 2014). Thus most of the studies of closed-loop GSHP systems are focused on vertical GHEs due to their high efficiency and high installation costs. Major studies on the GSHP system design available in the public domain are briefly reviewed in below sections.

2.5.2.1 General design procedures

Designing GSHP systems is an important issue since it has a direct influence on the operating performance of GSHP systems. Eskilson (1987) and Hellstrom (1991) provided a detailed thermal analysis of heat extraction vertical GHEs and described important parameters influencing the performance of vertical GHEs. The five most important parameters identified are: borehole thermal resistance; soil thermal conductivity; undisturbed soil temperature; heat rejection/extraction rates; and the heat carrier fluid flow rate.

The thermal performance of a vertical GHE is found to be approximately proportional to the thermal conductivity of the ground. A considerable amount of research has been conducted over the past decades on in-situ testing (or thermal response testing) to determine the soil thermal conductivity for better design (Bandos *et al*. 2011, Witte *et al*. 2013, Lhendup *et al*. 2014). The borehole thermal resistance is defined by a number of design variables including the fluid flow rate, fluid thermophysical properties, borehole diameter, pipe material, arrangement of flow channels, and grout material. A large thermal resistance of the individual borehole will negatively affect the heat transfer rate between the heat carrier fluid and the surrounding soil, which may lead to a

larger length of vertical GHEs and add extra installation costs. It is therefore desirable to minimise the borehole thermal resistance as much as possible in the design stage. The undistributed soil temperature is normally taken as an average value. The borehole depth designed is essentially proportional to the temperature difference between the undistributed soil temperature and the minimum (or maximum) design heat pump entering water temperature. Accurate identification of this temperature difference is essential to the optimal design of GHEs. The heat extraction or rejection rate directly influences the design capacity of GHEs, which is normally determined based on the building peak heating/cooling load. As mentioned by Eskilson (1987), mass flow rate is commonly considered in the borehole thermal resistance calculation. However, the mass flow rate should be large enough to ensure turbulent flow in the pipe channels. A good understanding of the impact of important parameters on the performance of GSHP systems is essential in order to develop appropriate design guidelines. A general design procedure for different types of GSHPs has been provided by Kavanaugh *et al.* (1997) and Omer (2008) and is summarised in Fig 2.2.

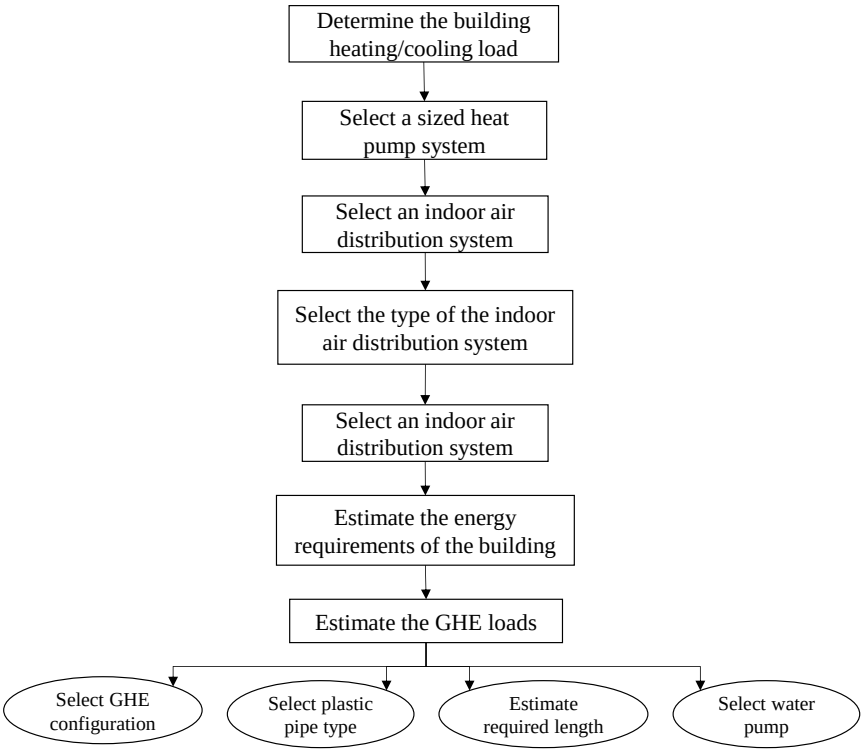

Fig. 2.2 Flow chart of the design routine (Kvavnaugh *et al*. 1997, Omer 2008).

2.5.2.2 GHE sizing methods and tools

In general, design of GSHP systems refers to proper size of the ground heat exchangers (GHEs) to meet a desired result by accomplishing the required tasks. The overall aim of the design is to ensure rises or falls of the soil temperature and the circulating fluid temperature are within acceptable values over the system life-span. One design method was derived from the solution of the heat transfer process in terms of a cylinder buried underground. The cylinder source equation was developed and evaluated by Carslaw *et al*. (1959) and had been suggested by Ingersoll *et al*. (1954) as an appropriate method for sizing GHEs. Kavanaugh (1997) further modified the equation by taking into account the arrangement of U-bends and the variations of hourly heating rates. In any design method, several parameters must be known in advance, including: soil thermal properties and undistributed temperature; thermal properties and heat transfer fluid flow rate; the rated coefficient of performance of the heat pump unit; the minimum and maximum design entering water temperatures to the heat pump units; and building load profile. The commonly used methods for sizing GHEs are briefly summarised below.

1) "Rule of Thumb" method for heating applications

The "Rule of Thumb" method has been used in the practical engineering field for a long time, and were investigated by Ball *et al.* (1983). "Rule of Thumb" also refers to the specific installed thermal outputs or specific heat extraction in W/m. The values of specific heat rate are obtained based on extensive analysis of monitored systems. Detailed analysis and conclusions of various projects led to the establishment of international guidelines for sizing vertical and horizontal GHEs (Rosen 2001). Some "Rule of Thumb" methods used in different countries are presented below.

- In United States, 68-82 W/m were reported for vertical GHEs with single U-tubes;

- In Germany, for vertical GHEs, 20-25 W/m were recommended for soil thermal conductivity less than 1.5 W/mK, 50-60W/m for medium thermal conductivity, and 70-84 W/m for soil thermal conductivity greater than 3.0 W/mK;
- In Europe, 62 W/m was estimated for vertical GHEs with single U-tube.

Based on the "Rule of Thumb" method, ASHRAE (2011) summarised the recommended trench lengths for various types of commonly used excavation methods, see Table 2.4 below. "Rule of thumb" methods might be a good beginning point for sizing GHEs due to their great convenience with arriving at a quick decision. However, excessive reliance on these rules might be risky (Banks 2012). A simple rule of thumb (i.e. a certain number of watts per drilled meter) may lead to significant errors since, as discussed in Section 2.1.1.1, the performance of a GSHP system is influenced by a range of parameters to various extent.

Table 2.4 Recommended lengths of trench or borehole per kW for residential GSHPs (ASHRAE 2011)

Type		Pitch	Ground temperature (°C)						
		m of Pipe per m Trench/Bore	7-8	8-11	11-13	13-15	15-17	17-19	19-21
Horizontal ground heat exchanger	6-pipe /6-pitch spiral	6	16	14	13	14	16	17	20
	4-pipe /4-pitch spiral	4	19	17	17	17	19	22	26
	2-pipe	2	26	24	22	24	26	30	35
Vertical ground heat exchanger	19 mm pipe	2	16	15	14	15	16	17	20
	25 mm pipe	2	15	14	13	14	15	16	19
	32 mm pipe	2	14	13	12.5	13	14	15	17

2) International Ground Source Heat Pump Association (IGSHPA) method

The IGSHPA modelling procedure developed based on Kelvin's infinite line source (ILS) theory is mainly used for the design of vertical GHEs. Bose (1984) sized the length of the ground heat exchanger (GHE) by assuming the equivalent pipe diameter for the period of coldest and hottest months of the year. The monthly bin method was then applied to analyse the seasonal performance and energy consumption of the system. Based on the IGSHPA method, the ground formation resistance of a single vertical GHE is defined as follows:

$$R_s = \frac{1}{4\pi k_s} E_1\left(\frac{r_b^2 \rho_s c_s}{4 k_s \tau}\right) \tag{2.3}$$

where r_b is the borehole radius, k_s is the soil thermal conductivity, τ is the simulation time, $E_1(x)$ is the exponential integral function, N is the borehole number, ρ_s is the soil density, and c_s is the specific heat of the soil.

For multiple vertical GHEs, the multiple boreholes are simplified into one single vertical GHE with an equivalent radius. The thermal resistance of adjacent GHEs are super-imposed and added to the ground formation resistance of the simplified single vertical GHE. Determining maximum and minimum entering water temperatures is important to determine the annual heating and cooling run fractions in the IGSHPA method. Both Bose (1984) and Cane *et al*. (1991) recommended that the minimum design entering water temperature (EWT) should be around 1.1 - 4.4°C higher than the lowest ambient air temperature and the maximum design EWT was to be 37.8 °C. The total length of the vertical GHEs can be determined by using the following equations.

For heating,

$$L_{h,tot} = \frac{Q_{c,h} \times \frac{COP_h - 1}{COP_h} \times (R_p + R_s \times RunFraction_h)}{T_{s,\min.annual} - T_{f,\min}} \tag{2.4}$$

For cooling,

$$L_{c,tot} = \frac{Q_{c,c} \times \frac{COP_c - 1}{COP_c} \times (R_p + R_s \times RunFraction_c)}{T_{f,\max} - T_{s,\max.annual}} \tag{2.5}$$

where, $T_{f,min}$ and $T_{f,max}$ are the minimum and maximum fluid temperatures, $T_{s,min,\ annual}$ and $T_{s,max,\ annual}$ are the minimum and maximum annual soil temperatures, $Runfraction_c$ and $Runfraction_h$ are the proportions of the time the pump has to run to provide the required cooling load and heating load, $Q_{c,h}$ and $Q_{c,c}$ are the heating capacity and cooling capacity respectively, COP_c and COP_h are the heating COP and cooling COP of the heat pump, respectively.

3) ASHRAE method

Ingersoll *et al*. (1954) proposed a design method which was derived from the following steady state heat transfer equation.

$$q = \frac{L(t_s - t_f)}{R} \tag{2.6}$$

where q is the heat transfer rate, L is the required vertical GHE length, t_s is the undistributed soil temperature, t_f is the fluid temperature, and R is the effective thermal resistance of the soil.

Kavanaugh *et al*. (1997) modified this equation by defining a range of constant heat-rate "pulses" to represent the ground heat exchanger heat transfer variations. Calculations of the required GHE lengths are based on Eq. (2.7) and Eq. (2.8), respectively.

For heating,

$$L_{h,tot} = \frac{q_a R_{sa} + (C_{fh} q_{lh})(R_b + PLF_m R_{sm} + R_{sd} F_{sc})}{t_g - \frac{t_{fi} + t_{fo}}{2} - t_p} \tag{2.7}$$

For cooling,

$$L_{c,tot} = \frac{q_a R_{sa} + (C_{fc} q_{lc})(R_b + PLF_m R_{sm} + R_{sd} F_{sc})}{t_g - \frac{t_{fi} + t_{fo}}{2} - t_p} \tag{2.8}$$

where q_a can be calculated by Eq. (2.9).

$$q_a = \frac{C_{fc} q_{lf} EFLH_c + C_{fh} q_{lh} EFLH_h}{8760} \tag{2.9}$$

where, F_{sc} is the short-circuit heat loss factor, $L_{c,tot}$ and $L_{h,tot}$ are the required total length of GHEs to meet the cooling and heating load, respectively, PLF_m is the part-load factor, q_a is the net annual average heat transfer to the ground, Q_{lc} and Q_{lh} are the design cooling load and heating load, R_{sa} , R_{sd} and R_{sm} are the effective thermal resistances of the ground in annual, daily and monthly pulse respectively, R_b is the borehole thermal resistance, t_s is the undisturbed ground temperature, t_p is the temperature penalty, t_{fi} and t_{fo} are the water temperature at heat pump inlet and heat pump outlet, respectively C_{fc} and C_{fh} are correction factors that account for the amount of heat rejected/absorbed by the heat pump units, and $EFLH_c$ and $EFLH_h$ are the annual equivalent full-load cooling hours and heating hours, respectively.

Table 2.5 Summary of software programs for GHE design (Chiasson 2007)

Software	Vendor
CLGS	International Ground-Source Heat Pump Association, Stillwater, OK, USA
ECA	Elite Software, Inc., Bryan, TX, USA
Earth Energy Designer (EED)	University of Lund, Sweden
Lund Programs	University of Lund, Sweden
GEOCALC	Ferris State University, Big Rapids, MI, USA
GeoDesigner	ClimateMaster, Oklahoma City, OK, USA
GchpCalc E	Energy Information Services, Tuscaloosa, AL, USA
GL-Source	Kansas Electric Utility, Topeka, KS, USA
GLHEPRO	Intl. Ground-Source Heat Pump Assoc., Stillwater, OK, USA
Ground Loop Design (GLD)	Gaia Geothermal; GBT, Inc., Maple Plain, MN, USA

Design of GHEs for GSHP systems in commercial buildings is generally achieved using software programs. For single-zone residential systems, design tables are often used. Software programs vary widely in calculation approach and assumptions used. A summary

of commercially available software design programs for GHEs can be found in Table 2.5 (Chiasson 2007).

The above methods and tools simplified the modelling process to some extent, which normally led to variations in the predicted GHEs length (Shonder *et al.* 2000). However, the drilling cost of a deep borehole is relatively expensive, and the high installation cost will counteract the interests of using GSHP systems. Therefore, design optimisation of the GHEs is necessary to reduce the system upfront cost and ensure good performance of GSHP systems.

2.5.3 Overview on the studies of optimal design of GSHP systems

A majority of studies on the design optimisation of GSHP systems are now in the public domain and they were mainly focused on the development and modification of mathematic models of GSHPs for system design. Zogou *et al*.(1998) performed a design optimisation study of heat pump systems by examining the effect of climatic characteristics on the design of the system. This study indicated that a heat pump system was favoured in the Mediterranean milder climates and subtropical climates . Spitler *et al.* (2005) optimised the main components of a GSHP system. The optimisation also considered the effects of building loads on the design of the heat exchanger length. Kjellsson *et al.* (2010) performed a design optimisation of a solar collector combined GSHP system with a vertical GHE. The results showed that the combination can be optimal by using solar collectors to supply the hot water during summer cooling period and to recharge the ground during winter heating season. Hackel *et al.* (2008) performed a design optimisation study of a GSHP system hybridised with a cooling tower based on TRNSYS (transient system simulation) simulation studio. The results suggested that the capacity of the GHSP in a hybrid system used in cooling-dominated buildings, should be designed to meet the building heating load. Bazkiaei *et al.* (2013) proposed a method to optimise the performance of a horizontal GHE system by using homogenous and non-homogenous soil profiles. It was concluded that the non-homogenous soil profiles would enhance the performance of horizontal GHEs. The above reviewed studies provide fundamental background and theories for future development of optimisation design methodologies for GSHP systems.

In formulating a design optimisation problem, it is important to find one or more appropriate objective functions to be minimised or maximised, as well as to determine the design variables that can be optimised. Single objective optimisation and multi-objective optimisation can be used to formulate the optimisation problem for GSHP systems and their applications are briefly reviewed below.

Single-objective optimisation

A general optimisation problem can be stated as (Aravelli 2014):

Find $X = \{x_1, x_2 ... x_n\}^T$ which minimises the objective function of $f(X)$

$$\text{Subject to} \quad \begin{aligned} & g_i(X) \le 0, && j = 1,2,...m \\ & h_k(X) = 0, && k = 1,2,...p \\ & x_i^{(l)} \le x_i \le x_i^{(u)} && i = 1,2,...n \end{aligned} \qquad (2.10)$$

where x_i is the design variable, $g_j(X)$ and $h_k(X)$ are the constraints. $x_i^{(l)}$ and $x_i^{(u)}$ denote the lower and upper bounds on x_i. The above problem is called a single objective optimisation problem, since there is only one objective function to be minimised.

The objective function is a key component in formulating an optimisation methodology. From the perspective of mathematics, optimisation can be redeemed as a procedure of finding the inputs that can minimise or maximise the objective function that may subject to certain constraints. The objective functions employed in the optimisation studies of GSHP systems can be categorised into two groups, i.e. economic and thermodynamic. The objective functions derived based on economic aspects include total annual cost, life cycle cost, etc. Thermodynamic objective functions include the system irreversibility, exergy loss and entropy/enthalpy generation, the system COP/EER, etc.

- *Economic optimisation of GSHP systems*

Economic optimisation of GSHP systems is normally based on thermo-economic analysis by taking into account the related the thermodynamic inefficiencies costs in the total product cost of an energy system. Thermo-economic analysis is useful for designers to identify the process of cost in a thermal system (Bejan *et al.* 1996). A significant number of publications have employed thermo-economic analysis, evaluation, and optimisation

techniques to tackle with practical issues in the process of improving the design and operation of energy systems (Frangopoulos 1987). There are various economic analysis methods that can be used to analyse and optimise GSHP systems, and these methods include, but are not limited to, the life cycle cost method (Kreith *et al.* 2008), the net benefits (net present worth) method (Peterson *et al*. 2012), the overall rate-of-return method, the exergy and cost energy mass method, and the analytical hierarchy process (Nikolaidis *et al*. 2009).

The earliest work using thermo-economic analysis on heat pump systems was performed by Wall (1985). He pointed out that thermo-economic optimisation could be regarded as an economic optimisation incorporated with thorough thermodynamic description of the system. Bejan *et al.* (1996) established the principles and methodologies of thermo-economics and provided guidelines for performing thermo-economic analysis. Zhao *et al.* (2003) presented an integrated optimal mathematical model for a ground water heat pump (GWHP) system by analysing its operating characteristics. An optimisation study was performed to minimise the annual total costs of the system according to technical and economic optimal principles. In Khan *et al.* (2004), a life cycle cost (LCC) analysis was applied to the GSHP system for a typical Canadian residential building by using a simulation procedure implemented in HVACSIM+. The LCC analysis considered the capital costs of the heat pumps, water pumps, materials and drilling costs, electricity costs of the heat pumps and water pumps. Esen *et al.* (2006) conducted a detailed techno-economic analysis of a GSHP system with horizontal GHEs in comparison with traditional heating systems in the heating season in Turkey. The economic analysis showed the advantages of GSHP systems over the electric resistance, fuel oil, liquid petrol gas, coal and oil heating methods. Pulat *et al.* (2009) conducted an experimental study to analyse the performance of a horizontal GSHP for mild climates in Turkey. The economic analysis indicated that GSHP systems were more cost effective than the other conventional heating systems. Sanaye *et al.* (2009, 2010) proposed a thermal-economic optimal design method to size a vertical GSHP system and a horizontal GSHP system, respectively. The objective function to be minimised was the sum of annual operating cost and investment cost of the system. Two optimisation techniques, namely, Nelder-Mead and genetic algorithm, were

applied to determine the optimal decision variables. Kalinci *et al.* (2008) conducted an economic and energy performance analysis of GSHP heating systems. The energy and exergy analysis methods were applied to determine the optimum pipe diameters. The system with a nominal diameter of DN300 pipeline was found to have a minimum cost of USD 561,856 per year, with system energy efficiency and exergy efficiency values of 40.21% and 50.12%, respectively. Garber *et al.* (2013) evaluated the performance of a GSHP system by comparing it with four alternative HVAC system configurations based on the probability approach in terms of economic and CO_2 savings. The results showed that the potential savings by using a GSHP system are significantly affected by the efficiency of HVAC system, and the prices of energy resources (e.g. electricity, gas, etc.). The evaluation found that the most cost- efficient configuration is that a GSHP with its maximum capacity equal to the full design load, backed up with an auxiliary device. Alavy *et al*. (2013) proposed a new methodology and computing approach for optimisation of the capacity of GSHPs in hybrid systems in terms of NPV (net present value). The results indicated that, in most cases, the GSHP needs to meet around 80% of total design load. Robert *et al*. (2014) established a new design method to optimally size the vertical GHEs of GSHP systems by minimising the total cost including the initial costs of drilling, excavation, heat pump, and piping, as well as the electricity cost. Retkowski *et al*. (2014) developed a new mixed-integer nonlinear programming (MINLP) approach to optimal sizing GSHP systems. A case study was performed to validate the effectiveness of the proposed method and the results showed that the total annual costs (TAC) can be reduced by more than 10%.

- *Thermodynamic optimisation of the GSHP systems*

Thermodynamic optimisation of the GSHP systems is usually studied based on the theory of the second law of thermodynamics or exergy analysis. Exergy analysis is a powerful tool for developing, evaluating and optimising the design and operation of energy systems and which can be used to identify the main sources of thermodynamic irreversibility and to minimise the entropy generation of a given energy and material transfer process (Bejan 2006).

Piechowski (1996) introduced an optimisation method to identify the optimal combination of pipe radius and water flow rate of a GHE based on the principle of second law of

thermodynamics. Ozgener *et al.* (2007) conducted a series of exergy analysis and performance assessment of conventional GSHP and hybrid GSHP systems. An energetic and exergetic modelling was developed and used to evaluate the system performance in terms of thermodynamic parameters, i.e. energy efficiency, exergy efficiency, exergetic improvement etc.

Bi *et al.* (2009) conducted a comprehensive exergy analysis of a GSHP system used for heating and cooling buildings. This study attempted to find out the key energy saving components to minimise exergy efficiency and thermodynamic perfection of the GHEs. The results validated the effectiveness of optimising GHE design from the aspect of thermodynamic performance. Lohani *et al*. (2010) performed an energy and exergy analysis of a fossil plant, an air source heat pump and a ground source heat pump system respectively, to determine which system can provide the highest efficiency of conversion and supply of energy/exergy. The exergy analysis and comparisons revealed that the GSHP heating system was more efficient than the air source heat pump and the fossil plant heating system. Ally *et al.* (2012) presented an exergy and energy analysis of the horizontal GSHP system operated in a low-energy test house. The average monthly rate of entropy production and percent entropy contribution for each segment of the system was calculated through exergy analysis. Li *et al.* (2013) utilised an entropy generation minimisation method to derive the analytical expressions for optimising total borehole length and flow velocity of a GSHP system. The analysis showed that the pure heat transfer and thermodynamics analysis can be an effective way to find the optimum parameters of GSHP systems. Yekoladio *et al*. (2013) optimised a downhole coaxial heat exchanger for an enhanced geothermal system. The objective was to minimise the heat transfer and fluid friction irreversibility in terms of the entropy generation number (EGN). The optimal diameter ratio of the coaxial pipes was determined for the minimum pressure drop within the turbulent and laminar fully-developed flow regime. Moreover, an optimal mass flow rate in the downhole coaxial heat exchanger and the optimal dimensions of the heat exchanger were determined through maximising the net power output.

The above studies were mainly based on the single-objective design optimisation. Single-objective design optimisation may either increase the system upfront cost if the thermal

performance is used as the objective function, or may decrease the system thermodynamic performance if the economic cost is employed as the objective function (Ndao *et al*. 2009, Sayyaadi *et al*. 2011).

Multi-objective optimisation

A general multi-objective optimisation problem can be stated as below (Aravelli 2014):

Minimise the objective functions of $f_1(X), f_2(X), \ldots f_k(X)$.

$$\text{Subject to} \quad \begin{matrix} g_i(X) \le 0, & j = 1,2,...m \\ h_k(X) = 0, & k = 1,2,...p \end{matrix} \tag{2.11}$$

where $X=\{x_1, x_2 \ldots x_n\}^T$ is an n-component design vector.

Unlike single objective optimisation, multi-objective optimisation considers two or more objective functions simultaneously and provides useful information on the effects of different objective functions to decision makers and help them to find appropriate compromised solutions from the obtained Pareto-solutions (Lu *et al*. 2015). Note that multi-objective optimisation problems could be converted into single-objective problems by applying weight coefficients (Xu *et al*. 2002). However, the computational effort required to perform this procedure is much higher because it is necessary to perform an optimisation run for every combination of the weight coefficient. For a multi-objective optimisation method, the final solution can be obtained in a single optimisation run (Toffolo *et al*. 2002).

In terms of the optimisation of GSHP systems, the multi-objective approaches to optimising both thermodynamic and thermoeconomic objectives simultaneously have been studied. Gholap *et al*. (2007) applied a multi-objective optimisation procedure by considering energy consumption and material cost as the two different objective functions to optimise the design of heat exchangers for refrigerators. The results demonstrated that this proposed method was technically feasible and effective in the design optimisation of refrigeration equipment with the vapour compression cycle. Sayyaadi *et al.* (2009) proposed a multi-objective design optimisation method of a vertical U-tube GSHP system to minimise both the total levelized cost of the system product and the exergy destruction of the system. Seven temperature differences (e.g. between inlet brine and sub-cooled refrigerant in the

condenser, between the outlet air and superheated refrigerant in the evaporator, etc.) and the pipe diameter of the GHE were chosen as the decision variables. The sensitivities of the interest rate, operating hours and the cost of electricity for the optimisation were also studied. Shi *et al*. (2012) developed a thermo-economic model for analysis and optimisation of a seawater source heat pump (SWHP) system in a residential building. The modelling results indicated that the exergy loss and EER increased by 22.7% and 13.9% respectively, whereas the annual production cost reduced by 29.1% using thermo-economic optimisation compared with using thermodynamic optimisation. Khorasaninejad *et al*. (2014) employed the multi-objective particle swarm optimisation algorithm to optimise a solar-assisted heat pump system. The two objective functions of total annual cost (TAC) and coefficient of performance (COP) were used to formulate the optimisation problem. The results from the case studies showed great improvement of both the TAC and COP of optimised systems as compared with those of original systems.

From the above review, it can be seen that the research effort on the optimisation of GSHP systems has increased dramatically in recent years and the optimisation focus has gradually been developed from single-objective to more comprehensive multi-objective optimisation of GSHP systems. With technology development, computer-based tools such as MATLAB Toolbox, GENOPT etc. are now readily available to help researchers perform optimisation studies (Asadi *et al.* 2012). With the aid of these optimisation tools, the investigation of different ways to decrease the high initial cost of the GSHP system by reducing the size of a GHE, and possibly the heat pump unit itself, while maintaining satisfactory system performance, becomes more desirable.

2.6 Control optimisation of GSHP systems

The major function of the control strategies for GSHP systems is to maintain satisfactory indoor thermal comfort with the minimal energy consumption. In practice, control systems can use a variety of control devices such as digital, mechanical, electrical and electric devices to meet different control purposes. Development of control strategies for GSHP system can be complicated and complex as it is challenging to fully understand the interactions among the system components. The parameters of the system components are

likely to interact with each other, changing one parameter will have potentially unpredictable effects on the operation of other components.

For a GSHP system, its performance is affected by climatic conditions, the heat distribution system (such as hydraulic loop or forced-air), the building load conditions and the ground characteristics, etc. simultaneously. To better understand the control concept, the operation of GSHP systems can be considered into three levels, including building level, heat pump level and ground loop level (Verhelst 2012).

Building level control is to ensure the indoor thermal comfort of the buildings is within an acceptable range. Research on the building level control is normally used to develop simplified and accurate building models to predict both the thermal comfort and building heating and cooling demands. Thermal comfort is a function of the operative temperature T_{op}, which in turn is a weighted sum of the room air temperature and the radiative temperature. An accurate prediction of the operative temperature requires a detailed building model which distinguishes between convective and radiation heat transfer processes into and inside the building zones.

The study of Zhai *et al.* (2012) indicated the strong implications of the indoor temperature set-point on the energy performance of GSHP systems applied for the cooling-dominated buildings. A series of experiments were conducted and results showed that both the heat rejection during the cooling period and the heat extraction during the heating period were significantly affected by the set values of the indoor temperature. For air-conditioning cooling dominated buildings using GSHP systems, the increase in indoor temperature settings can alleviate the thermal imbalance of the ground, which would be of benefits to the long-term operation of GSHP systems.

At the heat pump level control, extensive research has been done on the development and evaluation of control strategies for both cooling-dominated and heating-dominated buildings (Ahn *et al.* 2001, Jin *et al*. 2005, Ma *et al*. 2009, Li *et al*. 2013, West *et al*. 2014, Sichilalu *et al*. 2014). The research relied primarily on the development of the operational modes or sequence control strategies for different HVAC equipment, such as determining the strategies for charging and discharging of active thermal energy storage devices (e.g. ice storage), determining the logics of switching among active cooling, free cooling and night

ventilation, etc. In general, the control methods can be categorised into three groups, including the constant set-point based method, the temperature differential based method and the schedule based method (Gang *et al.* 2014).

Yavuzturk *et al*.(2000) discussed a comparative research method for investigating the benefits and drawbacks of various operating and control strategies for hybrid GSHP systems. One of the control strategies to avoid the soil temperature rise in the long run was to recharge the soil utilizing cooling towers. The recharge was realized by turning on the cooling towers for 6 hours during the night. In addition, one of the advantages of this control strategy is that it used the peak and valley electric charges to improve economic efficiency. Man *et al.* (2011) presented a novel hybrid GSHP (HGSHP) system, in which, the GSHP is combined with a nocturnal cooling radiator (NCR). The NCR was used as a supplemental heat rejecter and was only operated under certain conditions to alleviate the heat accumulation around GHEs. From 10:00 pm to 6:00 am, the water circulation pump was activated to pump the water flowing through the NCR installed on the roof to reject the accumulated heat around the GHE. In an attempt to reuse the waste rejected heat, this HGSHP system was also incorporated with a de-superheater used to produce domestic hot water. Madani *et al*. (2011) compared the annual operational performance of GSHPs using on/off control and variable speed control. The results showed that variable speed control can achieve 5-30% energy savings as compared to on/off control. Ouyang *et al.*(2012) proposed a new operating and control strategy of a hybrid GSHP (HGSHP) with the aim to dissipate the accumulated heat within the ground during the night. The cooling tower was connected with the condenser and the GHE was connected with the evaporator, so that the soil could be cooled during night to reduce the soil temperature. In this way, the energy performance of the HGSHP system can be improved during the daytime to a significant extent. However, the extra energy was consumed by the heat pump during the night also increased the total electricity consumption of the system. Yang *et al.* (2014) analysed the intermittent operation strategies for a hybrid GSHP system with double-cooling towers for hotel buildings. On the basis of the hotel load patterns, four operating conditions were designed for this system including one continuous condition and three intermittent conditions. The results showed that the optimal intermittent operating condition favoured

both energy consumption reduction and soil temperature recovery.

When the GSHP system is designed to cover the entire heating and cooling demands of a building, the control at the ground loop level is straightforward. The ground loop can be used permanently when the temperature limits are met at the end of the design lifetime. In order to facilitate optimal operation, efforts have been made to accurately predict the exiting fluid temperature from the ground loop. Gang *et al.* (2013) increased the accuracy of prediction of the fluid temperature circulating the GHEs based on artificial neural network (ANN). Based on the ANN theory, Gang *et al.* (2014) proposed an ANN predictive control method for a hybrid GSHP (HGSHP) system. The cooling water temperature exiting the ground heat exchanger was predicted by the ANN model and then compared directly with the cooling water temperature exiting the cooling tower. Four years' performance analysis of the HGSHP system showed that the ANN predictive method was more energy-efficient and could make full use of the heat exchange advantage of outdoor air and the soil.

As reviewed above, among the control studies for GSHP systems, the main efforts were concentrated either on the evaluation and comparison of different operational strategies to determine the best control strategy, or on the model predictive control by developing predictive component mathematical models based on neural network theory. Although GSHP systems with these control strategies can allow the systems to operate more energy efficiently and cost effectively, it is hard to conclude whether the selected control strategy is the optimal one or near-optimal one.

To optimise the operation of a process, a strategy for determining the optimal set values of the controlled variables at given conditions should be applied. Moreover, a control system is needed to change the controlled variables to the optimal state. Similar to the formulation of design optimisation methodologies, the control optimisation also needs to satisfy at least one objective function which is subjected to certain operating constraints, as illustrated in Section 2.5.3. The objective function is normally defined as electrical energy or power consumption. The constraints function represents the limitations of the GSHP system. The constraints function is represented by a system model. The system model could be a physical model, a grey-box model or a black-box model (Shan 2013).

With regard to control optimisation of GSHP systems, few research works have been published. Therefore, one of the objectives of the study is to develop an optimal control method for GSHP systems to maximise the overall operating efficiency without sacrificing indoor thermal comfort and violating the operating constraints.

2.7 Summary

A literature review on the energy performance evaluation, design and control optimisation of the GSHP system has been provided. The reviewed literature revealed that GSHP systems can be confirmed as the most energy-efficient and environmentally clean air conditioning system. The main disadvantage of GSHP systems compared to conventional ones is higher initial costs. Despite certain disadvantages, a good GSHP system can be justifiable from both the economic aspect and system efficiency point of view through appropriate design and optimisation methods. Below are some conclusions from this review:

1) Soil thermophysical properties significantly influence the performance of GSHP systems. Accurate determination of the soil thermal characteristics of the constructive sites is essential before the design of a GSHP system.

2) Performance evaluation of GSHP systems through experimental tests and simulations showed that GSHP systems are generally more energy-efficient when compared with conventional HVAC systems.

3) The results from feasibility studies showed that GSHP systems are economically and environmentally preferred in most of the conditions. The feasibility of using GSHP systems is influenced by many factors, such as different types of buildings, climate conditions, and technologies employed etc. It is not possible to reach a common conclusion on whether GSHP systems are feasible for every single building. It is necessary to assess energy performance and economic competitiveness of GSHP systems case by case.

4) Both analytical and numerical models have been developed for modelling and sizing ground heat exchangers. The analytical GHE models are usually used for

long-time-period simulation and are not suitable for short temperature response calculation. Numerical models are not suitable for direct incorporation in a building simulation program with hourly or sub-hourly time steps due to the high computational time required.

5) Several design procedures and software tools are now commercially available for appropriate sizing vertical GHEs. However, deviations between the real optimal length and the predicted GHEs length via using these different design methods may occur due to the simplifications and assumptions made during the modelling process. It is, therefore, hard to make sure the designed length is an optimal value or a near-optimal value. Design optimisation is worth further investigation to determine optimal values of design parameters such as total GHE length, buried GHE depth etc. in order to minimise the high upfront cost of GSHP systems.

6) A number of control strategies for GSHP systems have been developed. These include constant the set-point based method, the temperature differential based method and the scheduling based method. However, current available operational strategies might be far from optimal and application of these strategies might lead to energy losses due to the complexity of system operational conditions. Operational optimisation is worth further investigation to maximise the overall performance of GSHP systems, in order to further compensate high upfront cost of GSHP system and improve the economic feasibility of GSHP system in the long run.

This dissertation will, therefore, focus on analysing the energy performance of GSHP systems under major Australian climatic conditions. To maximise the benefits due to the use of GSHPs, a design optimisation methodology for vertical GHEs and an optimal control strategy for ground source-air source combined heat pump systems will also be developed.

Chapter 3

Ground Source Heat Pump System Design, Installation and Experimental Investigation

The literature reviewed in Chapter 2 demonstrated that proper design of ground source heat pump (GSHP) systems is essential to reduce the high installation cost of GSHP systems to facilitate the wide deployment of the GSHP technology. Ground heat exchangers (GHEs) are one of the major components in GSHP systems and the majority of installation costs related to the use of a GSHP system are from the installation of GHEs. In order to facilitate a better understanding of the performance of a GSHP system, a flexible GSHP system with both vertical and horizontal ground heat exchangers, which can operate in either parallel or series, has been designed and implemented in the Sustainable Buildings Research Centre (SBRC) at the University of Wollongong (UOW).

This chapter describes the design and implementation of the ground source-air source combined heat pump system of the UOW SBRC building and the experimental investigation of the effects of the series and parallel operation of ground heat exchangers on the energy performance of the GSHP system. The experimental data obtained was also used to validate the water-to-water heat pump model and ground heat exchangers models used in this study, which will be presented in Chapter 4.

This chapter is organised as follows. A brief description of the SBRC building is provided in Section 3.1. The design and installation of the ground source-air source combined heat pump system of the SBRC building are presented in Section 3.2. Section 3.3 describes the experimental tests and data analysis. The key findings in this chapter are summarised in Section 3.4.

3.1 Description of the SBRC building

The Sustainable Buildings Research Centre (SBRC) building is a net-zero energy university

building located at the Innovation Campus of the University of Wollongong, Australia (see Fig 3.1). The total floor area of the building is 2,600 m^2. The building forms part of a local initiative funded by the Australian Commonwealth Government that focuses on upgrading and retrofitting of existing buildings for energy efficiency and sustainability.

Fig. 3.1 Location of the SBRC building.

The building consists of two rectangular wings, each with the long axis orientated east-west for optimal solar access and shading as shown in Fig. 3.2. The southern “office” wing is a two-storey structure, the top floor of which is an open plan office. The ground floor includes an exhibition space, a training room, three multi-function laboratories and service areas. The northern wing is a high-bay facility with flexible functional capability, housing large-scale equipment and test facilities such as an indoor environmental quality test facility. Based on optimised passive design principles, natural ventilation and careful equipment selection, the building was designed to be an ultra-low energy building. The building is equipped with a 155 kWp PV array, a PV-thermal system, a ground source-air

source combined heat pump system, transpired solar collectors, green roofs and a low energy IT systems.

Fig. 3.2 Sustainable Buildings Research Centre building.

3.2 Design and installation of the ground source-air source combined heat pump system

The ground source-air source combined heat pump system installed consisted of an air-to-water heat pump (AWHP) and two identical water-to-water heat pumps (WWHPs), which were used to provide the heating and cooling necessary to maintain desired indoor thermal comfort conditions within the building. Both water-to-water heat pumps were sized to provide 20% of the total heating and cooling demand of the building under design conditions. However, the annual heating and cooling energy provided by the two water-to-water heat pumps will be significantly higher than 20% of the total due to the fact that the majority of the time building operates under part-load conditions and these units are sequenced to cover base-load heating and cooling demand. The two water-to-water heat pumps were integrated with a ground loop system, which consists of three vertical GHEs and a total of twelve horizontal GHEs. Three vertical GHEs can operate either in parallel or

in series. The six horizontal GHEs in the south side can only operate in parallel while the other six horizontal GHEs in the north side were categorised into three groups, which can operate either in parallel or in series. Such flexible design can allow the experimental investigation of potential benefits due to the change of the configurations of the ground heat exchangers, to determine the best approach to operating the GSHP system in order to achieve better energy performance. Two constant water pumps were dedicated to each water-to-water heat pump both in the load side and source side and a variable speed boost water pump was used in the ground loop to provide sufficient force to circulate the water flowing through the GHEs. Fig 3.3 is a schematic diagram of the ground source-air source combined heat pump system implemented. Fig 3.4 shows the hydronic loop of the ground source-air source combined heat pump system implemented in the SBRC building. The detailed ground heat exchanger design diagram and the hydronic loop system are presented in Appendix A and B, respectively.

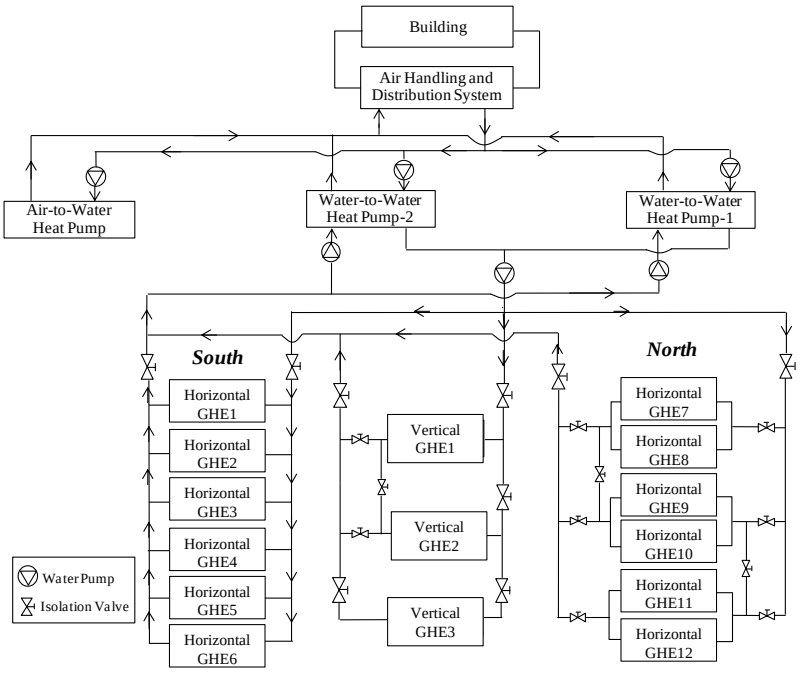

Fig. 3.3 Schematic of the ground source-air source combined heat pump system.

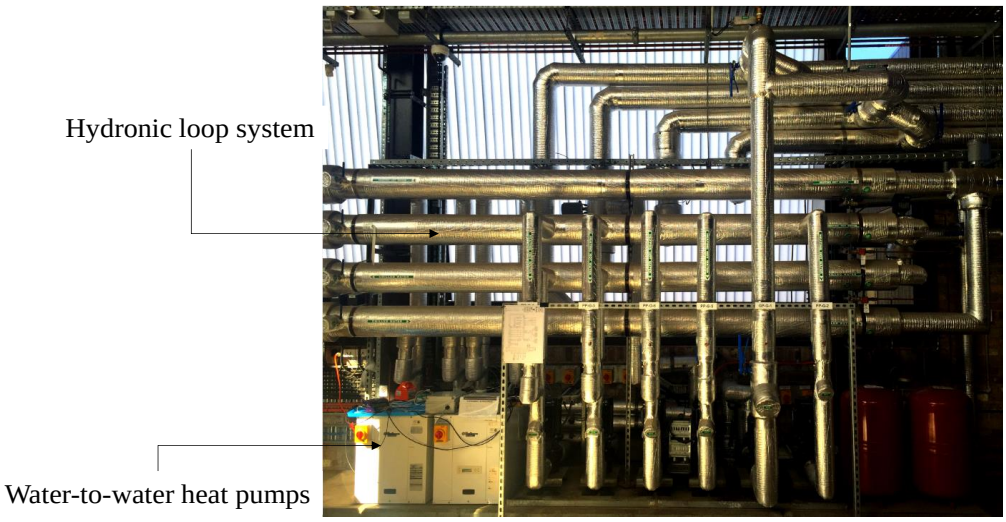

Fig. 3.4 Hydronic loop of the ground source-air source combined heat pump system.

Fig. 3.5 shows the *in-situ* arrangement of the horizontal heat exchangers, which were buried with a loop pitch of 1.5 m beneath the SBRC garden as shown in Fig. 3.6. The manifold box for changing the configurations of the GHEs is shown in Fig. 3.7. The specifications of the heat pumps and ground heat exchangers installed in this system are summarised in Table 3.1.

Fig. 3.5 Installation of the horizontal ground heat exchangers.

Fig. 3.6 SBRC garden beneath which the horizontal ground heat exchangers buried.

Fig. 3.7 Ground loop manifold box.

Table 3.1 Specifications of the ground source-air source combined heat pump system

Two water-to-water heat pumps	Rated cooling capacity/power (kW/kW)	32.8/8.2
	Rated heating capacity/power (kW/kW)	40.8/11.0
Air to water heat pump	Rated cooling capacity/power (kW/kW)	109.4/36.4
	Rated heating capacity/power (kW/kW)	133.9/37.9
Vertical heat exchangers	Number of boreholes	3
	Diameter of borehole (mm)	150
	Depth of borehole (m)	91
	Borehole spacing (m)	8
Horizontal heat exchangers	Loop pitch (m)	2
	Number of pipes	12
	Length per pipe (m)	125
	Trench length (m)	17

3.3 Experimental investigation and evaluation of the performance of the ground heat exchangers

3.3.1 Description of the experimental tests

A series of experimental tests were designed and carried out to investigate the performance of the GSHP system with different operating configurations of the ground heat exchangers (e.g. in parallel or in series operation) and with different water flow rates circulating through the GHEs. The changes from parallel to series operation were achieved through manually opening/closing the isolation valves installed in the manifold box shown in Fig. 3.7.

Table 3.2 summarises the six test scenarios. Test scenarios 1-3 focussed on the parallel configuration of the GHEs with three different water flow rates (i.e. 1.33 L/s, 1.89 L/s and 2.31 L/s) in the ground loop. The change of the water flow rates was achieved by adjusting the differential pressure set-point between the supply and return of the main pipelines in the ground loop to 20 kPa, 40 kPa and 60 kPa, respectively. The test scenarios 4-6 focussed on

the series operating configuration of the GHEs. Due to the increased flow resistance in the ground loop, during the tests, the differential pressure set-points were increased to 90 kPa, 110 kPa and 130 kPa, respectively. The resulting water flow rates in the ground loop were 1.41 L/s, 1.56 L/s and 1.71 L/s. The highest flow rate tested in the series configuration was smaller than that in the parallel configuration, since the increased pressure resistance in the ground loop meant that the boost water pump could not provide sufficient pressure to circulate at the highest water flow rate as for parallel operation. During the whole test period, the air source heat pump was turned off. During each test, the two water-to-water heat pumps were operating simultaneously for 3 hours. The experimental test results from the cooling mode operation are presented below. It is worthwhile to mention that, only a limited range of experiments were carried out due to the contractual delays in completing the system and the faults that needed to be rectified by the contractors.

Table 3.2 Summary of the test scenarios

Scenarios	Vertical heat exchangers	Horizontal heat exchangers		Ground loop water flow rate (L/s)
		South	North	
1	Parallel	Parallel	Parallel	1.33
2	Parallel	Parallel	Parallel	1.89
3	Parallel	Parallel	Parallel	2.31
4	Series	Parallel	Series	1.41
5	Series	Parallel	Series	1.56
6	Series	Parallel	Series	1.71

3.3.2 Data acquisition system

The data logging system used in the experimental tests consisted of temperature measurement, differential pressure measurement and the power consumption measurement.

Temperature sensors: Eight PT100 RTD temperature sensors were installed at the inlet and outlet of both the load side and source side of each water-to-water heat pump. The PT100

RTD sensors can be applied to the temperature range of -200-700 ºC with a measurement error of ±0.15 ºC.

Pressure sensors: Four wet/wet differential pressure transmitters (Model: 629-03-CH-P2-E5-S1) were installed in the source side and load side of the two water-to-water heat pumps to measure the pressure differences. Linear interpolation was employed to derive the water flow rates on the load and source sides of the heat pumps based on the pressure difference and flow rate table shown in Table 3.3, provided by the manufacturer. The measurement accuracy of the differential pressure transmitters was ±0.5% of the measurement range.

Table 3.3 Pressure difference and flow rate of the water-to-water heat pump

Flow rate	Pressure difference (kPa)				
(L/s)	0 °C*	15 °C	25 °C	35 °C	50 °C
0.6	22.1	20.7	19.5	18.3	17.2
0.9	37.9	36.5	35.2	33.5	32.1
1.2	54.5	52.4	50.3	48.7	46.9
1.5	79.3	77.9	75.8	74.5	72.4

*Temperatures are entering water temperatures

Power meters: The power consumption of the two water-water heat pumps was measured by a 3-Phase 4-Wire power quality analyser. The power consumption of the water pumps was not measured during the tests as there was no power meter installed in the system to measure the power consumption of the water pumps and there was no additional power quality analyser available during the tests. The accuracy grade of the power consumption acquisition by the HIOKI PW3198 used was ±0.2%.

The data transmitted from the HIOKI PW3198 was logged by its implanted commercial hardware and software, while the temperature and pressure difference signals were processed by a data logger. The DataTaker DT80 cooperated with the PT100 RTD temperature sensors and differential pressure transmitters for temperature acquisition and pressure difference acquisition, respectively.

The DataTaker was connected to a personal computer to monitor and record as well as retrieve the operational data. The schematic diagram of the data acquisition system is described in Fig. 3.8. In the experimental tests, the temperature, pressure difference, and the power consumption were recorded in every five minutes.

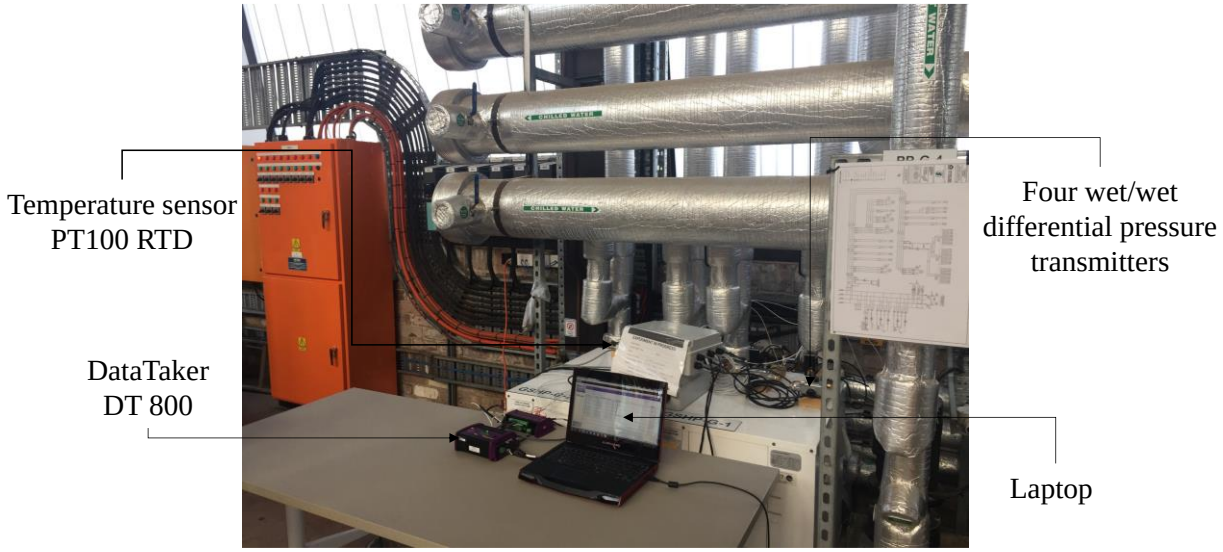

Fig. 3.8 The data log system used in the experimental tests.

3.3.3 Experimental test data analysis and discussion

As mentioned earlier, the data presented hereafter is for cooling mode operation only, where the load side and source side refer to the evaporator side and condenser side of the water-to-water heat pump, respectively (vice versa for the heating mode operation). The Coefficient of Performance (COP_{WWHP}) of the water-to-water heat pumps in the GSHP system was calculated by the following equation.

$$COP_{WWHP} = \frac{\sum Q_{load}}{\sum W_{HP}} \tag{3.1}$$

where $\sum Q_{load}$ is the total cooling energy provided by the two water-to-water heat pumps, and $\sum W_{HP}$ is the total power consumption of the two water-to-water heat pumps. The total cooling energy provided by the two water-to-water heat pumps was calculated by Equation (3.2).

$$Q_{load} = m_{load} c_{p,load} (T_{load,in} - T_{load,out}) \quad (3.2)$$

where, m_{load} is the water mass flow rate in the load side of the water-to-water heat pump, $C_{p,load}$ is the water specific heat capacity, and $T_{load,in}$ and $T_{load,out}$ are the inlet and outlet water temperatures in the load side of the water-to-water heat pump, respectively.

3.3.4 Uncertainty analysis

Experimental uncertainties can result from a number of elemental error source, such as instrument condition, instrument calibration, reading errors and others. In order to provide the accuracy of experimental tests, uncertainty analysis is necessary. In this experiment, uncertainty analysis of error estimations for both measured and calculated parameters is carried out. The measured parameters include the temperature, pressure difference and power consumption. The calculated parameters include the COP of the water-to-water heat pump (COP_{WWHP}) and the cooling energy provided by the water-to-water heat pumps (Q_{load}), which were calculated by using Equations (3.1) and (3.2), respectively.

The relative uncertainties of the measured parameters (σRx_i) and the calculated parameters (σRF) can be obtained from the Equation (3.3) and the Equation (3.4) (Yang *et al*. 2015, Moffat 1988).

$$\delta Rx_i = A\frac{\gamma_i}{x_i} \quad (3.3)$$

where, A is the upper limit of the measurement range, and γ_i is the accuracy grade according to the manufacturer's data.

$$\delta RF = \frac{\sqrt{\sum_1^n (\frac{\partial F}{\partial x_i} \cdot A \cdot \gamma_i)^2}}{F} \quad (3.4)$$

where F is a function of a series of independent measured variables.

The relative uncertainties in the inlet and outlet water temperatures at the load side of the water-to-water heat pumps were estimated to be 0.70% and 0.73%, respectively, whereas the relative uncertainties of the inlet and outlet water temperatures at the source side of the

water-to-water heat pumps were 0.60% and 0.58%, individually. The relative uncertainties of the pressure difference at the load side and source side of the water-to-water heat pumps were 0.53% and 0.63%, respectively. For the power consumption of the water-to-water heat pumps, the relative uncertainty was found to be 0.2%. The cooling load calculated showed a relative uncertainty of 0.9% by taking into account of both the temperature measurement uncertainty and pressure difference measurement uncertainty. The relative uncertainty in the COP was 1.26%.

3.3.5 Experimental test results and analysis

Parallel operation of the ground heat exchangers

Three experimental tests with different water flow rates were carried out when the GHEs were in parallel operation. The water flow rates used can be found in Table 3.2.

Fig. 3.9 shows the total cooling energy delivered by the two water-to-water heat pumps. It can be seen that, the total cooling energy provided by the two water-to-water heat pumps with different water flow rates in the ground heat exchangers was relatively stable within the range of 29-33 kW. The average cooling energy provided for the low source flow rate, medium source flow rate and high source flow rate were 31.2 kW, 30.9 kW and 31.0 kW, respectively. Due to the variations of the weather conditions and the internal building loads, the building loads were slightly different for the three test cases.

Fig. 3.10 presents the total power consumption of the two water-to-water heat pumps for the three test scenarios. It can be seen that, the water-to-water heat pumps (WWHPs) consumed an average power of 8.53 kW with the low source flow rate in the GHEs, approximately 0.32 kW and 0.63 kW higher than the power consumed with the medium source flow rate and high source flow rate in the ground loop, respectively.

Fig. 3.11 presents the coefficients of performance of the water-to-water heat pumps (COP_{WWHP}) under the three different test scenarios. It can be seen that the COP_{WWHP} values varied with the variations of the load conditions. The average coefficients of performance of the water-to-water heat pumps with the low, medium and high source water flow rates in the ground loop were 3.66, 3.76 and 3.92, respectively. Clearly, the water-to-water heat

pumps with the high source water flow rate in the ground loop gave the best performance for the three scenarios tested. A larger flow rate in the GHEs is beneficial to the operation of the water-to-water heat pumps. However, increasing the water flow rates in the GHEs can lead to the increase in the power consumption of the water pumps in the source side of the GSHP system (Cervera-Vázquez *et al*. 2015).

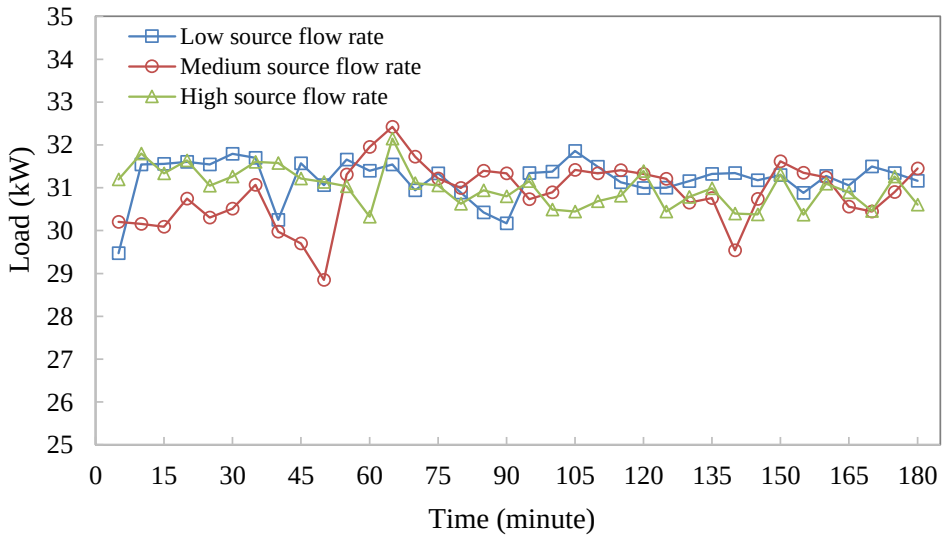

Fig. 3.9 Cooling energy provided by the two water-to-water heat pumps with different source flow rates - parallel operation.

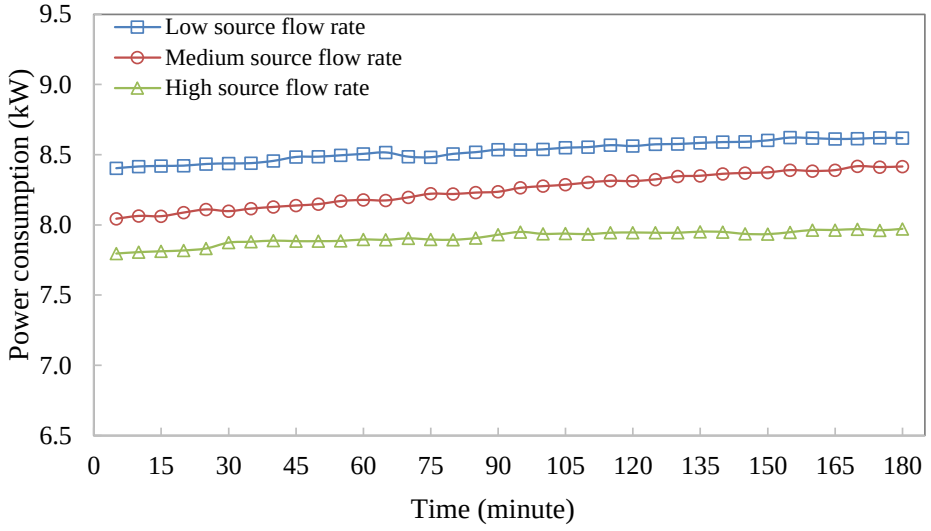

Fig. 3.10 Power consumptions of the two water-to-water heat pumps with different source flow rates - parallel operation.

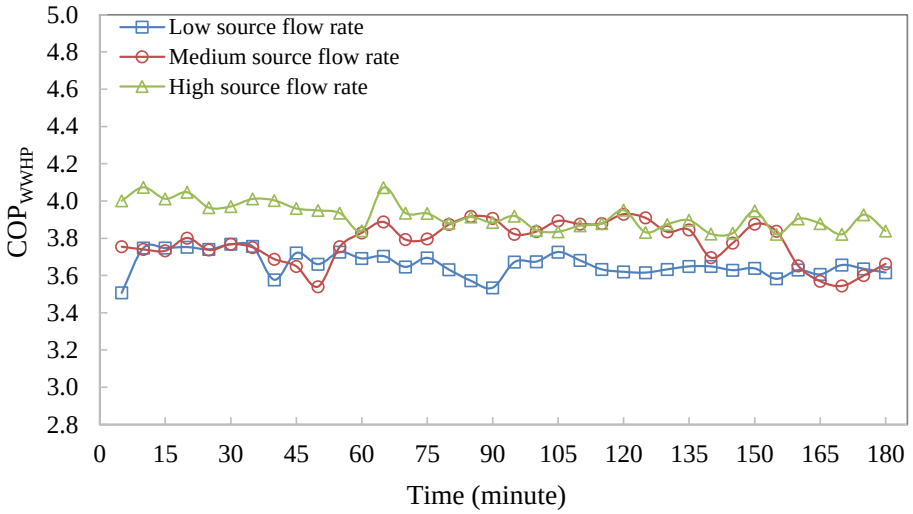

Fig. 3.11 COP of the two water-to-water heat pumps with difference source flow rates - parallel operation.

As mentioned earlier, the power consumption of the water pumps was not measured directly during the tests. In order to quantify the effects of the water flow rate on both the water-to-water heat pump and water pumps, the power consumption of the dedicated source side constant speed water pumps was estimated using the Equation (3.5) (Klein 2010).

$$W_{pump} = W_{p,rated} \times (\beta_0 + \beta_1 \times \frac{m_s}{m_{f,rated}} + \beta_2 \times (\frac{m_s}{m_{f,rated}})^2 + \beta_3 \times (\frac{m_s}{m_{f,rated}})^3) \qquad (3.5)$$

where, W_{pump} is the power consumption of the water pump, $W_{p,rated}$ is the rated power of the water pump, $m_{f,rated}$ is the rated fluid rate of the water pump, m_s is the water flow rate circulated by in the water pump, and β_0, β_1, β_2 and β_3 are the constant coefficients determined based on the performance data of the water pump provided by the manufacturer. This data is presented in Table 3.4.

Table 3.4 Coefficients used in the constant speed water pump model

Coefficients	$W_{p,rated}$	β_0	β_1	β_2	β_3
Source side water pump	1.6	0.4199	0.5914	0.2976	-0.306

For the boost water pump, due to the insufficient pump performance data provided by the manufacturer, the pump affinity laws presented below were used to predict the power consumption of the water pump under different operating speeds (Branan 2012). Once the power consumption, flow rate and pump head at the design condition are known, the corresponding values under the other conditions (i.e. operating speeds) can be easily determined using the affinity laws.

$$\frac{V_1}{V_2} = \frac{n_1}{n_2} \tag{3.6}$$

$$\frac{H_{p1}}{H_{p2}} = (\frac{n_1}{n_2})^2 \tag{3.7}$$

$$\frac{W_1}{W_2} = (\frac{n_1}{n_2})^3 \tag{3.8}$$

where, n is the pump speed, V is the volume flow rate, H_p is the pump head and W is the pump power consumption, and subscripts 1 and 2 refer to the two different pump speeds.

The estimated total energy consumptions of the water pumps for each test period of 3 hours (i.e. test scenario) are shown in Table 3.5. The source side water pumps included the two dedicated constant speed water pumps and one variable speed boost water pump. The total power consumption of the GSHP system included the power consumptions of the two water-to-water heat pumps and all water pumps in the source side of the water-to-water heat pumps. It can be seen that the increased source flow rate led to an increase in the power consumption of the water pumps, which would have offset the savings achieved by the water-to-water heat pumps. As a result, the system with the low source flow rate resulted in the lowest power consumption of 30.84 kWh with a COP_{WWHP} of 3.04 for the three scenarios studied under the test conditions. As the working conditions for the three test scenarios were slightly different, it is difficult to draw a simple conclusion as to which water flow rate can provide the best performance for the GSHP systems. However, it is clearly shown that the optimisation of the water flow rate in the ground loop is essential to minimise the total power consumption of the GSHP systems, in particular for the systems with boost water pumps.

Table 3.5 Comparison of energy performance of the system with different source water flow rates

	Test Scenarios	Total power consumption (kWh)			COP_{sys}
		Source side water pumps	Water-to-water heat pumps	Total	
1	Low (1.33 L/s)	5.25	25.59	30.84	3.04
2	Medium (1.89 L/s)	6.27	24.63	30.90	3.00
3	High (2.31 L/s)	7.38	23.70	31.08	2.99

Series operation of the ground heat exchangers

Similar tests were also carried out for the series operation of the vertical and horizontal heat exchangers with three different water flow rates in the GHEs as described in Table 3.2.

The total cooling energy, the total power consumption and the COP_{WWHP} of the water-to-water heat pumps for the three test scenarios in the series configuration of the GHEs are presented in Fig. 3.12, Fig. 3.13 and Fig. 3.14, respectively. From Fig. 3.12, it can be observed that the cooling energy supplied by the two water-to-water heat pumps under the three test scenarios were relatively stable within the range of 24.5-27.5 kW. The average cooling loads provided under the low, medium and high source flow rates were 25.7 kW, 25.5 kW and 25.3 kW, respectively. From Fig. 3.13, it can be seen that the average power consumed by the two water-to-water heat pumps with the low, medium and high source flow rates were 8.21 kW, 8.05 kW and 7.89 kW, respectively. The average coefficients of performance of the water-to-water heat pumps, as shown in Fig. 3.14, with the low, medium and high source flow rates were 3.13, 3.17 and 3.21, respectively. A similar study of the effects of the source flow rate on the performance of the water-to-water heat pumps and water pumps was also carried out but the results are not presented here since the conclusions were essentially the same as for the parallel operation of the ground heat exchangers.

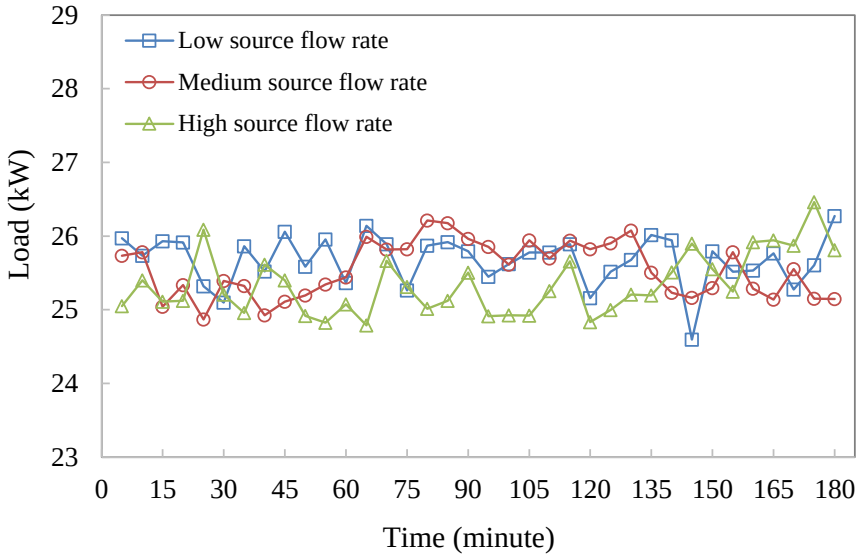

Fig. 3.12 Cooling energy provided by the two water-to-water heat pumps with different source flow rates - series operation.

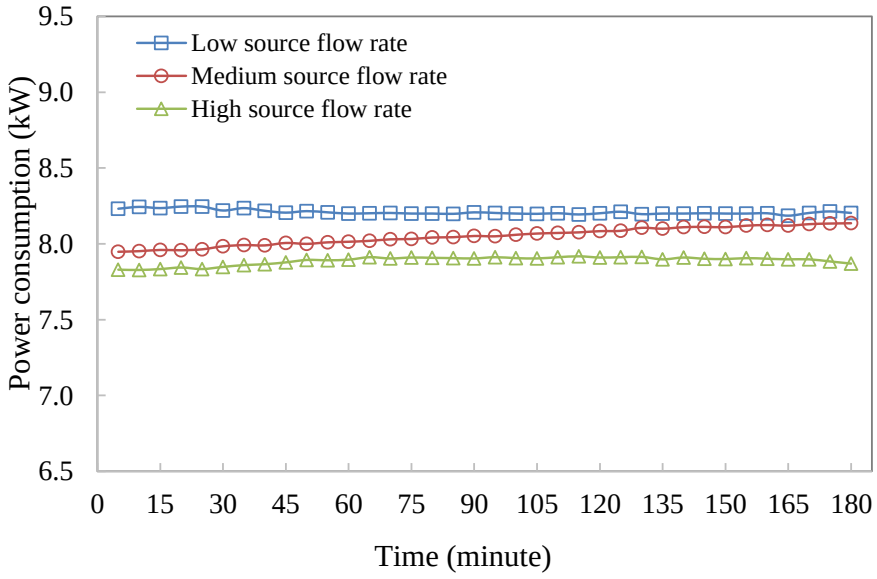

Fig. 3.13 Power consumption of the two water-to-water heat pumps with different source flow rates - series operation.

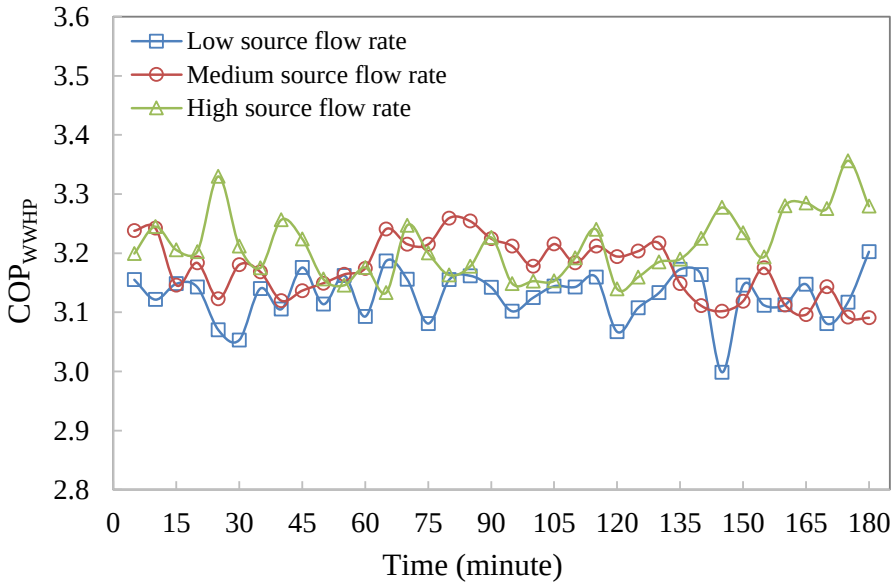

Fig. 3.14 COP of the two water-to-water heat pumps with difference source flow rates - series operation.

A comparison between the GSHP system with the GHEs in parallel and in series operation in terms of the average COP of water-to-water heat pumps is shown in Table 3.6. It can be seen that, the average COP of the water-to-water heat pumps with the GHEs in parallel operation were 17.0%, 18.6% and 22.0% higher than those of the GSHP system with the GHEs in series operation for the low, medium and high source flow rates, respectively. These results demonstrated that parallel operation of GHEs provides a better performance of the water-to-water heat pumps than that of GHEs in series.

Table 3.6 COP of the water-to-water heat pumps in parallel and series operation of the GHEs

Source water flow rate	Average COP_{WWHP}		
	Series	Parallel	Difference (%)
Low	3.13	3.66	17.0
Medium	3.17	3.76	18.6
High	3.21	3.92	22.0

3.4 Summary

This chapter describes the design, installation and evaluation of a ground source-air source combined heat pump system implemented in a net-zero office building at the University of Wollongong, Australia.

A monitoring system was set-up to examine the performance of the GSHP system with series and parallel operation of the ground heat exchangers, as well as the influence of different water flow rates circulating through the GHEs on the performance of the water-to-water heat pumps and water pumps. The experimental analysis showed that, for the GSHP system studied here, the GHEs in a parallel configuration offered a better performance for the water-to-water heat pumps than that in series. The results also showed that, for both series and parallel operation of the GHEs, a larger water flow rate in the GHEs can help reduce the power consumption of the water-to-water heat pumps. However, the power consumption of the water pumps in the ground loop will increase because of the increased water flow rate. Due to the limitations of equipment available, the power consumption of the water pumps was not measured directly during the experimental tests. However, results for the estimation of the effect of water flow rate in the GHEs on the energy consumption of the water pumps in the source side the GSHP system demonstrated that optimisation of the water flow rate in GHEs is essential to improving the overall energy performance of the GSHP system.

Chapter 4

Dynamic Characterisation and Performance Evaluation of Ground Source Heat Pump Systems

This chapter presents the dynamic characterisation and performance evaluation of ground source heat pump systems. This study is performed in order to understand the effects of the variation of system variables and working conditions on the energy performance of GSHP systems, as well as to evaluate the energy performance of a ground source-air source combined heat pump system. A thorough understanding of the dynamic characteristics and energy performance of GSHP systems is useful for development of design and control optimisation strategies for GSHP systems.

This chapter is organised as follows. Section 4.1 presents a brief introduction of the research background on performance evaluation and analysis of GSHP systems. The development of the simulation platform for the ground source-air source combined heat pump system implemented in the UOW Sustainable Buildings Research Centre is described in Section 4.2, which serves as the test platform for investigation of the dynamics and performance of GSHP systems. Section 4.3 presents the simulation results and discussions. Key findings are summarised in Section 4.4.

4.1 Introduction

GSHP systems have been used for many years worldwide to replace or supplement to the traditional air conditioning systems due to their higher energy efficiency (Yuan *et al*. 2012, Chung *et al*. 2012.). Over the last two or more decades, significant efforts have been made on the development of GSHP systems in building applications. Many studies have also been conducted to develop effective approaches for decreasing the initial cost of GSHPs and increasing their operational performance (Zhai *et al*. 2011). All the studies reviewed in Chapter 2 demonstrated that GSHP systems have high energy efficiencies and reliabilities when compared with conventional air conditioning systems.

In this chapter, the ground source-air source combined heat pump system introduced in Chapter 3 is used as a reference system to analyse the dynamic characteristics and energy performance of GSHP systems. A parametric study is first performed for both vertical and horizontal ground heat exchangers (GHEs) to analyse the effects of different variables on the system performance. In order to evaluate the energy performance of the ground source-air source combined heat pump system, an air source heat pump (ASHP) system and a GSHP system with vertical ground heat exchangers are also simulated.

4.2 Development of the simulation system

This section describes the processes undertaken in the simulation of the ground source-air source combined heat pump system. The main purpose of the simulation is twofold: i) to understand the effects of the key parameters on the performance of the GSHP systems, and ii) to examine the energy performance of ground source-air source combined heat pump systems, in comparison to standalone ground source heat pump systems and air source heat pump systems.

The Sustainable Buildings Research Centre (SBRC) building is used as the reference building and the ground source-air source combined heat pump system implemented in this building is used as the reference system. The detailed information of the building and system can be found in Section 3.1, Chapter 3. The heating and cooling loads of the building were simulated using DesignBuilder (Tindale 2004). The simulation of the ground source-air source combined heat pump system was performed based on TRNSYS simulation platform (Klein 2010) by using major component models available in TRNSYS library.

4.2.1 Building load simulation and analysis

DesignBuilder simulation program is used to simulate building heating and cooling loads. The building heating and cooling loads were only simulated for the southern “office” wing of the building, as the second wing is a naturally ventilated high-bay facility. Fig. 4.1 shows the simplified building model constructed in DesignBuilder.

The weather data used was the Representative Meteorological Years (RMY) data of Sydney (Tindale 2004). The necessary inputs in the DesignBuilder simulation included the detailed description of envelope, floors and ceiling of the building, design occupancy, lighting power and power, and the operation schedules, the indoor temperature and relative humidity set-points etc. As the building studied is an office building, in the simulation it was only occupied from 8.00am-18.00pm during the working days and the air conditioning system was not in operation during the weekends and public holidays. Natural ventilation was applied when ambient weather conditions can ensure good thermal comfort in buildings with the natural ventilation set-point temperature of 2°C lower than the cooling set-point and of 2°C higher than the heating temperature set-point. The building was simulated for one year (8760 hours).

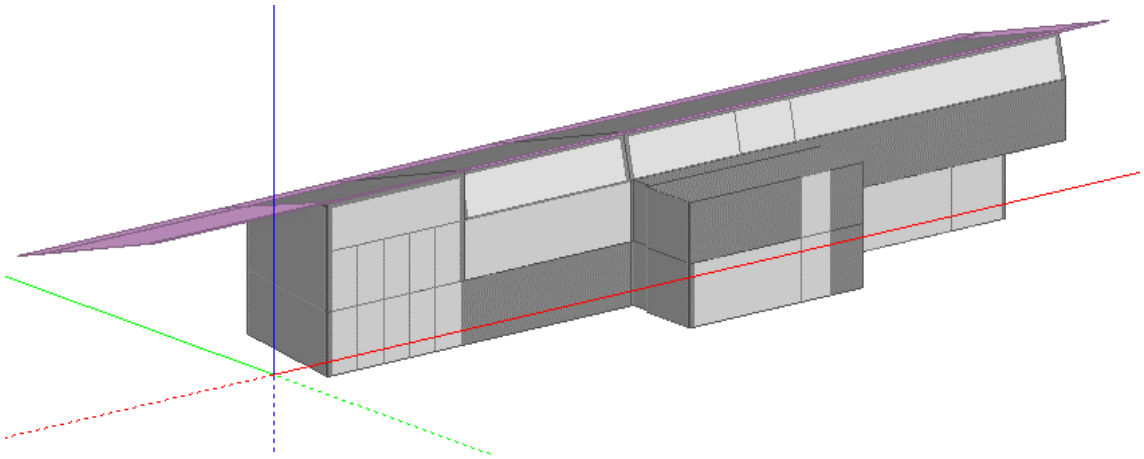

Fig. 4.1 Simplified building model developed in DesignBuilder.

Fig. 4.2 illustrates the simulated hourly-based cooling loads (positive values in the figure) and heating loads (negative values in the figure) of the building as well as the ambient air conditions. It can be found that the peak cooling load and peak heating load of the building are 120 kW and 81 kW, respectively. It is shown that the cooling demand in this office building is much higher than the heating demand, which indicates that the operation of the GSHP system may result in load imbalance within the vertical ground heat exchangers if the system is not well-designed and controlled. It is also shown that there is a relatively large variation of the building heating and cooling loads in different months over the course of the year. Such large variations may provide great opportunities for achieving energy

savings through using advanced control and operation strategies.

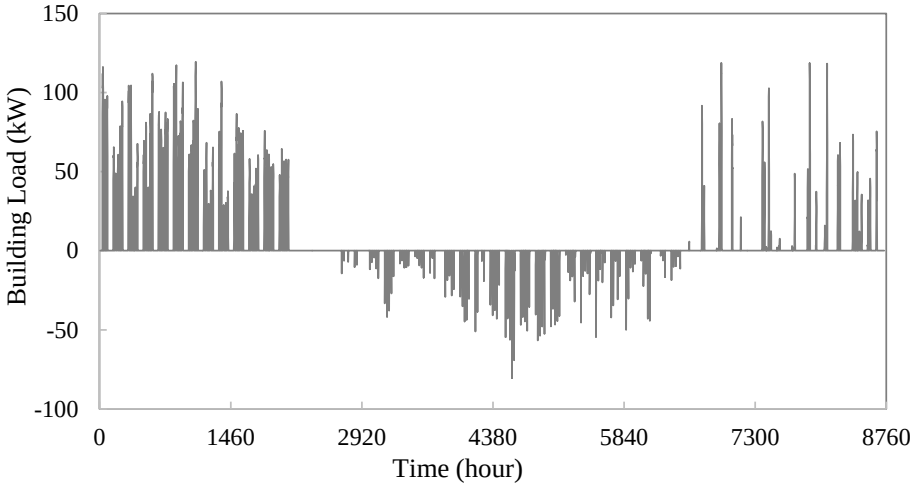

a) Heating and cooling loads

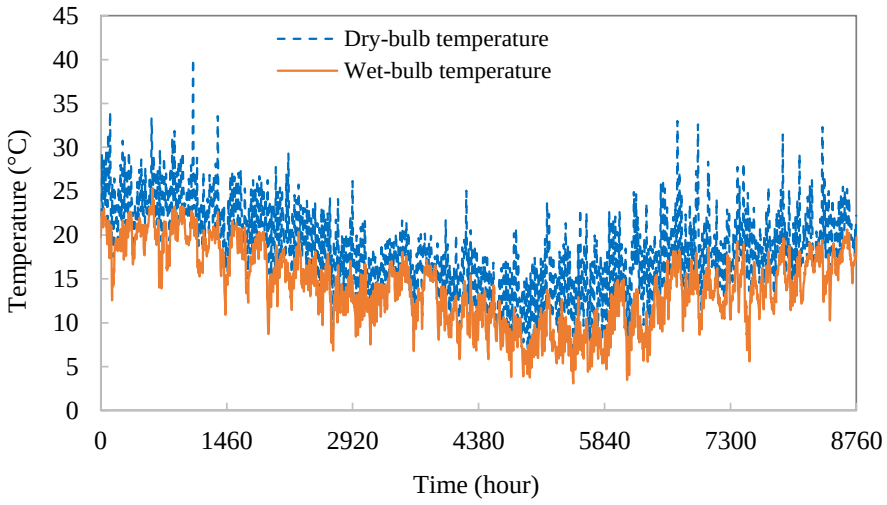

b) Weather condition

Fig. 4.2 Weather profiles and simulated hourly-based building loads.

4.2.2 Modelling and simulation of ground source-air source combined heat pump system

The ground source-air source combined heat pump system was simulated using the platform of Transient Systems Simulation Program, TRNSYS. TRNSYS is a comprehensive and extendable modelling environment for transient simulation of various

energy conversion systems. Its development was originally initiated by the Solar Energy Laboratory in 1974 in University of Wisconsin, USA, and was then continuously improved by users and programmers all over the world. It is widely used by engineers and researchers to validate new energy concepts. In the TRNSYS Simulation Studio, the user can specify the components of the system and the way in which they are connected.

Fig. 4.3 shows the schematic of the simulation system developed for the ground source-air source combined heat pump system of the SBRC building. The simulation system mainly consists of three parts, including a) a simplified building load distribution system, b) a ground source heat pump system and c) an air source heat pump system.

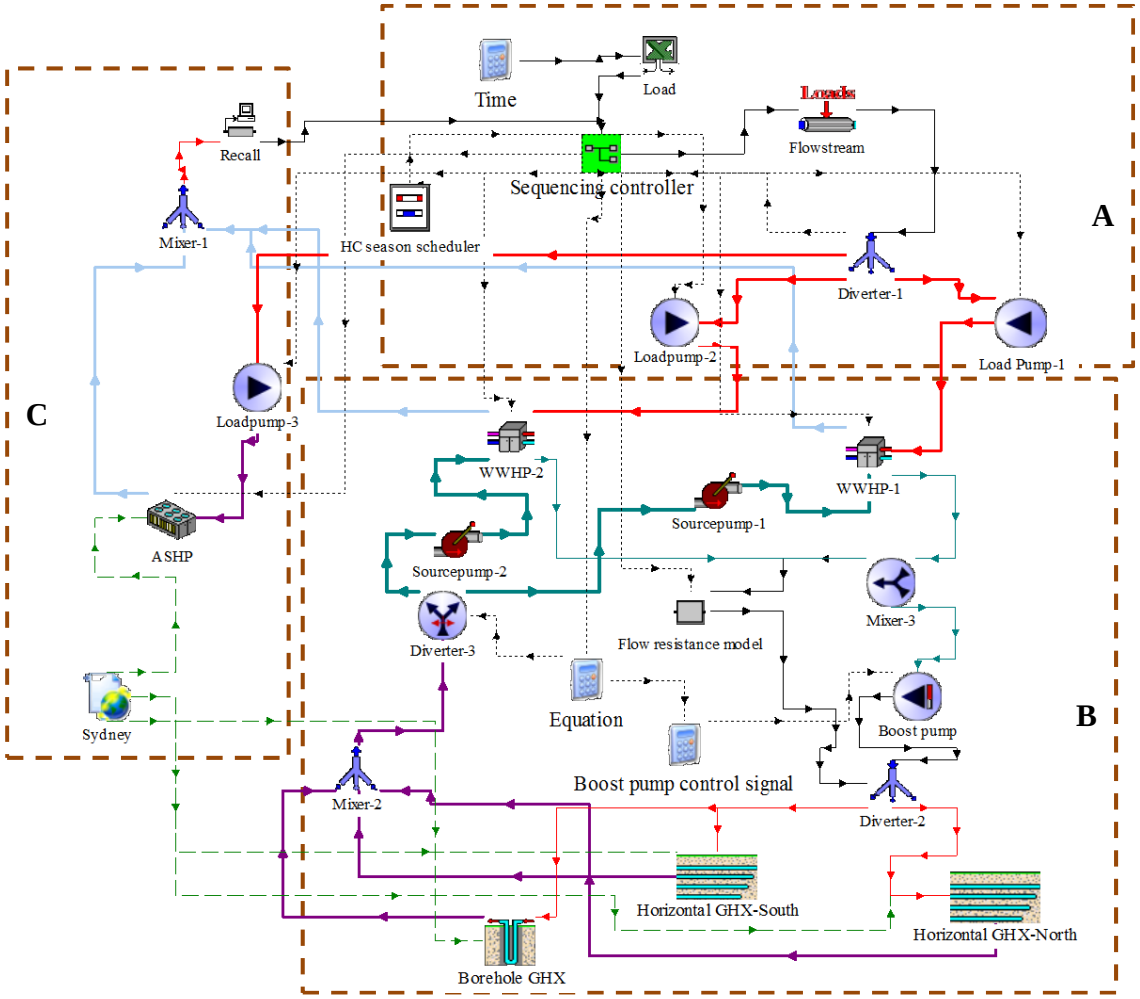

Fig. 4.3 Illustration of TRNSYS simulation system.

In order to simplify the simulation process, three following major assumptions were used in the simulation system.

1) The far-field soil temperature is constant at 20.0°C;
2) The borehole field is characterised as a single soil layer; and
3) Underground water movement is not considered.

The theoretical models of the major components used in the simulation system are described below.

- *Water-to-water heat pump*

Type 927 which is based on the user-supplied data files containing the heat pump catalogue data, was used to simulate the water-to-water heat pump. The catalogue data contains the power and capacity of the water-to-water heat pumps varying with the water flow rate, entering water temperatures of the evaporator and condenser. During the simulation, the cooling or heating capacity and power consumption can then be obtained from the two external files. It is worthwhile to note that, in order to better represent the part-load performance of the heat pumps, modifications have been made on the water-to-water heat pump model by adding external files containing the part-load performance data provided by the manufacturer. The model performs linear interpolation according to the entering source side and load side flow rates and temperatures. The COP and outlet conditions of the heat pump in the heating mode can be calculated by:

$$COP_{WWHP} = \frac{Q_{heating}}{W_{WWHP}} \tag{4.1}$$

$$Q_{absorbed} = Q_{heating} - W_{WWHP} \tag{4.2}$$

$$T_{load,out} = T_{load,in} + \frac{Q_{heating}}{m_{load} c_{p,load}} \tag{4.3}$$

$$T_{source,out} = T_{source,in} - \frac{Q_{absorbed}}{m_{source} c_{p,source}} \tag{4.4}$$

The COP and outlet conditions of the heat pump in the cooling mode can be calculated by:

$$COP_{WWHP} = \frac{Q_{cooling}}{W_{WWHP}} \tag{4.5}$$

$$Q_{rejected} = Q_{cooling} + W_{WWHP} \tag{4.6}$$

$$T_{load,out} = T_{load,in} - \frac{Q_{cooling}}{m_{load} c_{p,load}} \tag{4.7}$$

$$T_{source,out} = T_{source,in} + \frac{Q_{rejected}}{m_{source} c_{p,source}} \tag{4.8}$$

where $Q_{heating}$ and $Q_{cooling}$ are the heating and cooling load respectively, $Q_{absorbed}$ and $Q_{rejected}$ are the energy absorbed and rejected by the heat pump, $T_{source,in}$ and $T_{source,out}$ are the water temperature at the inlet and outlet of the source side of the heat pump, respectively, , $T_{load,in}$ $T_{load,out}$ are the water temperature at the inlet and outlet of the load side of the heat pump, respectively, W_{WWHP} is the heat pump power consumption, m_{source} and m_{load} are the source side and load side water mass flow rates, $c_{p,load}$ is the specific heat of the load fluid, and $c_{p,source}$ is the specific heat of the source fluid.

The performance of this water-to-water heat pump model was validated using the experimental data gathered from the GSHP system implemented in the SBRC building. Fig. 4.4 and Fig. 4.5 illustrate the comparisons between the experimental measurements and model predictions in terms of the power consumption and the COP of the water-to-water heat pump in the cooling mode operation. It can be seen that the model can provide acceptable estimates with a prediction accuracy of ±5%.

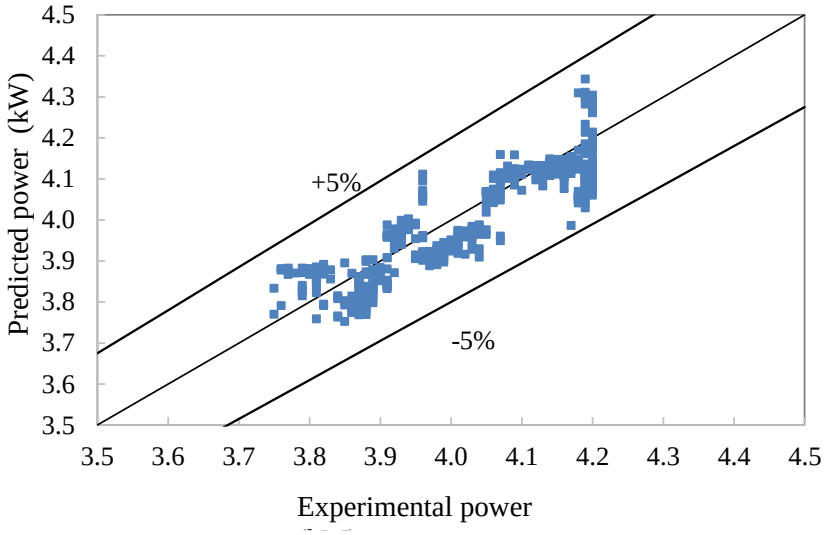

Fig. 4.4 Measured and predicted power consumptions of the water-to-water heat pump - cooling mode.

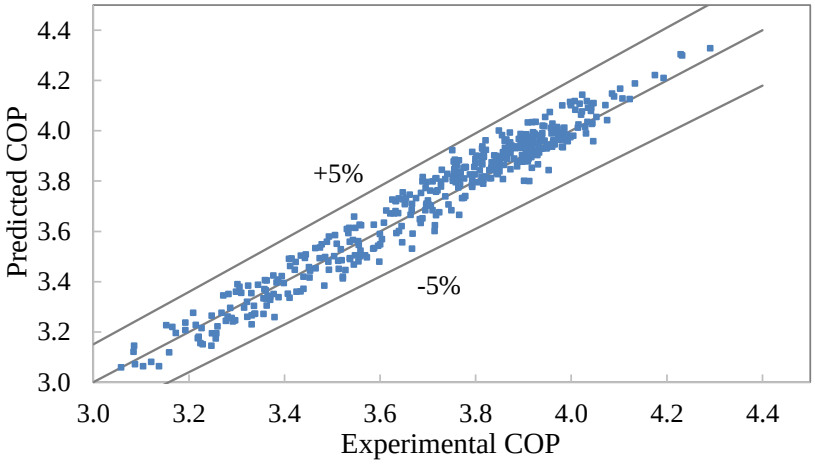

Fig. 4.5 Measured and predicted COP of the water-to-water heat pump - cooling mode.

- *Ground heat exchangers*

The TRNSYS mode Type 557 is commonly used to simulate the vertical ground heat exchanger of GSHP systems. This model assumes that the boreholes are placed uniformly within a cylindrical storage ground volume (V_b), which is expressed in the following equation:

$$V_b = \pi N_b H (0.525B)^2 \quad (4.9)$$

where N_b is the number of boreholes, H is the borehole depth, and B is the borehole space.

The model considers both the convective heat transfer between the heat transfer fluid flow and the pipe, and the conductive heat transfer between the pipe and the storage volume. The average temperature of the ground is calculated based on the following considerations:

1) a global temperature: which takes into account the large scale heat flow from the storage volume to the surrounding ground and is computed numerically;
2) a local radial solution: which covers the short-time variations and is computed numerically as well;
3) a steady-flux part: which redistributes the heat within a sub-region of the storage volume and is used for pulses varying slowly in time.

For the horizontal loop heat exchanger model, TRNSYS model Type 997 is used. This component model simulates the heat transfer process between the ground and a series of pipes which are buried in the ground. The configurations of these pipes can be various, i.e. in parallel, series, and serpentine etc. The model also takes into account the insulation on the soil surface and also down the edges of the pipe system. The model assumes that the pipes are buried within a 3D rectangular conduction model of the ground which considers the pipe to pipe interactions and energy storage within ground. The data obtained from the experimental tests were also used to validate the accuracy of the models. Here, the vertical and horizontal heat exchangers were validated by comparing the predicted and measured mixture outlet water temperatures from the whole ground loop. It is worthwhile to mention that the separate outlet water temperature from the vertical GHEs and horizontal GHEs was not measured, thus the validation is only performed for the whole ground loop field. Fig. 4.6 presents the comparisons between the measured and predicted outlet water temperatures from the whole ground loop. The results from the model prediction agreed well with the measurements. The errors between the predicted and measured temperatures were within the range of ±10%.

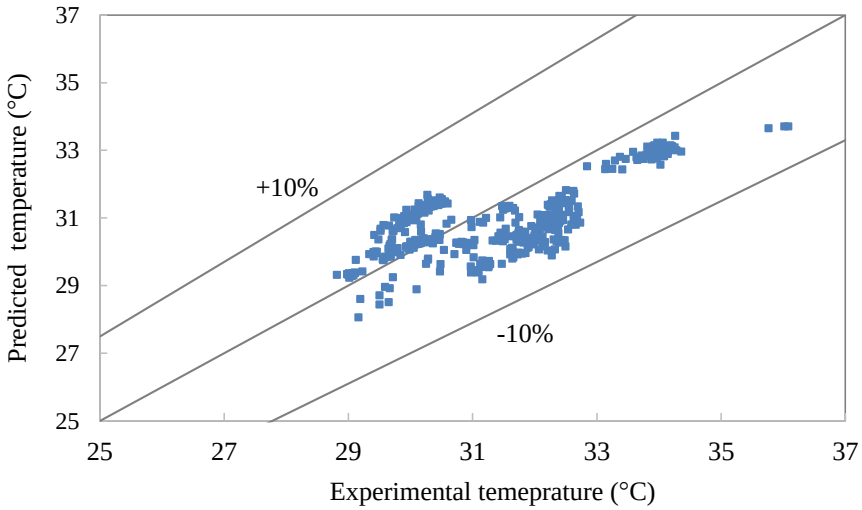

Fig. 4.6 Measured and predicted outlet water temperatures from the whole ground loop.

- *Air-to-water heat pump*

The air-to-water heat pump runs on the vapour compression cycle principle. In the heating mode the heat pump is extracting the energy from the air stream, while rejecting the heat to the air stream in the cooling mode. The efficiency of the air-to-water heat pump is a dynamic value and often called as the Coefficient of Performance (COP). The COP of the air-to-water heat pump depends on the outdoor temperature, and the inlet and outlet water temperatures. The TRNSYS component model Type 917 is used to simulate the air-to-water heat pump. Like Type 927, Type 917 is also based on the user-supplied performance data, which contains heat pump heating and cooling capacities and corresponding power consumptions. Modifications have also been made on the air-to-water heat pump model by adding the external files containing the part-load performance data provided by the manufacturers.

- *Flow resistance model*

A flow resistance model was developed and used to determine the water flow rate in each individual heat exchanger in the ground loop. In the simulation, the fluid diverters and mixers were used to allocate and mix the water flow rates into and from each ground heat exchanger loop. The model computes the total pressure drop across the individual heat exchanger and its fittings under the given water flow rate. The pressure drop along the

individual heat exchanger loop was calculated by using Eq. (4.10). The flow resistance includes the resistances of the heat exchanger, and all fittings and water pipe along the heat exchanger loop and is determined by Eq. (4.11).

$$\Delta H_p = S_{flow} \cdot V_f^2 \tag{4.10}$$

$$S_{flow} = \frac{8(f\frac{l}{d} + \sum \xi)}{\pi^2 d^4 g} \tag{4.11}$$

where, ΔH_p is the pressure drop, S_{flow} is the flow resistance, m_{flow} is the water mass flow rate, l is the length of the pipe, d is the pipe diameter, g is the gravitational acceleration, ξ is the local resistance coefficient, f is the friction coefficient and V_f is the volumetric flow rate.

Besides the above component models, other components, i.e. diverters and pumps, were also modelled using TRNSYS standard library components and are listed in Table 4.1.

Table 4.1 Summary of major component models used

Type	Description
Type 997	Multi-level horizontal ground heat exchanger
Type 557	Vertical U tube heat exchanger - DST model
Type 515	Heating and cooling season scheduler
Type 647	Flow diverter
Type 649	Flow mixer
Types 110/743	Water pumps
Type 917	Modified air source heat pump
Type 927	Modified water to water heat pump
Type 2300	Flow resistance model

4.3 Simulation results and discussion

4.3.1 Effects of design parameters on the performance of GSHPs

The performance of a GSHP system is dependent on a range of design parameters such as the depth and diameter of vertical ground heat exchangers, and operating parameters such as temperature settings and operation schedules. Based on the simulation system described above, a parametric study was performed to investigate the influence of different design parameters on the overall system performance of GSHPs in order to facilitate good system design and control. The tests were carried out based on the selected typical working conditions. As the heating condition has similar results (i.e. trends) as that of the cooling condition, only the results from the cooling case are presented below. Table 4.2 summarises the selected working conditions in the cooling mode operation. In the parametric study, the two water-to-water heat pumps and the air-to-water heat pump were all operating to meet the selected building load condition.

Table 4.2 Selected test conditions for the cooling mode operation

Dry-bulb temperature	Wet-bulb temperature	Building load	Load Ratio
°C	°C	kW	%
31	21	116	85

4.3.1.1 Test results for vertical ground heat exchangers

- *Effects of the borehole depth*

Fig. 4.7 shows the variations of the water temperatures at the inlet and outlet of the vertical GHEs, the GSHP COP, the heat transfer rate per meter of borehole depth and the total heat transfer rate in the vertical ground heat exchangers with the change of the borehole depth. It can be found that the total heat transfer rate of the vertical GHEs increased while the outlet water temperature from the vertical GHEs decreased with the increase of the borehole depth. This is because a deeper borehole provides a longer path for the heat transfer

between the borehole and its surrounding soil. The lower outlet water temperature from the vertical GHEs results in a lower inlet water temperature to the water-to-water heat pumps and a higher COP of the GSHP in the cooling mode operation. It is also shown that the inlet water temperature to the vertical ground heat exchangers decreased while the temperature difference between the inlet and outlet water temperatures of the vertical ground heat exchangers increased. The heat transfer rate per meter of borehole depth decreased with the increase of the borehole depth. However, the performance benefits will be counteracted when the borehole depth exceeds a certain value due to the high drilling cost.

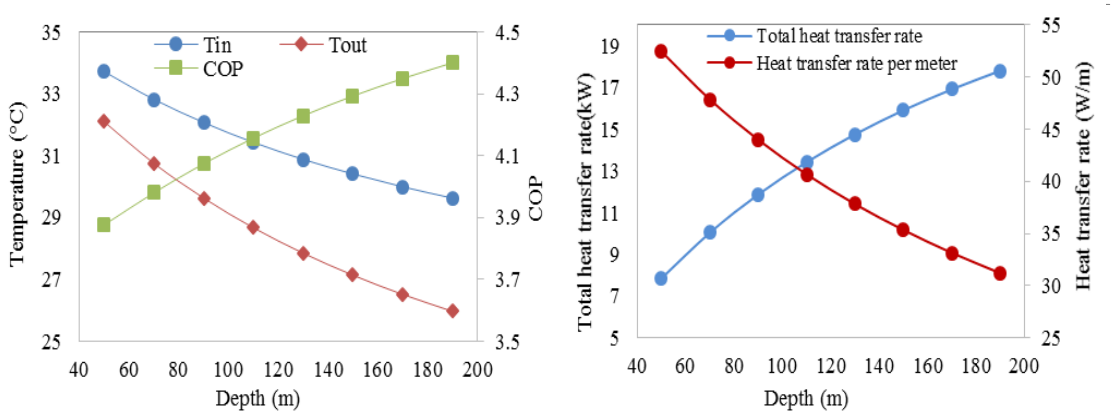

Fig. 4.7 Effects of the borehole depth - vertical heat exchangers.

- *Effects of the grout material*

The grout material also influences the performance of the vertical GHEs and the results are presented in Fig. 4.8. Increasing the thermal conductivity of the grout materials allows greater heat fluxes along the borehole wall, resulting in a slightly increased COP of the heat pumps. However, the COP of the heat pumps remains almost constant when the thermal conductivity of the grout material is larger than 1.47 W/m·K in this case studied. The total heat transfer rate and the heat transfer rate per meter of borehole depth increased with the increase of the thermal conductivity of the grout materials.

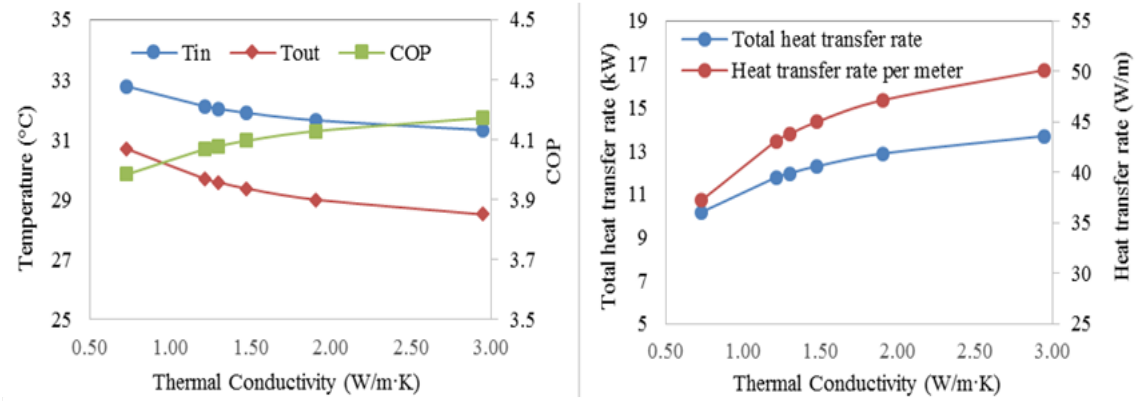

Fig. 4.8 Effects of the grout material - vertical heat exchangers.

- *Effects of the pipe diameter and shank space*

The thermal interference between the inlet and outlet pipes within the borehole is an important factor to be considered when designing the heat exchangers for GSHP applications. As shown in Fig. 4.9, the COP of the GSHPs, the total heat transfer rate of the vertical ground heat exchangers and the heat transfer rate per meter of the borehole depth increased with the increase of the pipe diameters and shank space. The larger pipe diameter provides a larger heat exchange surface between the fluid and pipe, leading to an increased performance of the GSHPs due to the lower inlet water temperature to the heat pumps. The larger shank space results in less interaction between the adjacent pipes, and thus the better performance of the GSHPs. However, the shank space has limited impacts on the system performance as the variation of the COP of the GSHPs is small when increasing the shank space.

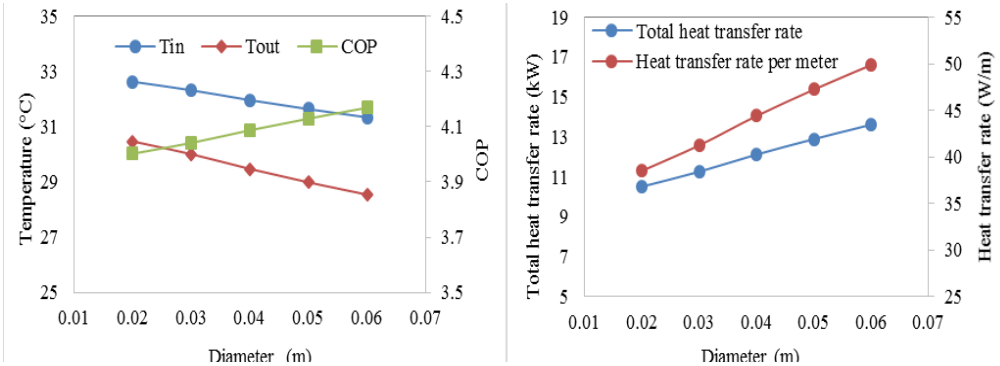

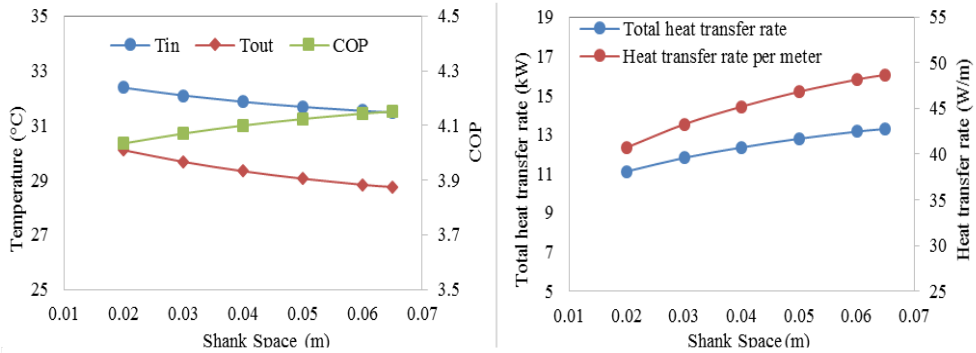

Fig. 4.9 Effects of the pipe diameter and shank space - vertical heat exchangers.

4.3.1.2 Test results for horizontal ground heat exchangers

Similar simulations have also been performed for the horizontal ground heat exchangers to analyse the effects of the pipe length, pipe diameter, separation space, and soil thermal conductivity on the heat transfer performance of the horizontal ground heat exchangers and water-to-water heat pumps.

- *Effects of the pipe length*

Fig. 4.10 shows the effects of the pipe length on the inlet and outlet water temperatures of the horizontal ground heat exchangers, the COP of the GSHP system, the heat transfer rate per meter of pipe length and the total heat transfer rate in the horizontal ground heat exchangers. The effect of the pipe length has similar trends as that of the vertical heat exchangers. The total heat transfer rate increased with the increase of the pipe length. This is mainly because a longer pipe provides a longer path for the heat transfer between the pipe and the surrounding soil. It is also shown that, when the pipe length increased, the inlet and outlet water temperatures from the horizontal ground heat exchangers decreased while the temperature difference between the inlet and outlet water temperatures of the horizontal ground heat exchangers increased. The lower outlet water temperature from the horizontal ground heat exchangers results in a lower inlet water temperature to the water-to-water heat pump which leads to a higher COP of the heat pump in the cooling operation. The heat transfer rate per meter of the pipe length decreased with the increase of the pipe length, which indicated that there is an optimal pipe length for horizontal ground heat exchangers

and its total length should be optimised in the design process.

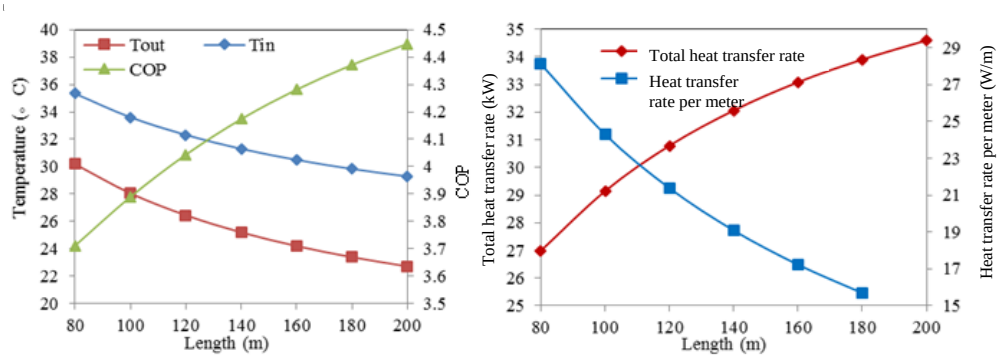

Fig. 4.10 Effects of pipe length - horizontal heat exchangers.

- *Effects of the pipe diameter - horizontal ground heat exchangers*

The effects of the pipe diameters on the performance of the horizontal ground heat exchangers and water-to-water heat pumps are presented in Fig. 4.11. It can be seen that the COP of the GSHP system, the total heat transfer rate of the horizontal ground heat exchangers and the heat transfer rate per meter increased with the increase of the pipe diameters. The larger pipe diameter provides a larger heat exchange surface between the circulating fluid and horizontal ground heat exchangers, leading to an increased performance of the GSHPs due to the lower inlet water temperature to the water-to-water heat pumps.

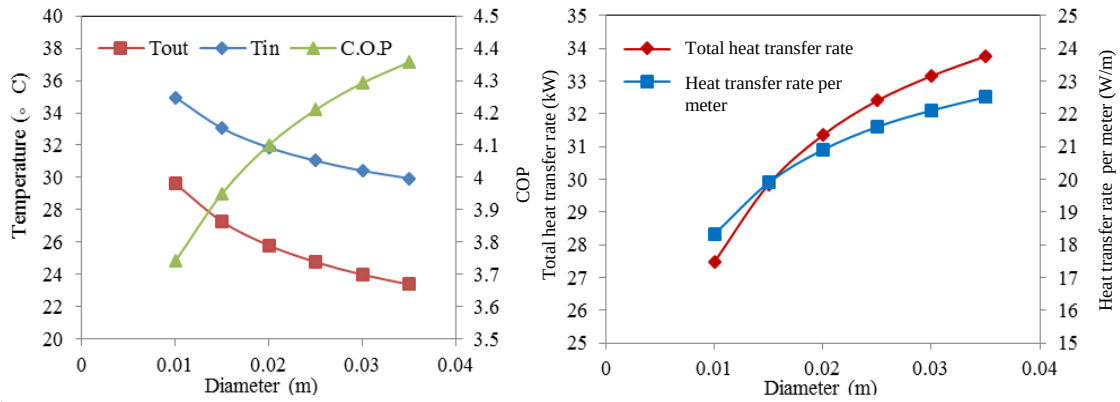

Fig. 4.11 Effects of the pipe diameter - horizontal heat exchangers.

- *Effects of the pipe separation distance*

The separation distance refers to the centreline to centreline distance between the two parallel pipes. A large separation distance requires a large trench area. The effects of the pipe separation distance on the performance of the horizontal ground heat exchangers and water-to-water heat pumps are shown in Fig. 4.12. It can be observed that the COP of the GSHPs first increased when the separation distance increased from 0.2 m to 0.6 m and then remained relatively constant if the separation distance was further increased. The optimal separation distance in this case is around 0.6 m. Similar trends can also be observed for the total heat transfer rate and heat transfer rate per meter of the pipe length.

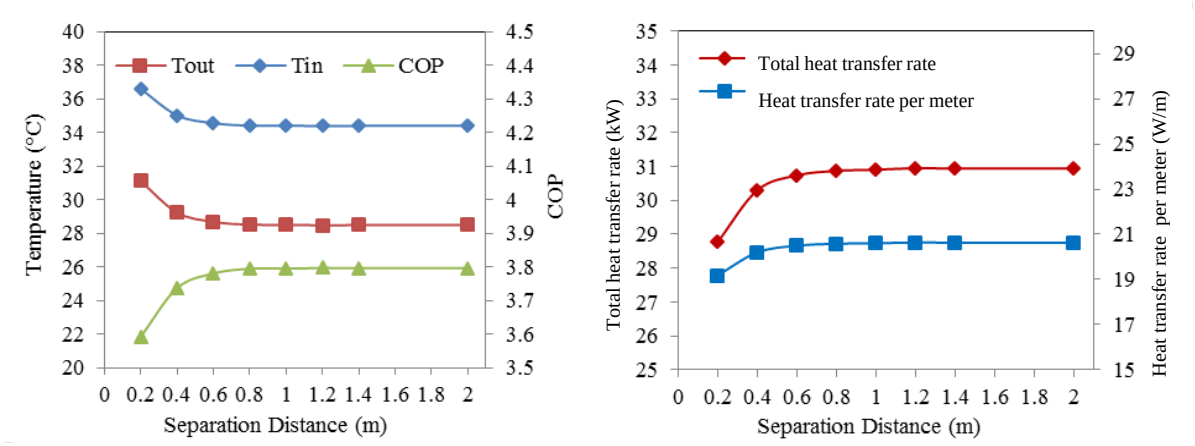

Fig. 4.12 Effects of the pipe separation distance - horizontal heat exchangers.

- *Effects of the soil thermal conductivity*

Fig. 4.13 shows the variations of the system performance when changing the soil thermal conductivity. Both the COP of the water-to-water heat pumps and the total heat transfer rate of the horizontal ground heat exchangers increased with the increase of the thermal conductivity, due to the decreased outlet water temperature from the horizontal ground heat exchangers in the cooling operation. This is because the higher soil thermal conductivity results in better heat transfer characteristics of the ground, and thus increased capability of the ground heat exchangers to reject the heat into the soil.

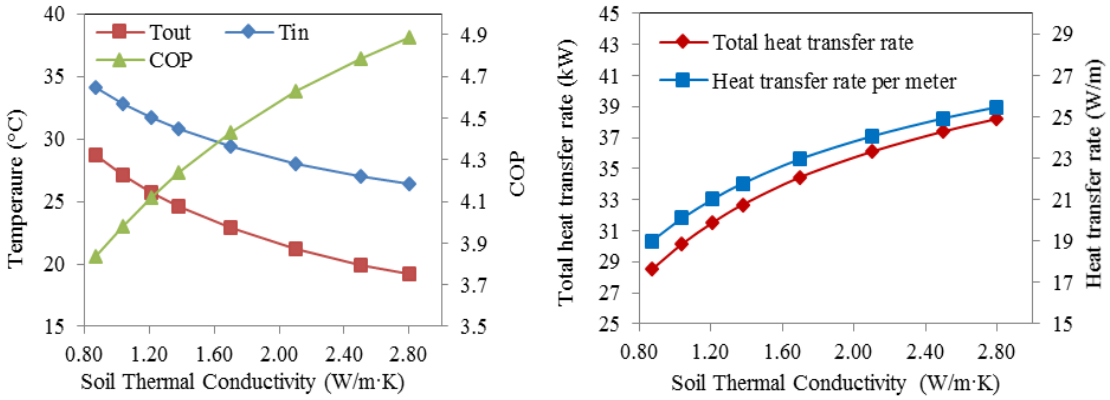

Fig. 4.13 Effects of the soil thermal conductivity - horizontal heat exchangers.

The above results showed that the design variables have significant impacts on the overall performance of the GSHPs. It is therefore essential to optimise these variables systematically when designing a GSHP system in order to ensure good operational performance and achieve long-term benefits.

4.3.2 Performance evaluation of different HVAC systems

The aim of the section is to evaluate the energy performance of the ground source-air source combined heat pump system by comparing with that of the other two systems. The other two systems considered are an ASHP system and a GSHP system with vertical ground heat exchangers. The performance simulation of the three systems was performed based on the TRNSYS simulation platform.

4.3.2.1 Description of the three HVAC systems

Ground source-air source combined heat pump system

The ground source-air source combined heat pump system studied is the system implemented in the SBRC building presented in Chapter 3. In this combined system, the GSHP system is first used to provide the heating and cooling demand of the building. The air-to-water heat pump will be switched on if the GSHP system cannot provide sufficient building heating and cooling demands.

Air source heat pump system

Air source heat pump (ASHP) configuration is composed by an air-to-water heat pump, an internal water pump and an air fan. Thermal energy is generated and supplied by the air-to-water heat pump when it is demanded by the building. The selection of the air-to-water heat pump was based on peak cooling demand of SBRC building. The heat pump capacities were then scaled proportionally based on the capacities of the air-to-water heat pump implemented in the Sustainable Buildings Research Centre (SBRC), University of Wollongong, which was descried in Table 3.1, Chapter 3.

Ground source heat pump system

The ground source heat pump system consists of two identical water-to-water heat pumps, vertical ground heat exchangers. The water-to-water heat pumps were also selected based on the peak cooling load and were sized based on the capacities of the water-to-water heat pump described in Table 3.1, Chapter 3.

Table 4.3 Specifications of the three HVAC systems

Equipment	Specification	ASHP	GSHP	GSASHP*
Water to water heat pumps	Rated cooling capacity/power (kW/kW)	-	65.6/16.4	16.4/4.1
	Rated heating capacity/power (kW/kW)	-	81.6/22	20.4/5.5
Air to water heat pump	Rated cooling capacity/power (kW/kW)	130.2/43.3	-	109.4/36.4
	Rated heating capacity/power (kW/kW)	159.1/45.0	-	133.9/37.9
Vertical ground heat exchangers	Number of boreholes	-	23	3
	Diameter of borehole (mm)	-	150	150
	Borehole spacing (m)	-	8	8
	Depth of per borehole (m)	-	91	91
Horizontal ground heat exchangers	Loop pitch (m)	-	-	2
	Number of pipes	-	-	12
	Length of per pipe (m)	-	-	125
	Trench length (m)	-	-	17

* GSASHP means the ground source-air source combined heat pump configuration.

The major specifications of the above three HVAC systems are summarised in Table 4.3. The total length of the vertical GHEs in the GSHP system was sized using Equation (2.8) based on the building peak cooling load simulated in Section 4.2.1. The other geometric parameters of vertical GHEs such as the borehole diameter/spacing, depth per borehole and pipe diameter were the same as the GHEs implemented in in the ground source-air source combined heat pump system.

4.3.2.2 Energy performance analysis of the three systems

The total energy consumptions of the three HVAC systems during 20-years operation are presented in Table 4.4. The total power consumption includes the power consumption of the heat pumps and the power consumption of all water pumps. The overall system efficiency (COP_{sys}) defined in Section 2.2, Chapter 2 was used as the performance indictor for performance analysis.

Table 4.4 Total power consumption and COP_{sys} for three HVAC systems

HVAC systems	Cooling load covered (kWh)	Power consumption (kWh)			COP_{sys}
		Heat pumps	Water pumps	Total	
Air source heat pump	938,890	390,530	69,710	460,240	2.04
Ground source heat pump	928,302	225,623	100,097	325,720	2.85
Ground source-air source combined heat pump system	938,859	248,711	113,783	362,494	2.59

From Table 4.4, it can be seen that:

- The overall system coefficient of performance of the air source heat pump system, GSHP system and ground source-air source combined heat pump system were 2.04, 2.85 and 2.59, respectively. In general, the GSHP system and the ground source-air source combined heat pump system are more energy efficient than the air source heat pump system.

4.4 Summary

In this chapter, the effects of the key design parameters on the performance of both vertical ground heat exchangers and horizontal ground heat exchangers were investigated through a detailed simulation system developed by using TRNSYS. The analysis was based on the GSHP system implemented in the UOW Sustainable Buildings Research Centre. The building heating and cooling loads simulated using DesignBuilder were used as the inputs and served as the working conditions in the TRNSYS simulation. The simulation results based on the typical working conditions showed that the optimisation of the key design variables, such as pipe diameter, pipe length and shank space, is essential to achieve good operational performance of GSHPs.

The energy performance of a ground source-air source combined heat pump system was also evaluated by using TRNSYS. The overall system coefficient (COP_{sys}) of the combined system was compared with that of an air source heat pump system and a GSHP only system. The overall system coefficient of performance (COP_{sys}) of ground source-air source combined heat pump system was 21% higher than that of the air source heat pump system, while 11% lower than that of the GSHP only system. The comparison results showed that employing GSHP only system and ground source-air source combined heat pump system are more energy efficient. This study also demonstrated that detailed simulations allow more detailed energy analysis to assist in understanding the effects of the key parameters on the system performance which can further facilitate the good design and control of the GSHP related systems.

Chapter 5

Feasibility Analysis of Ground Source Heat Pump Systems for Major Australian Climate Zones

This chapter presents an economic and environmental feasibility study of ground source heat pump (GSHP) systems for major Australian climate zones. The overall aim of this chapter is to quantify the extent to which the local climate influences the economic and environmental feasibility of implementation of GSHP systems. This chapter is organised as follows. Section 5.1 presents a brief introduction of current research status on feasibility analysis of GSHP systems. Section 5.2 describes the methods used in this study for feasibility analysis. The results of economic and environmental feasibility analysis are presented in Section 5.3. A brief summary of the key findings is provided in Section 5.4.

5.1 Introduction

GSHPs, like many other energy conservation technologies, usually require high initial investment, which is claimed to be offset by energy savings. Building function and climate conditions are probably the two most important factors in determining whether significant energy savings can be achieved due to the use of GSHP systems (Urchueguía *et al*. 2008, Rice *et al.* 2013, Aste *et al.* 2013). Feasibility analysis is therefore important in determining whether it is cost-effective and appropriate to invest the GSHP technology for a specific project.

A number of studies on the feasibility analysis of GSHP systems have been reviewed in Section 2.3, Chapter 2. Feasibility evaluation is normally conducted by means of economic and environmental analysis (Morrone *et al*. 2014). In economic analysis, economic indicators are needed to assess the economic effect of using GSHP systems. In general, cost analysis and payback period are frequently used (Aste *et al.* 2013, Cabeza *et al.* 2014). In environmental analysis, environmental indicators are used to reflect the impact of GSHP systems on environmental sustainability. Greenhouse gas (GHG) emissions and energy

efficiency are often used (Lucich *et al*. 2014, Zhang *et al*. 2015). The reviewed studies indicated that there are many factors such as building types, climate conditions and investment costs influencing the feasibility of using GSHP systems. It is therefore necessary to carry out a feasibility study before considering the deployment of GSHP system as an alternative option to provide heating and cooling to buildings.

This chapter will examine the economic and environmental feasibility of GSHP systems for major Australian climate zones. Typical cities were first selected to represent the major Australian climate zones. The SBRC net-zero energy office building, presented in Chapter 3, was used as the reference building and the building heating and cooling loads of the reference building under different Australian climate zones were then simulated using DesignBuilder with representative meteorological year (RMY) weather data for the selected cities. TRNSYS was used to simulate the 20-year operational performance of the GSHP systems as well as the air source heat pump (ASHP) systems for each selected city. The performance of the ASHP system was used as the baseline for performance comparison. The economic evaluation was performed by means of net present value (NPV), while the environmental impact was determined based on the CO_2 emissions related to building operation.

5.2 Methodology for feasibility analysis

5.2.1 Description of the heating and cooling systems

In this study, the performance of both ground source heat pump system and conventional air source heat pump system was simulated. The GSHP system was assumed to be equipped with vertical ground heat exchangers (GHEs) only, while the ASHP system was equipped with an air-to-water heat pump which utilises the ambient air as the primary heat source and sink.

5.2.2 Climate zones

Australian Bureau of Meteorology (BOM) has gathered 30 years detailed climate information of Australia (1961-1990), and compiled the data into six Australian climate zones (Australian Climate Average - Climate Classifications 2012). The classification of the

climate zones is based on the temperature and humidity conditions presented in Fig. 5.1. In Australia, most population is located in the coastal regions (Australian Bureau of Statistics 2012), and the majority of these areas are in the climate zones of warm summer/cold winter, warm humid summer, mild/warm summer and cold winter, hot humid summer, and hot dry summer/cold winter. Thus, the feasibility analysis is focused on the above five major climate zones.

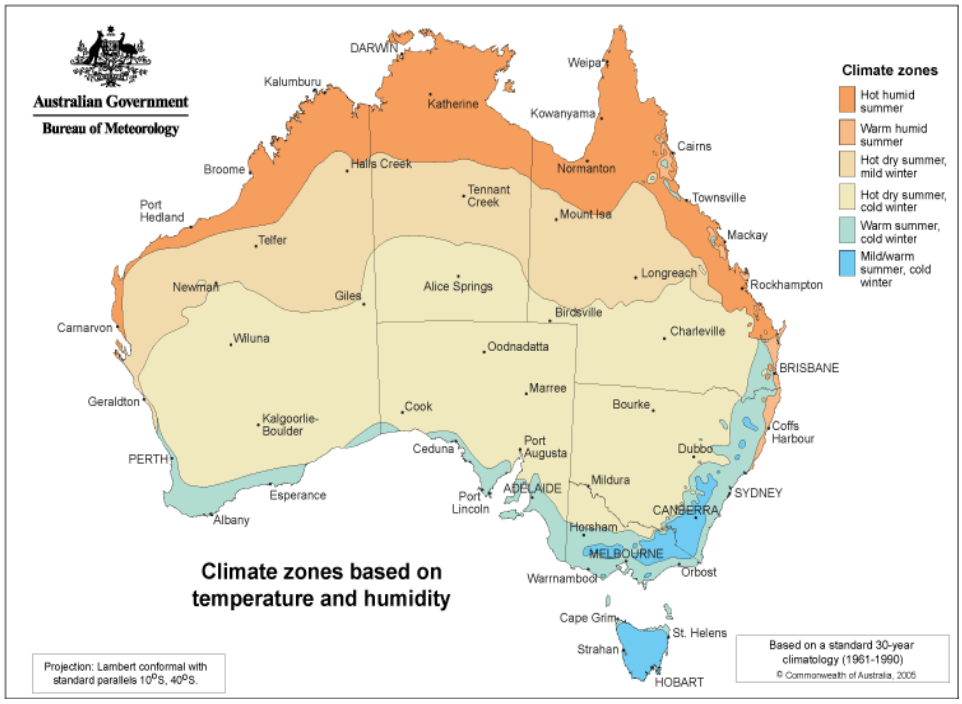

Fig. 5.1 Temperature and humidity climate zone classification (Australian Climate Average - Climate Classifications 2012).

In order to represent the above five climate zones in Australia, five typical cities were selected and are summarised in Table 5.1. Sydney was selected to represent warm summer and cold winter climate and Brisbane was chosen to represent warm humid summer climate. Hobart was selected to represent mild/warm summer and cold winter climate. Darwin and Alice Springs were selected to represent hot humid summer climate, and hot dry summer and cold winter climate, respectively.

Table 5.1 Selected typical Australian cities

State and territory	City	Climate zone
New South Wales (NSW)	Sydney	Warm summer, cold winter
Queensland (OLD)	Brisbane	Warm humid summer
Tasmania (TAS)	Hobart	Mild/warm summer, cold winter
Northern Territory (NT)	Darwin	Hot humid summer
Northern Territory (NT)	Alice Springs	Hot dry summer, cold winter climate

5.2.3 Reference building and building heating and cooling load simulation

The UOW Sustainable Buildings Research Centre (SBRC) building was considered as the reference building for heating and cooling load calculation under the different climatic conditions of the five cities selected. The detailed description of the SBRC building can be found in Section 3.1, Chapter 3. It is worthwhile to mention that the insulation of the reference building under different climate zones was kept constant although in reality it should be different for different climate conditions. The building heating and cooling demands were simulated using DesignBuilder based on the RMY weather data files (Tindale 2004). The simulated annual heating and cooling load profiles of the reference building under the climate conditions of the five cities are shown in Fig. 5.2.

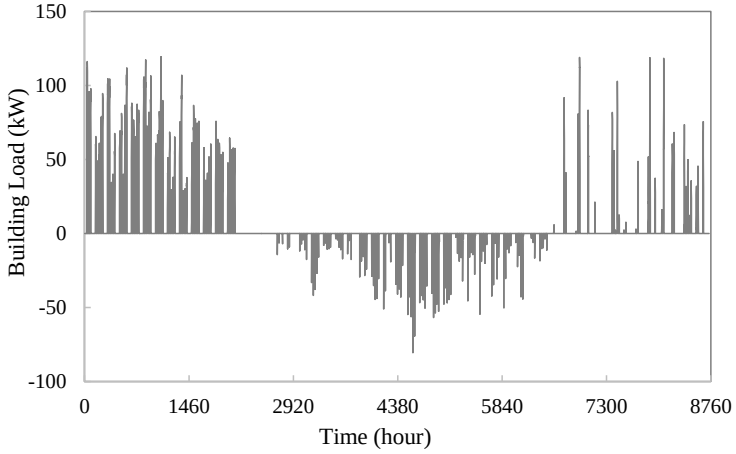

a) Sydney

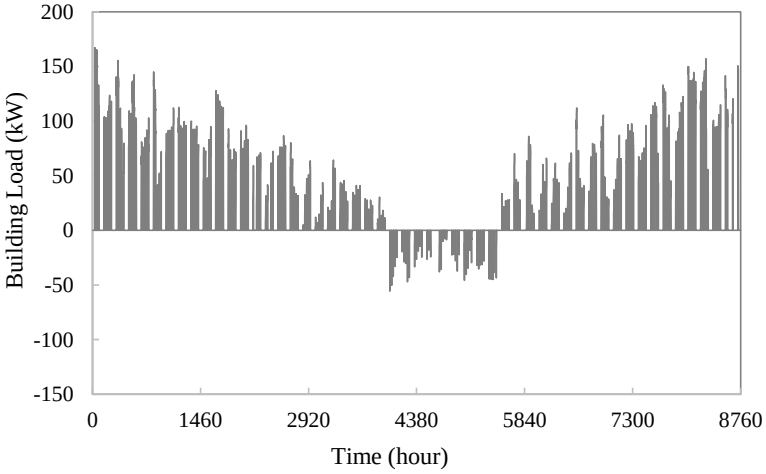

c) Alice Springs

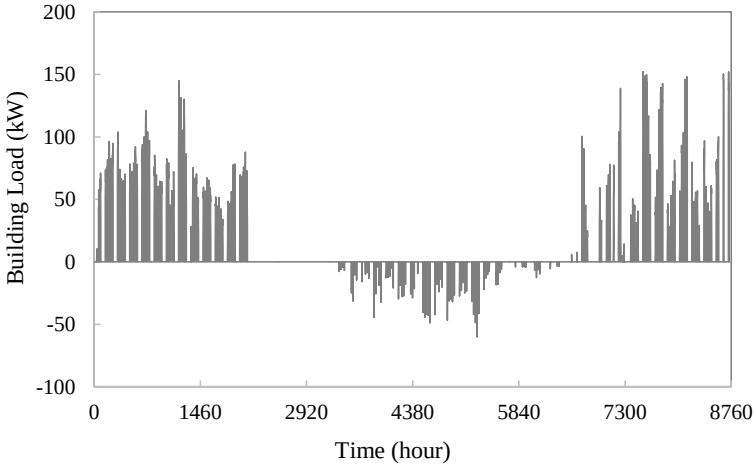

c) Brisbane

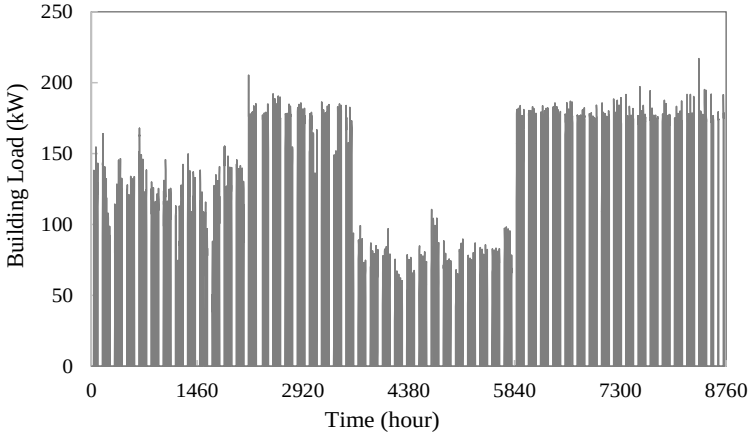

d) Darwin

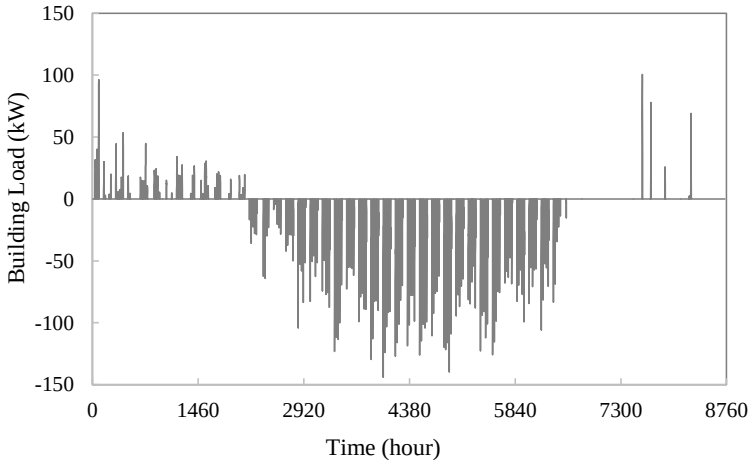

e) Hobart

Fig. 5.2 Load profiles of the reference building for the five selected cities.

It can be seen that the same building showed different load characteristics under the five different cities due to different climate conditions. In reality, the load characteristics will be different from the results presented in Fig. 5.2 as the design of the building needs to consider local climate conditions. The positive values in Fig. 5.2 represent the cooling demands, while the negative values represent the heating demands. It is shown that this reference office building in Sydney is cooling-dominated with the maximum cooling demand of 120 kW and maximum heating demand of 81 kW. The maximum cooling and heating demands of the reference building in Alice Springs were 167.2 kW and 55.3 kW respectively, while in Brisbane, both values were 152.1 kW and 60.2 kW, individually. The building load in Hobart represents the heating-dominated with the maximum heating demand of 143.9 kW and maximum cooling demand of 100.6 kW. The reference building in Darwin showed a totally different load profile as there is only cooling demand without any heating demand during the course of the year. The maximum cooling demand was 217 kW. It is worthwhile to note that the reference building studied is an office building, which was only occupied from 8.00am to 18:00pm in the simulation. The load characteristics for other types of buildings (i.e. residential buildings) in these selected cities might be totally different from those of the reference building presented.

For cooling only conditions such as in Darwin, GSHP systems are generally not recommended if there are no supplementary cooling devices such as fluid coolers or cooling towers used (ASHRAE 2011). In this study, feasibility analysis for Darwin is

therefore not performed. Table 5.2 summarises the annual accumulated heating and cooling demands and load imbalance ratios for the remaining four cities.

Table 5.2 Summary of the annual accumulated heating/cooling demands of the reference building under the four selected cities

Location	Accumulated annual cooling demand (kWh)	Accumulated annual heating demand (kWh)	Load imbalance ratio (χ)	Load characteristic
Sydney	42,701.7	3,723.7	0.913	Cooling-dominated
Alice Springs	104,604.7	2,103.0	0.980	Cooling-dominated
Brisbane	62,715.7	1,723.8	0.973	Cooling-dominated
Hobart	5,704.6	28,620.9	-0.801	Heating-dominated

where load imbalance ratio (χ) is defined as in Equation (5.1). The positive value of χ indicates that the accumulated cooling load is higher than the accumulated heating load, which often occurs in cooling-dominated buildings, and vice versa.

$$\chi = \frac{\sum Q_{cooling} - \sum Q_{heating}}{Max(\sum Q_{cooling}, \sum Q_{heating})} \tag{5.1}$$

Where $\sum Q_{cooling}$ and $\sum Q_{heating}$ are the annual accumulated cooling load and heating load, respectively.

From Table 5.2, it can be seen that the load imbalance ratios of the building demands for the four cities were all relatively high. The high load imbalance ratio indicates that the total annual heat extracted from the soil will not be equal to the total annual heat rejected into the soil.

5.2.4 GSHP system sizing and simulation system development

5.2.4.1 GSHP system sizing

Based on the load conditions and the maximum heating and cooling demands presented

above, the ASHP and GSHP system for the four selected four cities can be sized, respectively. In cooling-dominated conditions, the sizing of both GSHP and ASHP systems were based on the maximum cooling demand, whereas in heating-dominated conditions, the sizing of the GSHP and ASHP systems were based on the maximum heating demand.

To determine the required total borehole length, it is essential to consider the ground formation thermal resistance, maximal cooling or heating demands, fluid flow rate within the GHE, and borehole diameter should be considered. In this study, the required borehole length was determined using the sizing equation (Equation 2.7 or 2.8) for the total borehole length estimations provided by ASHRAE Handbook (2011) which was described in Section 2.5.2.2, Chapter 2. Other geometric parameters such as borehole diameter, borehole spacing and pipe diameter were the same as the vertical GHEs installed in the SBRC building which were described in Table 3.1, Chapter 3. The average soil temperatures of the shallow ground for the selected cities were assumed to be 1-3°C higher than the average air temperature in each city (Wu *et al.* 2013).

The ASHP system was assumed to be equipped with one air-to-water heat pump while the GSHP system was assumed to be equipped with two identical water-to-water heat pumps (i.e. similar to the system implemented in the SBRC building). The selection of the water-to-water heat pumps for the GSHP system and the air-to-water heat pump for the ASHP system were based on the peak heating/cooling demand. The heat pump capacities were then scaled proportionally based on the capacities of the heat pumps implemented in the SBRC building, as descried in Chapter 3. The specifications of the ASHP and GSHP systems for each location are summarised in Table 5.3.

Table 5.3 Specifications of the ASHP and GSHP systems for different cities

System	Specifications	Cities			
		Sydney	Alice Spring	Brisbane	Hobart
ASHP	Rated cooling capacity/power (kW/kW)	130.0/43.3	183.6/61.1	170.6/56.8	126.6/42.1
	Rated heating capacity/power (kW/kW)	159.1/45.0	224.7/63.6	208.8/59.1	155.0/43.9
	Number of AWHP	1	1	1	1
GSHP	Rated cooling capacity/power (kW/kW)	65.0/16.4	91.8/20.3	85.3/21.3	62.3/15.6
	Rated heating capacity/power (kW/kW)	81.6/22.0	114.2/30.8	106.1/28.6	77.5/20.9
	Number of WWHP	2	2	2	2
	Number of boreholes	23	32	29	21
	Borehole depth (m)	91	112	100	90
	Undistributed soil temperature (°C)	20	24	23	16

From Table 5.3, it can be seen that, for cooling-dominated conditions, a higher value of the maximum cooling load will result in larger design capacities of the GSHP and ASHP systems, which leads to the increased in the investment costs. In particular for the GSHP system, a greater number of deeper and more boreholes will be required, which add extra expensive drilling costs.

5.2.4.2 Simulation system development

In order to investigate the performance benefits of using GSHP systems and compare the performance difference between the use of GSHP systems and ASHP systems under the climate conditions of the four selected cities, the simulation systems for both the GSHP system and ASHP system were developed using the TRNSYS simulation program. Fig. 5.3 and 5.4 present the developed simulation systems for the ASHP system and GSHP system,

respectively.

In the simulation systems, the duct heat storage model (DST), Type 557, was used to simulate the vertical GHEs. The building load of each city calculated by DesignBuilder was imported using Type 62. A sequence control strategy was used to control the operation of the two identical water-to-water heat pumps in the GSHP system. When the building load is less than the rated capacity of one single water-to-water heat pump, only one water-to-water heat pump is in operation; otherwise, two heat pumps are in operation.

The simulation was performed for 20 years with a time step of 1 hour. The average soil temperature, system coefficient of performance (COP_{sys}) and electricity consumption can be obtained once the simulation is completed.

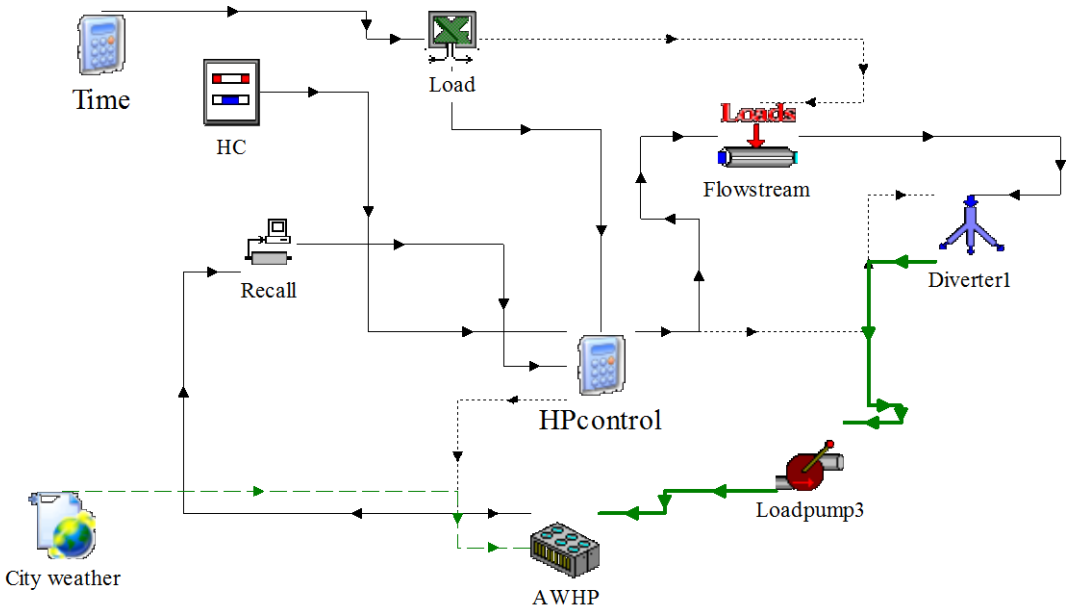

Fig. 5.3 Simulation system developed for the ASHP system.

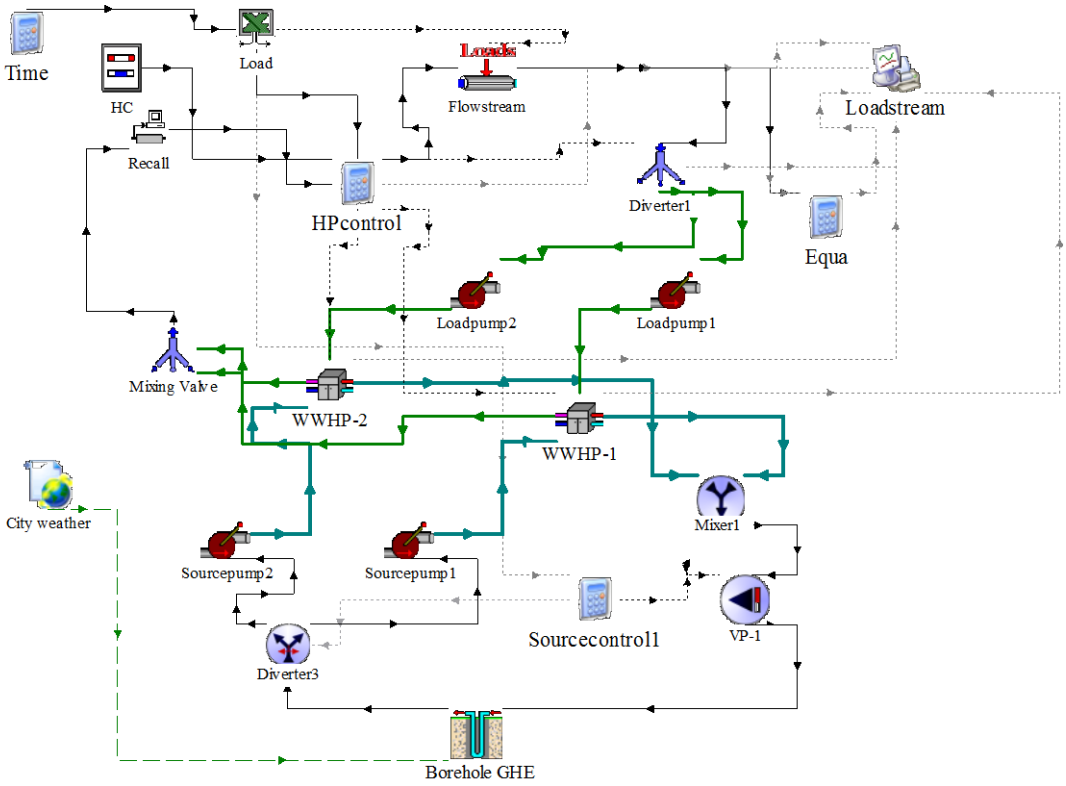

Fig. 5.4 Simulation system developed for the GSHP system.

5.2.5 Performance evaluation criteria

5.2.5.1 Calculation of the energy performance

The energy performance was evaluated by using the overall system coefficient of performance (COP_{sys}), which was calculated by:

$$COP_{sys} = \frac{Q_{load}}{\sum W_{HP} + \sum W_{pumps}} \tag{5.2}$$

where, COP_{sys} is the overall system energy efficiency, Q_{load} is the annual total cooling and heating energy provided by the system, and W_{pump} are the power consumptions of all water pumps in the field loop.

5.2.5.2 Average soil temperature

Previous studies have demonstrated that the average soil temperature in the borehole storage field can be used as an effective performance index to evaluate the thermal

imbalance within the vertical borehole field (Trillat-Berdal *et al*. 2007). It was therefore selected as a long-term performance indicator in this chapter.

5.2.5.3 Calculation of life cycle cost

In this study, the upfront costs and operating costs were combined into a single net present value considering 20-years of operation of the GSHP systems and ASHP systems for the four selected cities. The net present value (NPV) can be defined as the sum of the present values of all project cash flows (Kent *et al.* 2011).

$$NPV = \sum_{t=0}^{n} \frac{CF_t}{(1+IR)^t} \tag{5.3}$$

where, CF_t is the cash flow at time t, IR is the discount rate, and n is the duration of operation in years.

Economic feasibility was calculated in terms of the NPV. The GSHP system is considered to be economically feasible only when its NPV of cost is less than that of the ASHP system.

5.2.5.4 Calculation of environmental impact

The CO_2 emissions were calculated based on the power consumptions of GSHP and ASHP systems. In this study, the CO_2 emission density for the purchased electricity was determined by calculation principles provided by the National Greenhouse Accounts Factors (NGA) (DCCEE 2013).

The greenhouse gas emissions (tonnes of CO_2) were calculated using the following equation.

$$Y = Q \times \frac{EF}{1000} \tag{5.4}$$

where, Y is the measured GHG emissions, Q is the quantity of electricity consumed in kWh, and EF is the indirect emission factor for the consumption of the purchased electricity. The indirect emission factors for the four cities are provided in Table 5.4.

The environmental feasibility of the GSHP system was evaluated by comparing the predicted total CO_2 emissions with the ASHP system. The GSHP system is deemed to be

environmentally friendly when its total CO_2 emission is less than that of the ASHP system.

Table 5.4 Indirect emission factors for consumption of the purchased electricity (DCCEE 2013)

Cities	Emission factor (kg CO_2-e/kWh)
Sydney	0.87
Brisbane	0.82
Hobart	0.20
Alice Springs	0.69

5.3 Results and discussion

5.2.1 Energy performance analysis

5.2.1.1 Power consumption of the ASHP and GSHP systems

The total power consumption includes the power consumption of the heat pump units as well as the water pumps. Fig. 5.5 presents the power consumptions of the GSHP system and ASHP system for four selected cities.

It can be seen in Fig. 5.5 that, for Sydney, the GSHP system consumed 134,520 kWh less power than the ASHP system. For Alice Springs, the GSHP system saved 411,314 kWh power in comparison with the consumption of the ASHP system. For Brisbane and Hobart, 172,972 kWh and 128,983 kWh more power respectively can be saved when using the GSHP system instead of using the ASHP system. The variations of the energy savings among different cities are mainly due to different climatic conditions and building load characteristics. From the results presented in Fig 5.5, it can be concluded that, for all four cities studied, the GSHP system consumed less power than the ASHP system.

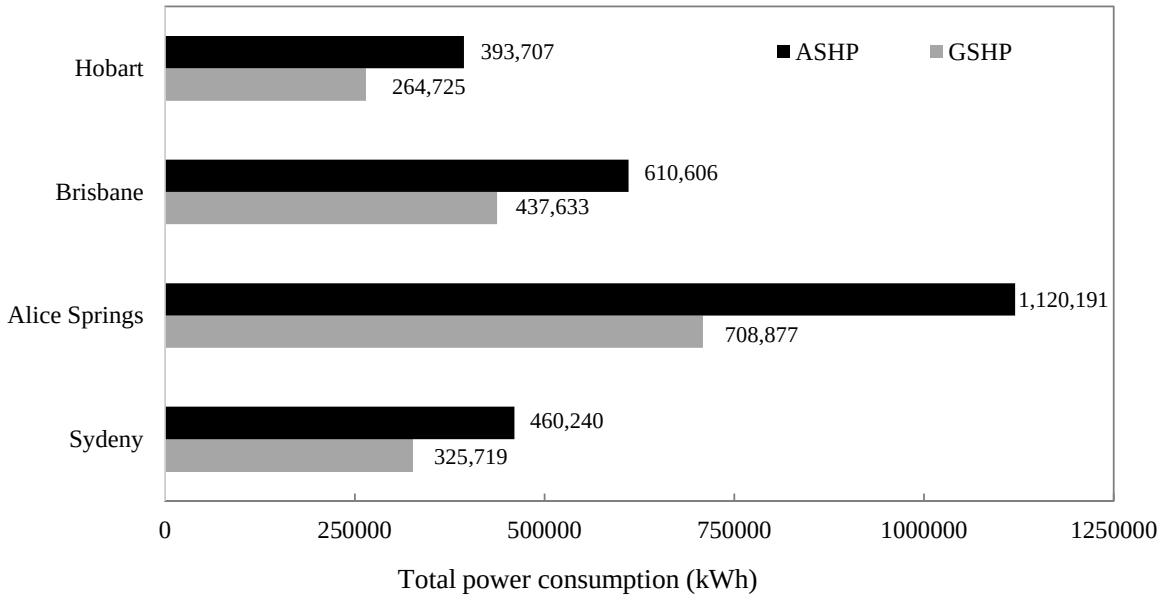

Fig. 5.5 Power consumptions of the ASHP and GSHP systems of 20-year operation for four cities selected.

5.2.1.2 The overall system coefficient of performance of the ASHP and GSHP systems

The overall system coefficients of performance (COP_{sys}) of the GSHP system and the ASHP system for the four cities are summarised in Table 5.5.

Table 5.5 System coefficients of performance (COP_{sys}) of using GSHP and ASHP system for four selected cities

Cities	System coefficient of performance		Difference
	ASHP	GSHP	(%)
Sydney	2.02	2.85	43
Alice Springs	1.91	3.01	58
Brisbane	2.11	2.94	40
Hobart	1.74	2.59	49

It can be seen that the overall system performance coefficient of the GSHP system is higher than that of the ASHP system. For 20-years operation, the COP_{sys} of the GSHP system in Sydney, Alice Springs, Brisbane and Hobart were 41%, 58%, 40%, and 49% higher than

that of using the ASHP system for the four corresponding cities, respectively.

5.2.1.3 Long-term performance evaluation of the GSHP systems

The variations of the hourly-based vertical borehole temperature over 20-year operation of the GSHP systems are shown in Fig. 5.6. It is clearly shown that the average soil temperature around the vertical ground heat exchangers varied to some extent when using the GSHP systems in all four cities.

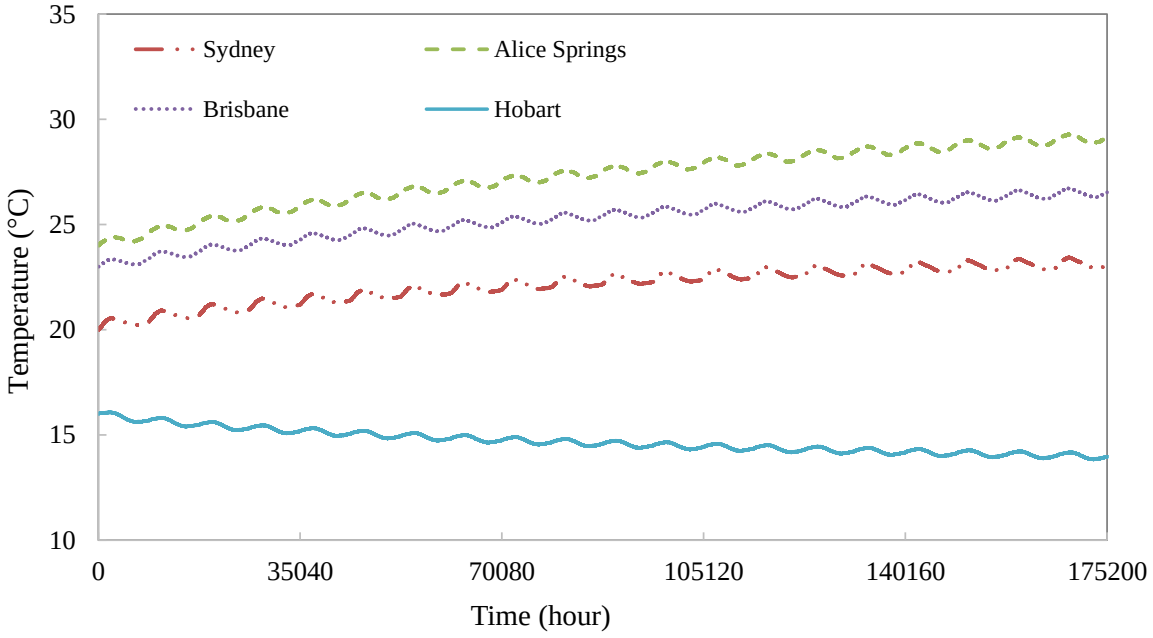

Fig. 5.6 Hourly average soil temperatures in 20-years operation of GSHP systems in the four selected cities.

It can be seen in Fig 5.6 that the borehole storage temperature first increased when more heat was rejected into the vertical loop, then the storage temperature decreased due to the extraction of the heat from the ground during the winter heating periods and then increased again due to the requirement of the cooling of the building. For Sydney, Alice Springs and Brisbane, due to more heat being rejected into the ground, the average soil temperature increased by 3.02°C, 5.16°C and 3.53°C respectively after 20 years of operation. On the contrary, for Hobart, as the amount of heat extraction is more than that of heat rejection, there is a decrease in the average soil temperature by 2.04 °C during the 20-years operation.

As mentioned earlier, the continuous increase/decrease in the soil temperature will result in performance degradation of GSHP systems.

- Entering water temperature to the water-to-water heat pumps

The performance of the GSHP systems is also influenced by the entering water temperature to the evaporator and condenser of the heat pump units. For cooling-dominated conditions, the increased soil temperature will undermine the heat transfer in the heat rejection process and increase the temperature to the condenser. The higher the inlet water temperature to the condenser, the lower the performance of the water-to-water heat pump in the cooling operation mode. For the heating-dominated conditions, the decreased soil temperature will undermine the heat transfer in the heat extraction process, which will decrease the inlet water temperature to the evaporator. The lower the inlet temperature to the evaporator, the lower the performance of the water-to-water heat pump in the heating operation mode.

Fig. 5.7 a-c) presents the annual maximum entering water temperature to the water-to-water heat pumps for cooling dominated conditions. The maximum entering water temperature continuously increased as a result of the thermal imbalance. By the end of 20-years operation, the maximum entering water temperature reached 37.2°C, 38.0°C and 37.3°C for Sydney, Alice Springs and Brisbane, respectively. Fig. 5.7 d) presents the annual minimum entering water temperature to the water-to-water heat pumps for the heating-dominated conditions. The load imbalance led to continuous decrease in the minimum entering water temperature to the evaporator. By the end of 20-years operation, the minimum entering water temperature reduces to 7.6°C for Hobart.

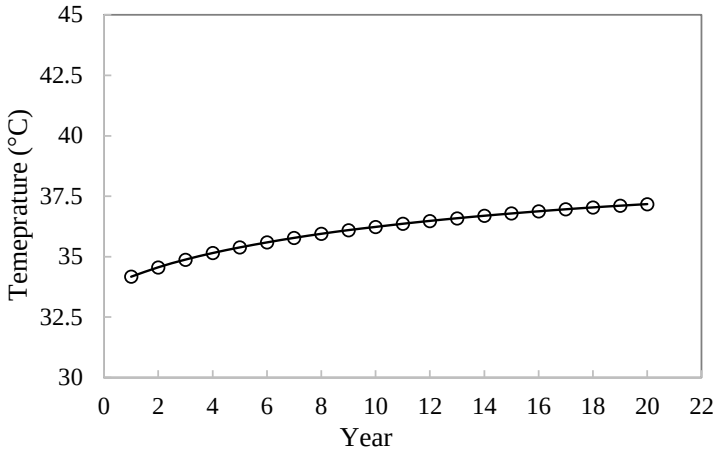

a) Maximal EWT - Sydney

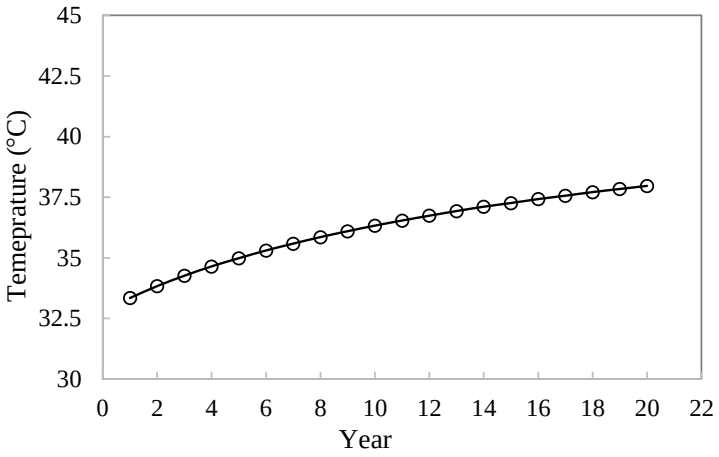

b) Maximal EWT - Alice Springs

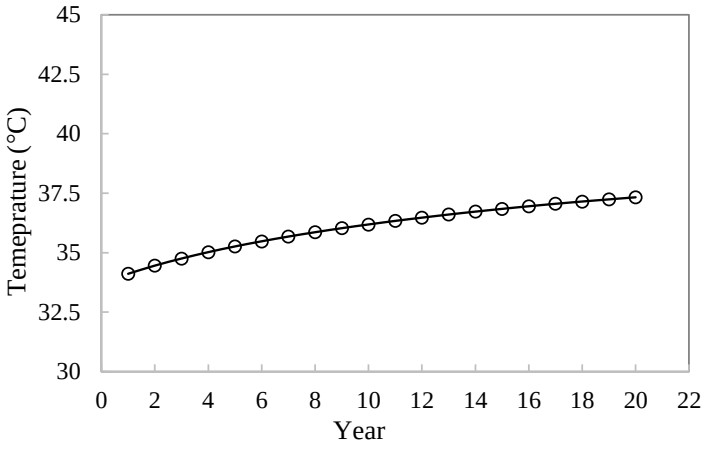

c) Maximal EWT – Brisbane

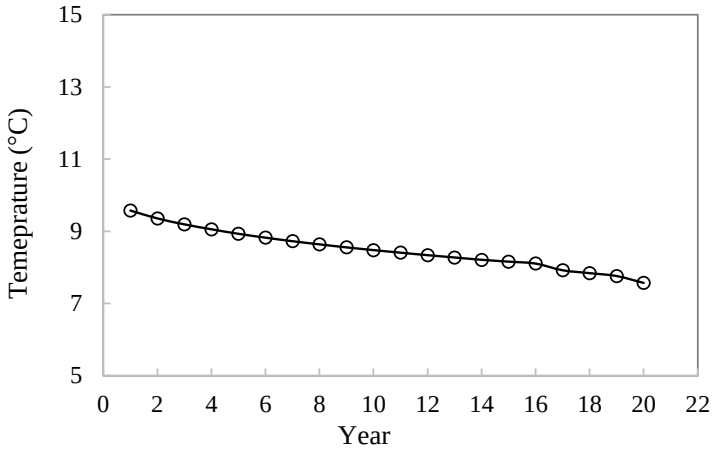

d) Minimal EWT - Hobart

Fig. 5.7 Entering water temperature to the water-to-water heat pumps.

The above analysis showed that the thermal imbalance within the ground will have negative consequences on the long-term operation of GSHP systems. The GSHP system performance will be deteriorated in the long run if the soil temperature increases or decreases (Li *et al*. 2006, Chen *et al*. 2011). Researchers have come up with different approaches like increasing borehole spacing, depth or numbers and installing supplementary HVAC devices, all these methods have been demonstrated to be effective in alleviating the thermal imbalance issue. As solving the imbalance issue is not the focus of this study, the details of these approaches can be found in the literature (Nguyen *et al*. 2014, You *et al*. 2014).

5.2.2 Economic feasibility

5.2.2.1 Life cycle cost analysis

Financial viability is an important factor influencing the users' decisions on installation of GSHP systems. An economic analysis is often performed to evaluate the economic feasibility and benefits of using GSHP systems. In this study, the net present value (NPV) defined in Equation (5.6) was used as the performance indicator for cost analysis. The service time of the ground source heat pump systems normally lasts more than 20 years (Alavy *et al*. 2013, Garber *et al*. 2013), in this study, the life span is set to 20 years. In formulating the NPV analysis, it is necessary to determine the upfront cost and operating

cost of the GSHP system and ASHP system, respectively. The upfront cost for the ASHP system is the capital cost of the air-to-water heat pump, while the upfront cost for the GSHP system is the sum of the capital costs of water-to-water heat pumps and vertical GHEs. As the upfront costs of the water pumps and valves in the pipelines are relatively small when compared to the costs of the air-to-water heat pump, water-to-water heat pumps, and vertical GHEs, their upfront costs were not considered in this study. The operating costs for both systems include the system maintenance cost and electricity usage cost.

- *Upfront cost*

The typical cost for drilling and installation of the vertical ground heat exchangers was assumed to be $75/m in consultation with GeoExchange Pty Ltd., Australia. The cost of the air-to-water heat pump was calculated by multiplying its rated capacity with the unit price of $0.73/W. As it was difficult to find the unit price of an air-to-water heat pump in Australia, the unit price of $0.73/W used in this study was derived from the unit price of 1-3 yuan/W in China (Wu *et al.* 2014) by converting it to Australian dollars by using the maximum value of 3 yuan/W. Similar assumptions were made for the determination of the capital costs of the two water-to-water heat pumps.

- *Maintenance cost and electricity cost*

In a life cycle cost study conducted by Chiasson (2006), the annual maintenance costs for the ASHP system and GSHP system were specified as $3.01/m^2 and $1.40/m^2, respectively. As the price was specified in 2006, an annual increase of the cost was assumed as 1.15% (Junghans 2015) and the annual maintenance costs were therefore derived as $3.30/m^2 for the ASHP system and $1.53/m^2 for the GSHP system in 2014 in this study. The electricity price for Australia was determined to be $0.25/kWh, and annual increase rate was assumed to be 3.76% (APVA, 2011).

For the calculation of NPV, the discount rate *IR* was assumed to be 5%. The results of the life cycle cost analysis are shown in Table 5.6. It is shown that the GSHP system has lower NPV values for Sydney, Alice Springs, Brisbane and Hobart, approximately 1.65% to 4.50% lower than that of the ASHP system. However, the economic benefit of using the GSHP system is small when compared to that of the ASHP system. This is mainly due to the high installation costs of the GSHP systems. For Sydney, Alice Springs, Brisbane and

Hobart, the upfront costs of the GSHP systems were 61%, 87%, 66% and 48% higher than those of the ASHP systems. The high installation costs of the GSHP systems undermined the NPV savings achieved as compared with conventional ASHP systems.

Table 5.6 Net present values of life cycle costs of the ASHP and GSHP systems

	Sydney		**Alice Springs**		**Brisbane**		**Hobart**	
	ASHP	GSHP	ASHP	GSHP	ASHP	GSHP	ASHP	GSHP
Upfront cost	$115,860	$186,856	$163,630	$306,165	$152,044	$253,081	$118,836	$171,631
1st year operating cost	$4,882	$2,690	$12,500	$6,100	$6,683	$3,046	$4,000	$2,742
1st year maintenance cost	$5,614	$2,607	$5,614	$2,607	$5,614	$2,607	$5,614	$2,607
NPV	$270,343	$261,628	$445,768	$440,920	$335,527	$330,691	$258,141	$246,517
NPV savings	-	3.22%	-	1.09%	-	1.44%		2.73%

The overall results of the economic feasibility study for the GSHP system in each location are summarised in Table 5.7, where the symbol "○" means that the utilisation of GSHP systems is feasible, while "×" means the system is unfeasible. The GSHP system is considered to be economically feasible when the NPV value is smaller than that of the ASHP system. It can be seen that GSHP systems are economically feasible in Sydney, Alice Springs, Brisbane and Hobart. In order to maximise the benefits of using GSHP systems, appropriate design and operational optimisation of GSHP systems is essential for further improving their economic feasibilities.

Table 5.7 The results from the economic feasibility study

Location	GSHP
Sydney	○
Alice Springs	○
Brisbane	○
Hobart	○

5.2.2.2 Sensitivity analysis

In this section, a sensitivity study is conducted to understand the influences of the drilling cost, electricity price and discount rate on the net present value (NPV) of the GSHP system. The three parameters were assumed to vary between 5% higher and 5% lower than the values described in section 5.3.2.1 with a 1.0% variation rate. For each city, the NPV of the GSHP system was calculated with the above varied parameters.

Fig. 5.8 shows the effects of the variations of the borehole drilling cost on the NPV of the GSHP system. An approximately linear relationship can be found between the borehole drilling cost and net present values. The higher the borehole drilling cost, the higher the GSHP system NPV, which will make the system less financially attractive. In general, the deviations of NPV were around 3% with ±5% variations of the borehole drilling cost in the four locations studied.

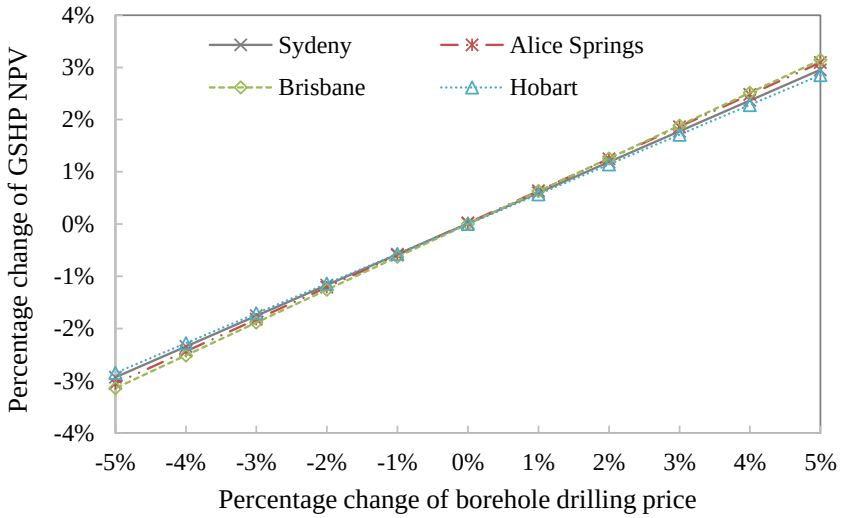

Fig. 5.8 Effects of the variations of borehole drilling cost on the NPV of GSHP systems.

Fig. 5.9 shows the effects of the variations of the electricity price on the NPV of the GSHP system. An approximately linear relationship can also be found between the two parameters. The higher the electricity price, the higher the GSHP system NPV. The deviations of NPV in the four cities studied were around 1.5% with ±5% variations of the electricity price.

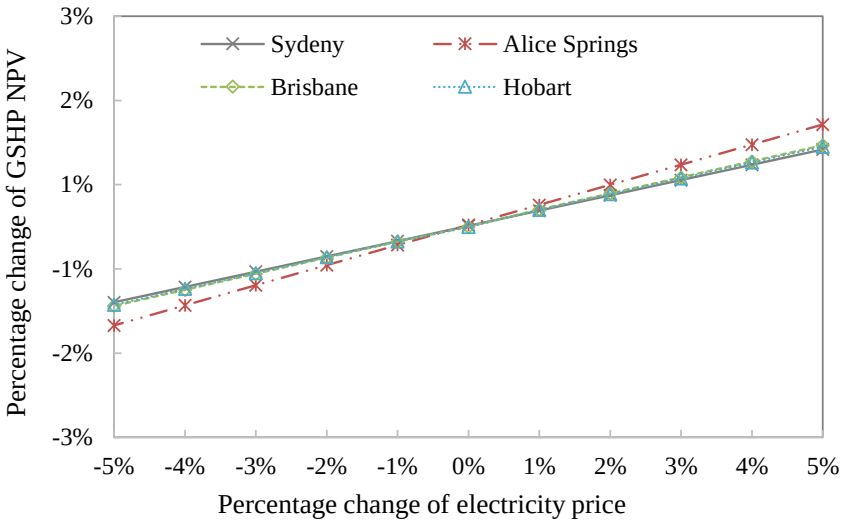

Fig. 5.9 Effects of the variations of electricity price on the NPV of GSHP systems.

Fig. 5.10 shows the effects of the variations of the discount rate on the NPV of the GSHP system. The GSHP system NPV approximately linearly decreased with the increase of the

discount rate. However, the deviations of NPV were small, less than 1.0% with the ±5% variations of the discount rate in the four locations studied.

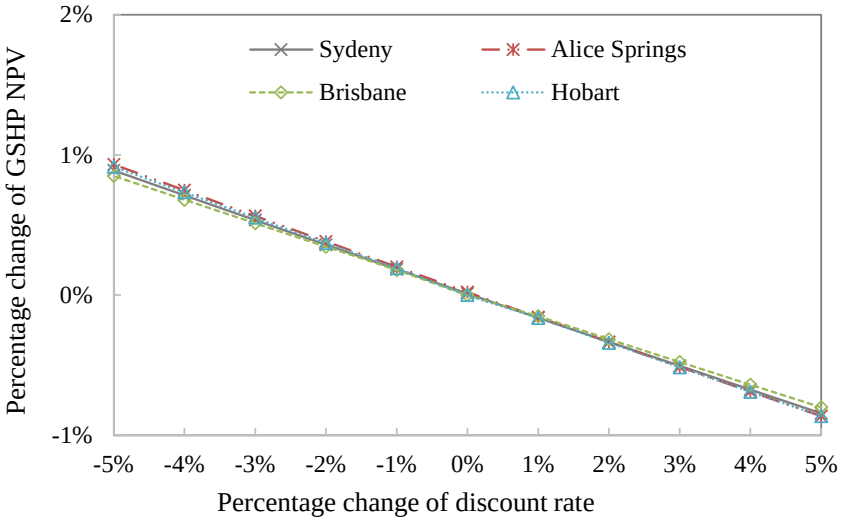

Fig. 5.10 Effects of the variations of discount rate on the NPV f GSHP systems.

5.2.3 Environmental feasibility

In this section, the CO_2 emissions of the GSHP system and ASHP system were estimated based on Equation (5.7) for the life span of 20 years. Table 5.8 summaries the CO_2 emissions of the GSHP and ASHP systems of the reference building under the four cities.

It can be found that the GSHP system emitted less CO_2 in comparison with the ASHP system, due to its higher system coefficient of performance. The reductions of CO_2 emissions by using the GSHP system were 117.0 tonnes for Sydney, 297.2 tonnes for Alice Spring, 141.8 tonnes for Brisbane, and 15 tonnes for Hobart, when compared to those of using the ASHP system. The average percentages of reduction in CO_2 emissions by using the GSHP system in comparison with the ASHP system for the four selected cities were around 32.5±4.2%.

Table 5.8 Summary of power consumption and CO_2 emissions of GSHP and ASHP systems.

	CO_2 emission (tonnes)		
	ASHP	GSHP	Difference (%)
Sydney	400.4	283.4	29
Alice Spring	772.9	475.7	37
Brisbane	500.7	358.9	28
Hobart	78.7	52.9	33

The results of the environmental feasibility study for the GSHP systems for four locations are summarised in Table 5.9. Similarly, the symbol "○" means that the system is feasible, while "×" means that the system is unfeasible. When the CO_2 emission from the GSHP system is smaller than that from the ASHP system, the GSHP system is deemed to be environmental feasible. It can be seen that, for Sydney, Alice Springs, Brisbane, Darwin and Hobart, GSHP systems are environmentally feasible with massive reduction of CO_2 emissions.

Table 5.9 Economic feasibility study results

Location	GSHP
Sydney	○
Alice Springs	○
Brisbane	○
Hobart	○

5.4 Summary

The chapter presented a feasibility analysis of using ground source heat pump (GSHP) systems to provide heating and cooling to a reference building under different Australian climate zones. The Sustainable Buildings Research Centre (SBRC) building was used as

the reference building, and the building heating and cooling load profiles of the reference building under the selected Australian cities including Sydney, Alice Springs, Brisbane, Darwin and Hobart, were modelled using DesignBuilder. The GSHP systems without using any supplementary heat rejecters are not recommended for Darwin as the reference office building in Darwin only requires cooling during the course of the year. The energy, economic and environmental performance of the GSHP systems were therefore evaluated and compared with an air source heat pump (ASHP) system for the remaining four cities only. It is worthwhile to mention that, the economic and environmental benefits obtained in this study are particular to the chosen conditions of our simulations. In Australia, different states often adopt different electricity rates for both residential and commercial electricity users. Using the same electricity price for different stages is a limitation of this analysis. Some key conclusions are summarised below.

1) The results from the energy performance analysis showed that, the system coefficient of performance (COP_{sys}) of the GSHP system was found to be 2.59-3.01, relatively higher than that of the ASHP system whose COP_{sys} was to be 1.74-2.11, for different locations selected.

2) The economic analysis showed that GSHP systems are economically feasible for major Australian climate zones. For Sydney, Alice Spring, Brisbane and Hobart, net present values (NPV) of using the GSHP system were reduced by approximately 1.09% to 3.22%, compared to the use of the ASHP system. The high drilling costs of vertical GHEs undermined the NPV savings of using GSHP systems in comparison with using ASHP systems to some extent.

3) The sensitivity analysis of the drilling cost, electricity price and discount rate on the NPV of GSHP systems showed that the drilling cost seems to have a relatively higher influence on the system NPV. Optimal sizing of the vertical GHEs is crucial to minimise the high installation costs of the GSHP systems to improve the economic benefits, which will be optimised in Chapter 6 and Chapter 7.

4) The environmental analysis showed that GSHP systems saved approximately 33.0±4.0%of CO_2 emissions in comparison with the savings due to using ASHP systems. Environmental analysis indicated that GSHP systems are environmentally

feasible with massive reduction of CO_2 emissions for major Australian climate zones.

Chapter 6

Entropy Generation Minimisation based Single-Objective Design Optimisation of Vertical Ground Heat Exchangers

GSHP system with vertical GHEs is usually believed to be more efficient than other types of GSHP systems. However, the high drilling cost of the vertical GHEs makes the short-term economics of this system unattractive. It is therefore highly desirable to optimise the vertical GHEs. This chapter presents the development and validation of an optimal design methodology for vertical U-tube ground heat exchangers (GHEs) used in HVAC systems. The dimensionless 'entropy generation number' (EGN) obtained by scaling the entropy generation due to heat transfer and pressure drop, on the ratio of the heat transfer rate to the average fluid temperature of vertical GHEs is employed as the objective function. A global sensitivity analysis based on Sobol's method (Sobol' 1993) is first performed to identify the key design variables. The identified variables are then optimised by a genetic algorithm optimisation technique. The entropy generation process combines the heat transfer and fluid mechanics with thermodynamic analysis. A vertical GSHP system which is part of the system implemented in the Sustainable Buildings Research Centre at University of Wollongong, Australia, is used as a case study to validate the effectiveness of the proposed design optimisation strategy by comparing the total system cost (i.e. the upfront cost and 20 years' operation cost) of the optimised system with that of the original system. The validation process is performed based on the simulation system developed using TRNSYS.

This chapter is organised as follows. Section 6.1 introduces the background of application of thermodynamic theories into GSHP system analysis. Section 6.2 outlines the formulation of the proposed design optimisation methodology based on entropy generation minimization which includes the objective function, optimisation constraints, system energy modelling and global sensitivity analysis. A case study for validating the

effectiveness of the proposed design optimisation methodology is provided in Section 6.3. A brief summary is provided in Section 6.4.

6.1 Introduction

Energy analysis based on the 1st law of thermodynamics is the most commonly used approach to evaluating the performance of GSHP systems. As reviewed in Chapter 2, the coefficient of performance (COP) is one of the key performance indicators to evaluate the operating efficiency of HVAC systems, and has been widely applied in the studies of various types of GSHP systems by experiments and simulations (Sanner *et al*. 2003, Hamada *et al*. 2007, Si *et al*. 2014, Dai *et al*. 2015). As the COP is converted based on the theory of energy conservation, it can only represent the relationship between the output energy and the input energy. This means that COP cannot be used to indicate the thermal irreversibility generated during the energy transfer within a thermal system (Wark 1995). Combining the principle of energy conservation with the 2nd law of thermodynamics can be an effective and efficient approach to facilitate the energy analysis and design of thermal systems (Dincer 2002).

Recently, the second law of thermodynamics (i.e. exergy analysis), has been used to investigate GSHP or other heat pump systems (Hepbasli *et al*. 2004, Bi *et al*. 2009, Lohani *et al*. 2010, Zhao *et al*. 2014).According to Bejan (2006), exergy analysis requires the application of both 1st and 2nd law of thermodynamics to assess the energy performance of a thermal system in terms of the irreversibility. Therefore, appropriate utilisation of this approach can be effective in identifying the key components with the potentiality of energy savings. Bi *et al*. (2009) discovered that, among all the components of a GSHP system, the GHE was found to be the potential energy saving component which needs to be improved, as the GHE has the minimum exergy efficiency.

The purpose of this chapter is to develop an optimal design methodology for vertical U-tube ground heat exchangers (GHEs) by using entropy generation minimisation (EGM) method. The EGM, or thermodynamic optimisation, is a method for modelling and optimisation of thermodynamic cycles, which has been widely applied to the optimisation design of various types of heat exchangers (Bejan 1996, Maheshkumar *et al*. 2011, Pussoli *et al*. 2012, Cheng

et al. 2014). Minimisation of the entropy generation of a system is equivalent to the optimisation of its thermodynamic performance. Usually, the application of EGM is referred as 'entropy generation number' (EGN) (Bejan 1996).

In this chapter, the entropy generation number (EGN) of vertical GHEs is first derived and defined as the objective function, and the infinite line source model is utilised for performance prediction. The global sensitivity analysis is then used to determine the non-influential design parameters to reduce the number of decision variables. A genetic algorithm is used as the optimisation technique to solve the optimisation problem and search for optimal values of major design parameters. Finally, an illustrative example is used to validate the effectiveness of the proposed optimal design methodology.

6.2 Formulation and development of the optimal design methodology

6.2.1 Outline of the optimal design methodology

The aim of the thermodynamic modelling of vertical U-tube ground heat exchangers is to evaluate and compare the thermal performance of alternative design options. Fig. 6.1 illustrates a block diagram of the optimal design methodology. The overall optimisation procedure consists of two steps. The first step is to use a global sensitivity analysis method to determine the major design parameters and their design constraints. The second step is to formulate the entropy generation minimisation (EGM)-based optimisation strategy, including the development of the objective function, and selection of the performance model and optimisation technique.

Genetic algorithm (GA) as an optimisation tool can provide good solutions with random initialization and has been widely used to solve the optimisation problems in engineering and science fields (Ma *et al*. 2011, Gutiérrez *et al*. 2012, Maehara *et al*. 2013, Iranmanesh *et al*. 2014, Sadeghzadeh *et al*. 2015). A general GA procedure is summarised in Fig. 6.2 (Shyr. 2010). The algorithm is maintained by a population of parent individuals that represent the latent solutions of a real-world problem. After some generations, the algorithm converges to a best individual, which probably represents the best or nearly optimal solution of the given problem (Houck *et al*. 1996, Gutiérrez *et al*. 2012). Typically, the most time-consuming step of the GA procedure is the evaluation of the objective

function, which involves several simulations for each individual. This might be a reason for simplifying the system modelling associated with the optimisation problem, rather than performing systematic simulations to evaluate each individual. The genetic algorithm used aims at finding a single set of input variables that will optimise one or more performance criteria synthesised into a single-objective function. A GA optimiser implemented by using MATLAB Optimisation Toolbox (Houck *et al*. 1996) is used in this study to search for optimal values of major design parameters.

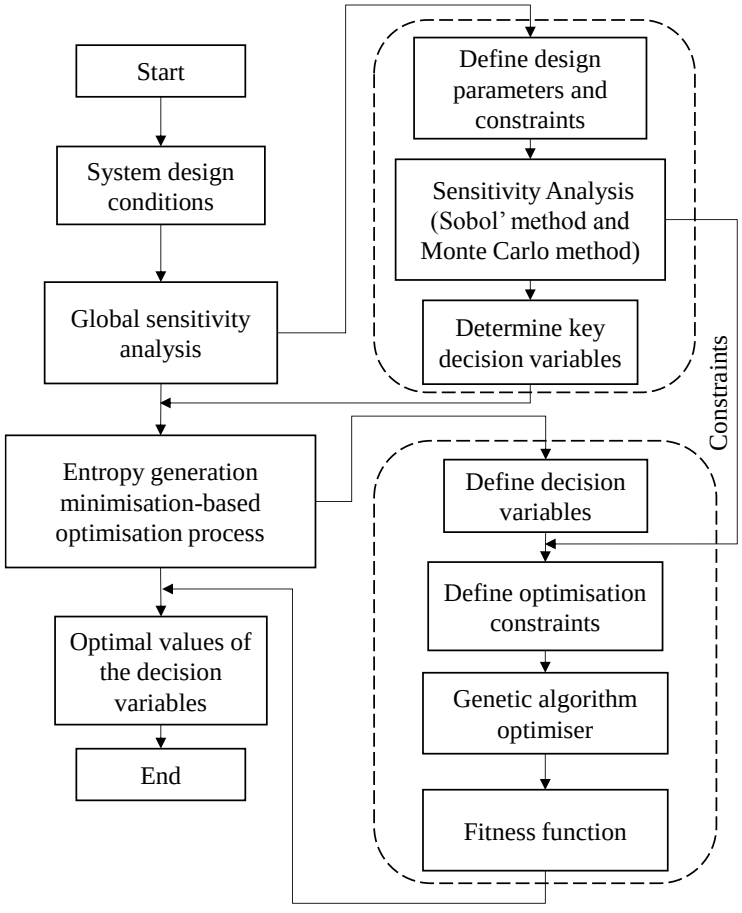

Fig. 6.1 Outline of the design optimisation methodology.

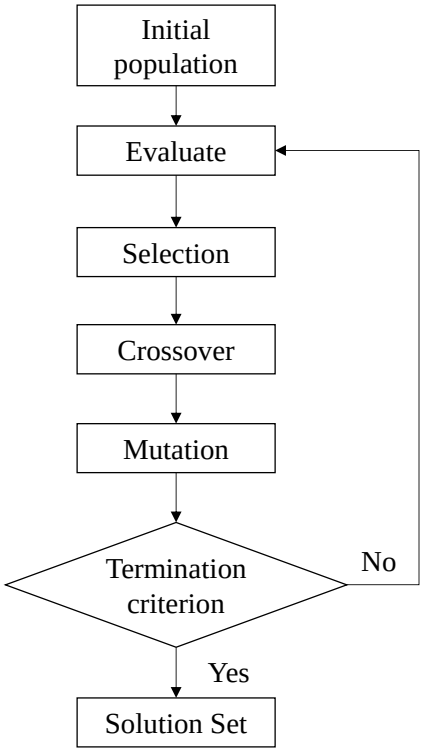

Fig. 6.2 Main steps of a typical genetic algorithm (Shyr 2010).

6.2.2 Objective function and design constraints

6.2.2.1 Objective function

The major objective of the optimisation in this study is to minimise the thermodynamic irreversibility due to the friction fluid flow and heat transfer driven by the finite temperature difference in the vertical GHEs. This will be achieved through identification of the optimal design values of vertical U-tube GHEs which are capable of accomplishing the designed thermal duty with minimum thermodynamic irreversibility. The objective function is denoted by the so-called entropy generation number (EGN) method generated based on the entropy generation rate (S_{gen}), and is expressed in Equation (6.1) (Bejan 1996).

$$N_s = \frac{S_{gen} \cdot T_{f,m}}{Q} \tag{6.1}$$

where, N_s is the dimensionless entropy generation number, S_{gen} is the entropy generation rate, $T_{f,m}$ is the logarithmic average fluid temperature of the vertical U-tube GHE, and Q is

the heat transfer rate.

The detailed procedure to be used to calculate the entropy generation rate (S_{gen}) of the vertical U-tube GHEs will be presented in section 6.2.2.3.

6.2.2.2 Design constraints

Mathematical models used in the optimisation process are typically simplified to represent the real process. Both the model mismatch and process disturbance can result in infeasible operation conditions. Hence, defining the constraints of the decision parameters is crucial in helping avoid this potential problem (Chachuata *et al*. 2008). In this study, the following constraints are applied in the optimisation process.

1) Constraints for geometrical parameters: the variation ranges of the geometrical parameters such as the number of boreholes, borehole depth, and borehole distance, as shown in Fig. 6.3, are determined based on the recommended values of practical engineering projects and summarized in Table 6.1 (ASHRAE 2011, Banks 2012).
2) Constraints for heat transfer process: the estimated total length of the vertical GHEs is associated with the possible maximal heat flux. The acceptable range of the maximal heat flux is dependent on the thermal conductivity of the soil on the site (Banks 2012). In this study, the acceptable range of the maximal heat flux (30 W/m - 130 W/m) recommended by Robert *et al*. (2014) was used.
3) Temperature constraints: the maximum and minimum outlet temperatures from the vertical GHEs in the cooling and heating conditions have a fairly limited range of acceptable values. The practical values of the temperature constraints are normally dependent on the mode of the heat pump used (ASHRAE, 2011). The minimum entering fluid temperature to the heat pump at the design condition in the heating condition can be determined by Equation (6.2), while the maximum entering fluid temperature to the heat pump at the design condition in the cooling condition can be determined by Equation (6.3) (ASHRAE, 2011).

$$T_{f,2,\min} = T_{s,\min} - 8.3°\mathrm{C} \tag{6.2}$$

$$T_{f,2,\max} = \min(T_{s,\max} + 11.1°\mathrm{C}, 43.3°\mathrm{C}) \tag{6.3}$$

where, $T_{f,2}$ is the outlet fluid temperature from the vertical U-tube GHE, $T_{s,min}$ is the minimal soil temperature over the year, and $T_{s,max}$ is the maximal soil temperature over the year. The average soil temperature was assumed as 20°C with a temperature variation of 5°C.

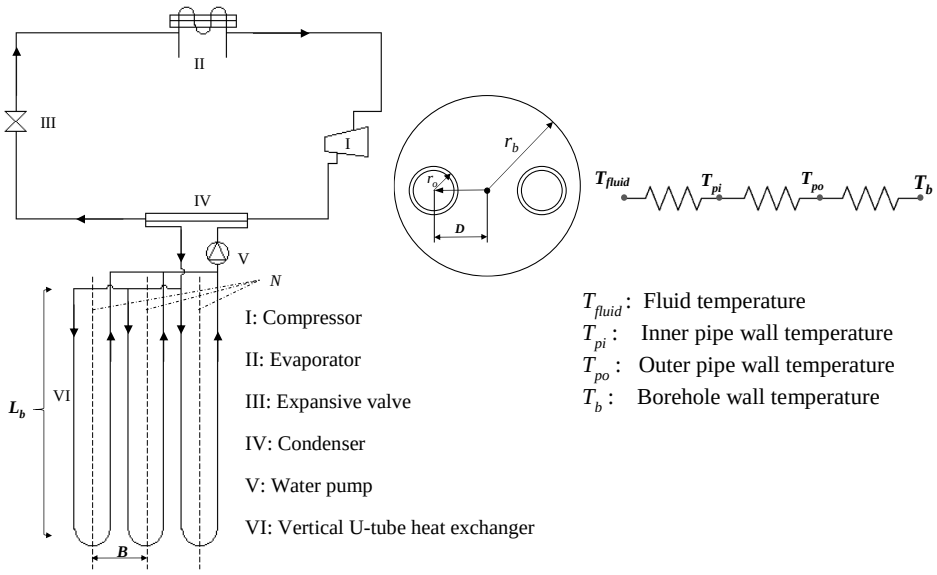

Fig. 6.3 Schematic of the vertical ground source heat pump.

Table 6.1 Ranges of the design parameters of vertical U-tube heat exchangers. (ASHRAE 2011, Banks 2012).

Design parameters		Values or ranges
Vertical U-tube GHE geometry parameters	Number of boreholes: N	$[1, \frac{Q_{tot}}{q_{\min} L_{b,\min}}]$
	Borehole depth L_b (m)	[50, 200]
	Borehole distance B (m)	[3, 10]
	Borehole radius r_b (m)	[0.0325, 0.1]
	Pipe outer radius r_o (m)	[0.012,0.022]
	Half shank space D (m)	[0, r_b-2r_o]
Material parameters	Pipe material conductivity k_p (W/mK)	[0.2, 0.6]
	Grout material conductivity k_b (W/mK)	[0.5, 2.5]
	Soil material conductivity k_s (W/mK)	[0.5, 2.5]
Operating conditions	Circulating fluid mass flow rate per pipe m_f (kg/s)	[0.1, 1]
	Undisturbed soil temperature $T_{s,0}$ (°C)	[10, 20]

6.2.2.3 Energy modelling

Heat transfer calculation

There are many methods of simulating the heat transfer process in and around a vertical GHE (Yang *et al*. 2010). Practically, the heat transfer process of a vertical GHE is analysed in two separated zones. One is the soil/rocks outside the borehole. The other is the zone inside the borehole, including the grout, U-tube pipes and the circulating fluid inside the pipes as shown in Fig. 6.3. The analytical model representing the heat transfer process of the vertical U-tube GHEs used in this study consists of the infinite line source model, and the thermal resistance of boreholes derived from the line-source approximation which is used in the well-known duct ground heat storage model (Lamarche *et al*. 2010).

The infinite line source model was developed based on Kelvin's line source theory (Yang *et al*. 2010). The whole borehole is considered as a semi-infinitely long line source in the ground which is regarded as an infinite medium with an initial uniform temperature. This approach has been widely utilised in some analytical design methods that are currently used to analyse the heat transfer of GHEs (Yang *et al*. 2010, Yuan *et al*. 2012). The simplifications of the model makes it suffer from limitations on time scale and it was estimated that the model may have acceptable accuracy when $t > 20r_b^2/a_s$. Otherwise, it may have noticeable errors (Yang *et al*. 2010, Yuan *et al*. 2012). In the vicinity of the borehole, for sufficiently long time scales and constant heat flux, the line source model gives the expression below to determine the borehole wall temperature (T_b).

$$T_b = T_s(r_b, \tau) = T_{s,0} + \frac{q}{4\pi k_s} \int_{\frac{r_b^2}{4\alpha_s \tau}}^{\infty} \frac{e^{-u}}{u} du \cong T_{s,0} + \frac{q}{4\pi k_s} E_1\left(\frac{r_b^2 \rho_s c_s}{4k_s \tau}\right) \tag{6.4}$$

$$q = \frac{Q}{NL_b} \tag{6.5}$$

where, $T_{s,0}$ is the undisturbed soil temperature, r_b is the borehole radius, q is the heat flux, k_s is the soil thermal conductivity, α_s is the thermal diffusivity, τ is the simulation time, $E_1(x)$ is the exponential integral function, N is the borehole number, L_b is the borehole depth, ρ_s is the soil density, and c_s is the specific heat of the soil.

Borehole thermal resistance is an important parameter in the determination of the inlet and outlet fluid temperatures of the vertical GHEs. The borehole thermal resistance driven by the line-source approximation can be determined by Equation (6.6) (Lamarche *et al*. 2010).

$$R_b = \frac{1}{4\pi k_b}[\ln\frac{r_b}{r_o} + \ln\frac{r_b}{2D} + \frac{k_b - k_s}{k_b + k_s}\ln(\frac{r_b^4}{r_b^4 - D^4})] + \frac{R_p}{2} \tag{6.6}$$

$$R_p = \frac{1}{2\pi k_p}\ln\frac{r_o}{r_i} + \frac{1}{2\pi r_i h_f} \tag{6.7}$$

where, R_b is the total borehole thermal resistance, R_p is the pipe thermal resistance, r_o and r_i the inner and outer radius of the U-tube respectively, D is the half shank space, h_f is the convective heat transfer coefficient, k_b is the thermal conductivity of grout material, and k_p is the thermal conductivity of U-tube.

The convective heat transfer coefficient (h_f) is determined by Nusselt number described in the Equations (6.8) and (6.9) (Bejan 2004).

For laminar flow:

$$Nu = \frac{2h_f r_i}{k_f} = \begin{cases} 4.36 & \text{for uniform heat flux} \\ 3.66 & \text{for uniform wall temperature} \end{cases} \tag{6.8}$$

For fully developed turbulent flow:

$$Nu = \frac{2h_f r_i}{k_f} = 0.023\,\mathrm{Re}^{0.8}\,\mathrm{Pr}^{0.3},\ (0.7 < \mathrm{Pr} < 160;\ \mathrm{Re} > 10^4) \tag{6.9}$$

Based on the IGSHPA approach reviewed in Chapter 2, the thermal resistance between the borehole wall and the undisturbed soil layer (R_s) can be derived as Equation (6.10) and the thermal resistance for multiple boreholes connected in parallel can be determined by Equation (6.11).

$$R_s = \frac{1}{4\pi k_s}E_1(\frac{r_b^2\rho_s c_s}{4k_s\tau}) \tag{6.10}$$

$$R_{s,N} = \frac{1}{4\pi k_s}[E_1(\frac{r_b^2\rho_s c_s}{4k_s\tau}) + \sum_{i=2}^{N}E_1(\frac{B_i^2\rho_s c_s}{4k_s\tau})] \tag{6.11}$$

where, R_s and $R_{s,N}$ are the soil thermal resistance for single borehole and multiple boreholes respectively, and B_i is the borehole distance.

The temperature difference between the circulated fluid (T_f) and undistributed ground temperature ($T_{s,0}$) for single borehole and multiple boreholes can be expressed in Equation (6.12) and Equation (6.13), respectively.

$$T_f(\tau) \cong T_{s,0} + q\{R_s + R_b\} \tag{6.12}$$

$$T_f(\tau) \cong T_{s,0} + q\{R_{s,N} + R_b\} \tag{6.13}$$

where, T_f is the average circulating fluid temperature, which is defined in Equation (6.14).

$$T_f = \frac{T_{f,1} + T_{f,2}}{2} \tag{6.14}$$

where, $T_{f,1}$ and $T_{f,2}$ are inlet and outlet fluid temperatures of the vertical U-tube GHE, respectively.

Pressure drop calculation

The pressure drop ($\triangle P$) along a single U-tube pipe can be determined by Equation (6.15) (Li *et al*. 2013).

$$\Delta P = f \frac{m_f^2 (2L_b)}{\rho_f \pi^2 r_i^5} \tag{6.15}$$

where, f is the friction factor, m_f is the mass flow rate per U-tube pipe. The friction number (f) is determined by the following well-known correlations (Bejan 2004).

For laminar pipe flow:

$$f \cong \frac{16}{\mathrm{Re}} \tag{6.16}$$

For fully developed turbulent pipe flow:

$$f \cong 0.046\mathrm{Re}^{-0.2}, (10^4 < \mathrm{Re} < 10^6) \tag{6.17}$$

where, Re is the Reynolds number of the pipe flow defined in Equation (6.18).

$$\mathrm{Re} = \frac{2m_f}{\pi \mu r_i} \tag{6.18}$$

where, μ is the dynamic viscosity of the fluid.

Entropy generation calculation

Entropy generation is a term used to evaluate the irreversibility losses of a heat exchanger. The entropy generation rate caused by the finite temperature difference ($S_{gen,\Delta T}$) can be expressed as follows (Bejan 1996).

$$S_{gen,\Delta T} = \frac{Q\Delta T}{T_{f,m}^2(1+\chi)} \tag{6.19}$$

where, χ is a dimensionless temperature difference defined by Equation (6.20) and can be negligible on the thermodynamic temperature scale (Bejan 1996), $T_{f,m}$ is the logarithmic average temperature of the fluid, and ΔT is the temperature difference between the average temperature of the fluid ($T_{f,m}$) and the borehole wall (T_b) (Bejan 1996).

$$\chi = \frac{\Delta T}{T_{f,m}} \tag{6.20}$$

The average fluid temperature in the U-tube ($T_{f,m}$) is computed in the logarithmic average way and expressed as:

$$\frac{1}{T_{f,m}} = \frac{1}{T_{f,1} - T_{f,2}} \int_{T_{f,2}}^{T_{f,1}} \frac{1}{T} dT \tag{6.21}$$

or as:

$$T_{f,m} = \frac{T_{f,1} - T_{f,2}}{\ln \dfrac{T_{f,1}}{T_{f,2}}} \tag{6.22}$$

The irreversibility caused by the fluid friction is expressed by Equation (6.23) (Yekoladio *et al*. 2013, Li *et al*. 2013). The total entropy generation rate in U-tube heat exchangers can be written as Equation (6.24):

$$S_{gen,\Delta P} = \frac{m_{f,tot}\Delta P}{\rho_f T_{f,m}} \tag{6.23}$$

$$\begin{aligned} S_{gen} &= S_{gen,\Delta T} + S_{gen,\Delta P} \\ &= \frac{Q\Delta T}{T_{f,m}^2(1+\chi)} + \frac{m_{f,tot}\Delta P}{\rho_f T_{f,m}} \end{aligned} \tag{6.24}$$

where, $m_{f,tot}$ is the total mass flow rate of the system.

6.2.2.4 Sensitivity analysis

Sensitivity analysis can be generally classified into two groups, the local sensitivity analysis (LSA) and the global sensitivity analysis (GSA) (Haaker *et al*. 2004). LSA measures the extent of the change of the output in accordance with the small variation of a random input around a reference point. The analysis results are partially dependent on the choice of the reference point. Unlike LSA, GSA analysis is totally unrelated to the selection of the reference point, as GSA focuses on the investigation of the contribution of each random input, within its entire range of space, to the variations of the output.

Design of vertical GHEs depends on a number of parameters such as the borehole depth, borehole numbers, borehole radius, and U-tube diameter. All these parameters affect the thermal irreversibility output. Since sensitivity analysis has been widely used to understand the relationships of input parameters on different simulation outputs (Cannavó. 2012), a global sensitivity analysis is performed in this study to screen the design parameters with a significant impact on the thermal irreversibility output.

The Sobol' method, which is a variance-based global sensitivity technique, is used in this study (Sobol′ 1993). The Sobol' method can test the contribution of each input parameter to the variance of the output (Cannavó 2012). The method can be represented in the form of Equation (6.25) (Fesangharya, 2009).

$$Y = f(x_1, x_2 \ldots, x_k) \tag{6.25}$$

where, Y is the model output, and x_1, x_2, …, x_k are the input factors. In this study, Y is the dimensionless entropy generation number, and $x_1, x_2, \ldots, x_k$ represent the design parameters listed in Table 6.1.

The total variance can be determined by Equation (6.26), which will be used to derive the total sensitivity index in Equation (6.27) and used as the measurement index in this study (Fesangharya, 2009).

$$V(Y) = \sum_{i=1}^{k} V_i + \sum_{1<i<j\leq k}^{k} V_{ij} \ldots + V_{1,2,\ldots k} \tag{6.26}$$

$$S_i^{tot} = 1 - \frac{V_{-i}}{V(Y)} \tag{6.27}$$

where, $V(Y)$ is the total variance of the output Y, V_i measures the main effect of the parameter x_i, V_{ij} and $V_{1,2,\ldots,k}$ measure the interaction effects among other parameters except x_i, V_{-i} is the sum of all variance terms that exclude the index i, and S_i^{tot} is the total sensitivity index for x_i which takes into account all effects including the parameter x_i.

The successful use of the Sobol' global sensitivity analysis method is related to the possibility of computing the multi-dimensional integrals (Tang *et al*. 2007). Usually, computing the Sobol indices numerically requires evaluating the correlation coefficients between the output vectors from pairs of model runs, and the Monte Carlo method based on the probabilistic interpretation of an integral is used to generate the random samples of the parameters to compute the Sobol' indices. The principle of Monte Carlo method and the detailed generation of randomly samples of parameters within permissible ranges and estimation of sensitivity indices have been shown in Fesangharya (2009).

6.3 Case study and test results

6.3.1 Illustrative example

The schematic of the system studied is shown in Fig. 6.3, in which a GSHP with the design cooling load of 15 kW is considered and the vertical ground heat exchangers are used. It is worthwhile to note that this GSHP system is a part of the system implemented in the Sustainable Buildings Research Centre at University of Wollongong, Australia. The detailed description of the building and the system can be referred in Chapter 3. For simplification of the optimisation process, only the vertical ground heat exchangers are considered in this

study. The specifications of the system studied and design conditions are shown in Table 6.2.

Table 6.2 Specifications of the system studied and design conditions.

Design condition	Design cooling load (kW)	15
	Indoor design temperature (°C)	24
	Outdoor design temperature (°C)	31
	Average undisturbed soil temperature (°C)	20
Water-water heat pump	Rated cooling capacity/power consumption (kW/kW)	16.4/4.1
	Rated heating capacity/power consumption (kW/kW)	20.4/5.5

6.3.2 Results from sensitivity analysis

Based on the design conditions and the ranges of design parameters provided in Table 6.1 and Table 6.2, global sensitivity analysis is used to evaluate the relative sensitivity of 11 design parameters (see Table 6.1) on the objective function. As mentioned earlier, the ranges of these parameters are determined based on practical engineering projects. Through using the extensive Sobol' method with Monte Carlo simulations, the design parameters can be classified into two groups. One is the parameters to be rather insensitive and called low sensitive parameters. In order to reduce the complexity of the GA search space and save computational time, this group of parameters will not be optimised in the entropy generation minimisation (EGM)-based global optimisation process and the constant values based on good design practices will be assigned for these parameters. The other group of design parameters is sensitive parameters and the changing of these parameters has relatively high effects on the dimensionless entropy generation number (EGN). These parameters will be used as the decision variables and are to be optimised in the EGM-based optimisation process.

For each design parameter studied, the sensitivity index of the entropy generation number (EGN) of the vertical GHEs with respect to the changes of the design parameters is calculated. The results from the global sensitivity analysis are summarized in Fig. 6.4. It

can be observed that the pipe material conductivity (k_p), half shank distance (D) and borehole distance (B) do not have significant effects on the model output of the entropy generation number, and can be considered as low sensitive parameters. These parameters will not be optimised in the EGM-based optimisation process, although the soil thermal conductivity (k_s), grout material thermal conductivity (k_b) and undisturbed soil temperature ($T_{s,0}$) are the three important parameters for the EGN of the vertical U-tube GHEs. However, k_s and $T_{s,0}$ can be determined once the construction site has been chosen. The grout material is normally a mixture of bentonite and S_iO_2 sand, and its thermal conductivity is normally around 2.04-2.42 (W/mK) (ASHRAE, 2011). Therefore, these three parameters are not optimised by the EGM optimisation in this study as well. The values of the low sensitive parameters and the construction site related parameters used in this study are summarised in Table 6.3, which are the recommendation values from practical engineering projects (ASHRAE 2011; Banks 2012). The other parameters will be globally optimised by the GA optimiser.

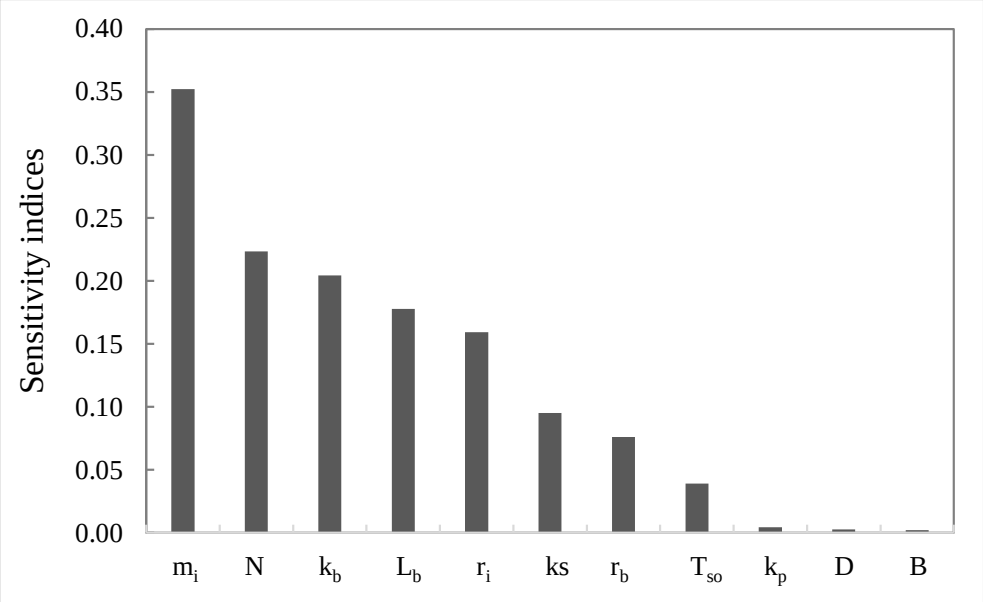

Fig. 6.4 Sensitivity indices of the EGN for different design parameters.

Table 6.3 Low sensitive parameters and the values used (ASHRAE 2011, Banks 2012)

Parameters	Values	Units
Pipe material conductivity (k_p)	0.5	W/mK
Borehole distance (B)	8	m
Half shank space (D)	r_b-2r_o	m
Soil material conductivity (k_s)	2.0	W/mK
Grout material thermal conductivity (k_b)	2.42	W/mK
Undisturbed soil temperature ($T_{s,0}$)	20	°C

Fig. 6.5 presents the variations of the entropy generation number (EGN) with respect to the change of the five design parameters to be optimised by the EGM-based optimisation process while keeping other parameters constant, which was based on the values of the parameters for the base design case provided in Table 6.3 and the variation ranges of each design parameter presented in Table 6.1.

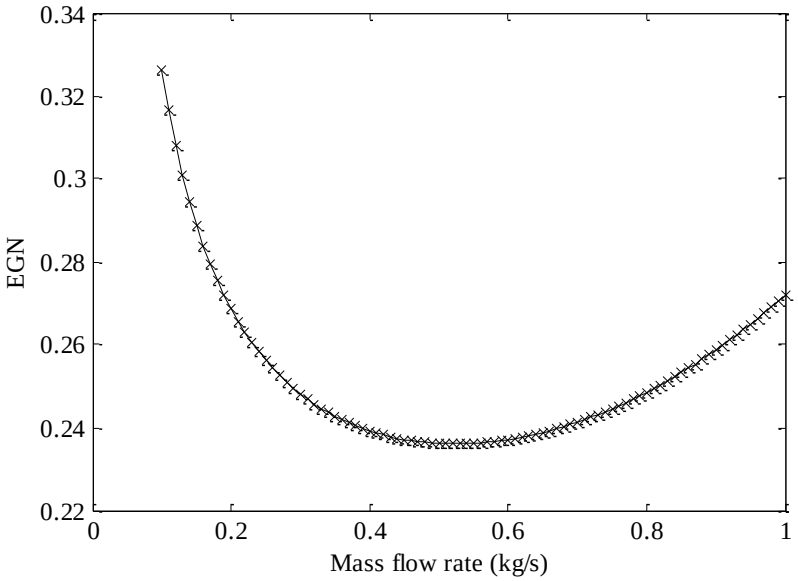

a) EGN versus mass flow rate

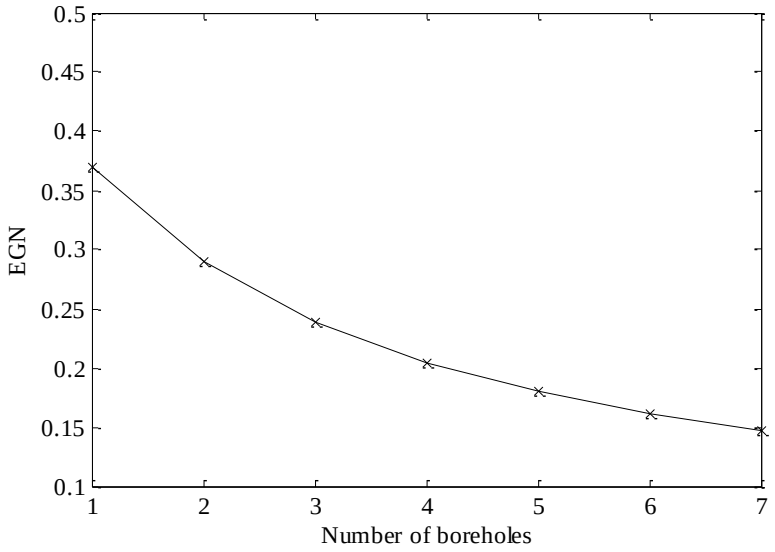

b) EGN versus borehole numbers

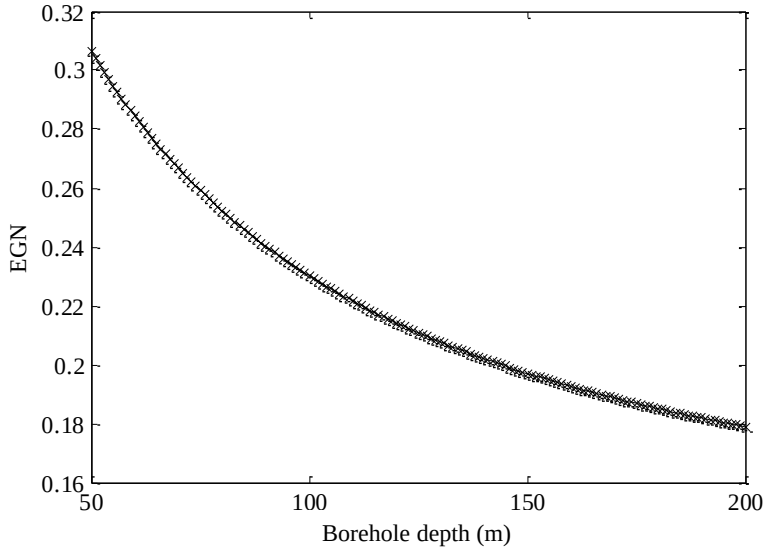

c) EGN versus borehole depth

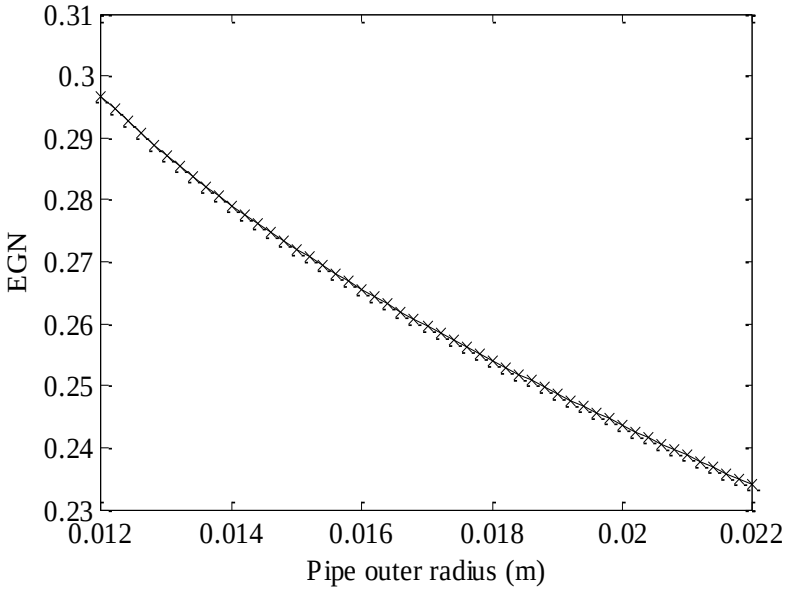

d) EGN versus pipe outer radius

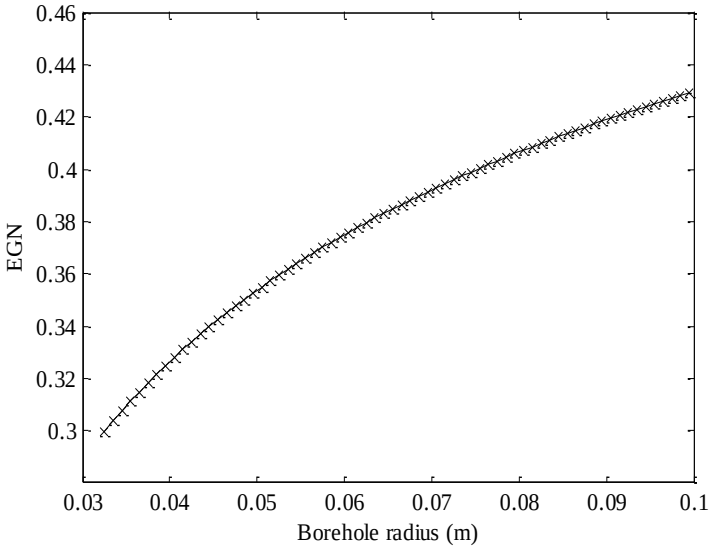

e) EGN versus borehole radius

Fig. 6.5 Variations of the entropy generation number for high sensitive parameters.

Fig. 6.5a shows the existence of the optimal mass flow rate (m_f) per U-tube for minimizing the EGN. From Fig. 6.5b–6.5d, it can be found that, with the increase of the borehole number (N), borehole depth (L_b) and pipe outer radius (r_o), the entropy generation number (EGN) decreases. As shown in Fig. 6.4e, the EGN decreases with the decrease of borehole radius (r_b). The reason is that the thermal performance of the vertical GHEs increases with the increase of the borehole depth (L_b) and pipe outer radius (r_o), and the decrease of

borehole radius (r_b). All the above results indicate that the undesirable thermodynamic irreversibility quantified by the entropy generation number decreases the thermal performance of the vertical U-tube GHE.

6.3.3 Results from the entropy generation minimisation (EGM) optimisation

For the given example with the design conditions, the selected parameters are globally optimised using genetic algorithm toolbox of MATLAB (Houck 1996). According to the ranges of the design variables, an initial random population is generated to carry out the iterative search process. The maximum number of generations used is 100, which was determined based on many trial tests. The normalized geometric selection, arithmetic crossover and adaptive feasible mutation were employed in the GA optimiser. The variances of the fitness function are shown in Fig. 6.6.

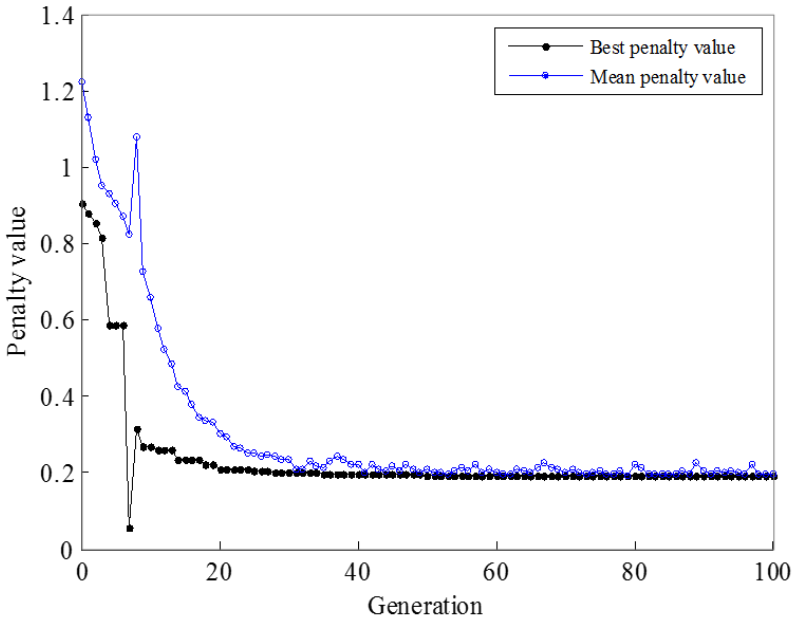

Fig. 6.6 Variations of the penalty value of the best individual in each generation.

It can be found that the fitness value was basically stable after 50 generations, and reached the optimum when the termination condition is met. After 100 generations, the optimal solution of the vertical GHE optimisation design problem is obtained and the results are summarized in Table 6.4 together with the results of the original design (i.e. base design

case). The entropy generation numbers of the base design case and optimal design case are 0.2180 and 0.1913, respectively. Compared to the base design case, a 12.2% reduction in the entropy generation number was achieved by using the optimal design values.

Table 6.4 Original and optimal design parameters of the vertical U-tube GHEs.

Case	r_b (m)	m_f (kg/s)	L_b (m)	N	r_o (m)	EGN	EGN reduction (%)
Base design	0.075	0.4	91	3	0.020	0.2180	-
Optimal design	0.06	0.595	126	2	0.016	0.1913	12.2

6.3.4 Economic analysis

In order to validate the effectiveness of the proposed EGM-based design optimisation method for the vertical U-tube GHEs, an economic analysis was performed for the optimal design and base design. There are a variety of economic analysis methods (e.g. life cycle cost method, payback period method etc.). These methods require a number of variables as input (e.g. general inflation rate, investment escalation rate etc.), and they are most commonly employed to perform detailed thermo-economic analysis of thermal systems or to solve practical problems in optimising the thermal systems (Sanaye *et al*. 2009, Alavy *et al*. 2013 Robert *et al*. 2014).

The purpose of the economic analysis in this section is to approximate the potential savings by using the GSHP system with optimised design parameters when compared to using the GSHP system with original design parameters. The sum of the first upfront cost and straight addition of 20 years' operating cost is the most simple and straightforward method to achieve the purpose. As a GSHP system is generally believed to have a life span of more than 20 years (Alavy *et al*. 2013, Garber *et al*. 2013), 20 years should be a reasonable assumption to approximately represent the lifetime of the concerned GSHP system.

The first upfront cost (*IC*) and operating cost (*OC*) were determined based on the cost data shown in Table 6.5, which was provided by GeoExchange Australia Pty Ltd. The total system cost (*TSC*) of the 20 years operation of the concerned GSHP systems is used as the

performance indictor and expressed in Eq. (6.28). For ground heat exchangers, the upfront cost can be determined by Eq. (6.29). For the water-water heat pump, the upfront cost can be determined by Eq. (6.30) and the operation cost can be determined by Eq. (6.31).

$$TSC = IC_{GHE} + IC_{HP}^{tot} + OC_{HP} \tag{6.28}$$

$$IC_{GHE} = C_p L_p + C_b L_{tot} \tag{6.29}$$

$$IC_{HP}^{tot} = IC_{HP} N_{HP} \tag{6.30}$$

$$OC_{HP} = C_{ele} P_{tot} \tag{6.31}$$

where, IC is the upfront cost, OC is the 20 years' operation cost, C_p is the cost of U-tube per meter, and C_b is the drilling and grouting cost of per borehole per meter, C_{ele} is the electricity price per kWh, L_{tot} is the total borehole length which is calculated by multiplying the borehole number and depth, and L_p is the U-tube length within one borehole.

Table 6.5 Installation cost for borehole heat exchangers

Component	Cost
U-shaped polyethylene pipe	2.5* ($/m)
Drilling cost	75 ($/m)
Grouting cost	8 ($/m)
Water-to-water heat pump	6000 ($/unit)
Electricity price	0.25 ($/kWh)

*Mean cost determined based on the installation cost for 40 mm and 32 mm outer diameters of the U-shaped polyethylene pipes.

In order to facilitate the economic analysis, a simulation platform representing the real vertical GSHP system shown in Fig. 6.3, was developed by using TRNSYS and is illustrated in Fig. 6.7. In the simulation platform, the major component models used were the mathematical models provided in the standard TRNSYS library. The key component models used are the water-to-water heat pump model (Type 927), vertical U-tube GHE model (Type 557), and water pump model (Type 110).

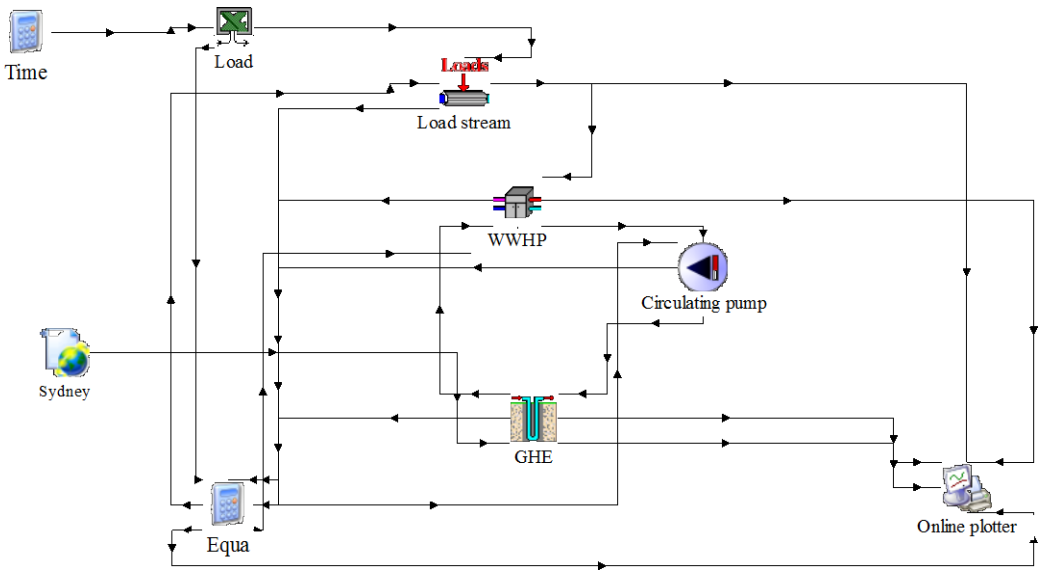

Fig. 6.7 Illustration of the simulation platform developed by TRNSYS.

The heating and cooling loads associated to the vertical GSHP system were estimated based on the total building loads simulated in the Chapter 4 and the load ratio of the vertical system at the design condition. The estimated building load profiles and Sydney weather conditions have been presented in Fig. 4.2, Chapter 4. The annual maximum entering water temperature to the water-water heat pump and the variation of the annual energy consumption of the GSHP system with the vertical U-tube GHEs in 20 years' of operation were estimated and the results are shown in Fig. 6.8 and Fig. 6.9. It is clearly shown that the annual maximum entering water temperature to the water-water heat pump in the optimal design case is larger than that of the base design case. This is due to the fact that the reduction of the total borehole length (L_{tot}) resulted in the increase of the heat flux in the optimal design case. The increase of the heat flux tended to increase the circulating fluid temperature in the vertical U-tube GHEs, and the increase of the entering water temperature led to the increase of the energy consumption of the water-water heat pump in the cooling operation condition, which can be derived from Equations (6.12)-(6.14).

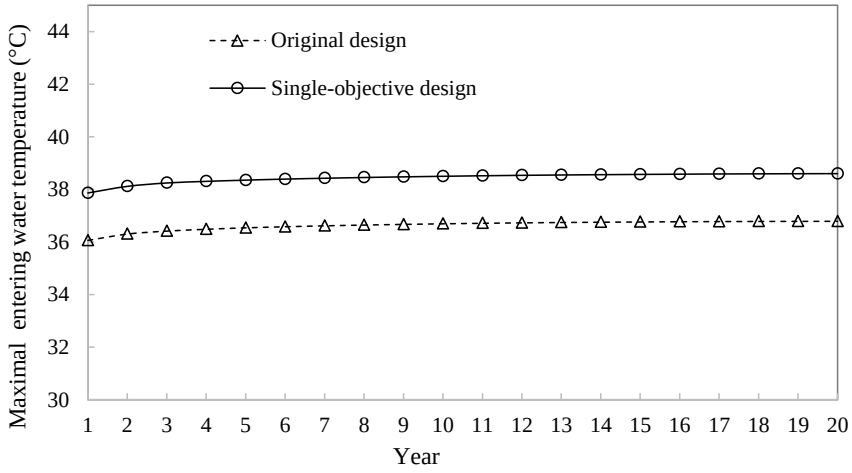

Fig. 6.8 Annual maximum entering water temperature (EWT) to the water-to-water heat pump in 20 years' operation.

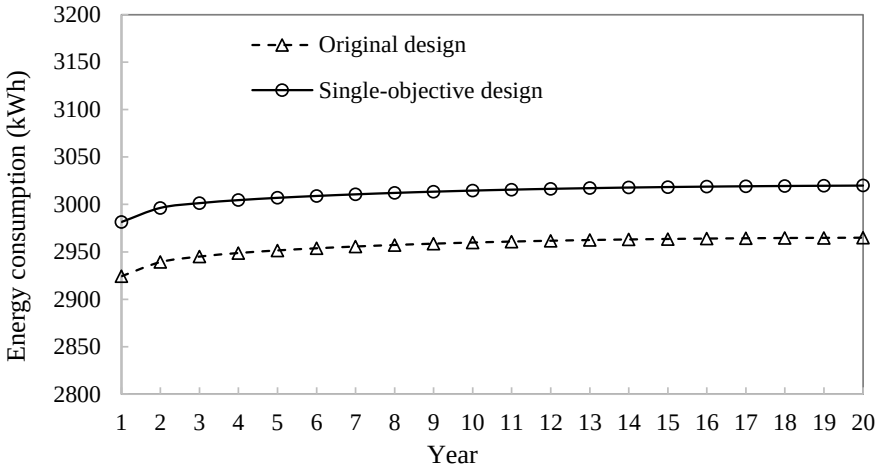

Fig. 6.9 Annual energy consumption of the vertical GSHP in 20 years' operation.

The results of the economic analysis for the optimal design case and the base design case are summarised in Table 6.6. It is clearly shown that the total system cost (i.e. the upfront cost and 20 years' operation cost) for the optimal design case is 3.5% lower than that of the base design case. However, the operating cost for the optimal design case is 1.9% higher than that of the base design case, while the upfront cost of the optimal design case is 6.2% lower than the base design case.

Table 6.6 Economic cost analysis of the system with two different designs

	Base case	Optimal case
Number of boreholes	3	2
Borehole depth (m)	91	126
Outer pipe diameter (m)	0.040	0.032
Borehole radius (m)	0.075	0.06
Energy consumption in 20 years' operation (kWh)	59,128	60,233
20 years' operating cost ($)	14,782	15,058
Total upfront cost ($)	30,024	28,176
Total system cost (i.e. Upfront cost and 20 years' operation cost) ($)	44,806	43,234
Total system cost savings (%)	-	3.5

Fig. 6.10 presents the relationship between the entropy generation number and the economic aspects of the GSHP with vertical U-tube GHEs under different entropy generation numbers. The entropy generation numbers were obtained from the EGM-based optimisation process. From Fig. 6.10, it can be observed that the operation cost slightly increases, while the total system cost and upfront cost decrease, with the increase of the entropy generation number. From the thermodynamic aspect, the smaller of the entropy generation number, the better the thermal performance of the vertical U-tube GHEs. However, from the economic aspects, it seems that a relatively larger value of the entropy generation number will decrease the upfront cost in the case studied. Therefore, it is necessary to optimise the entropy generation number by taking into account both the thermodynamic and economic aspects when using entropy generation minimisation method to design vertical ground heat exchangers.

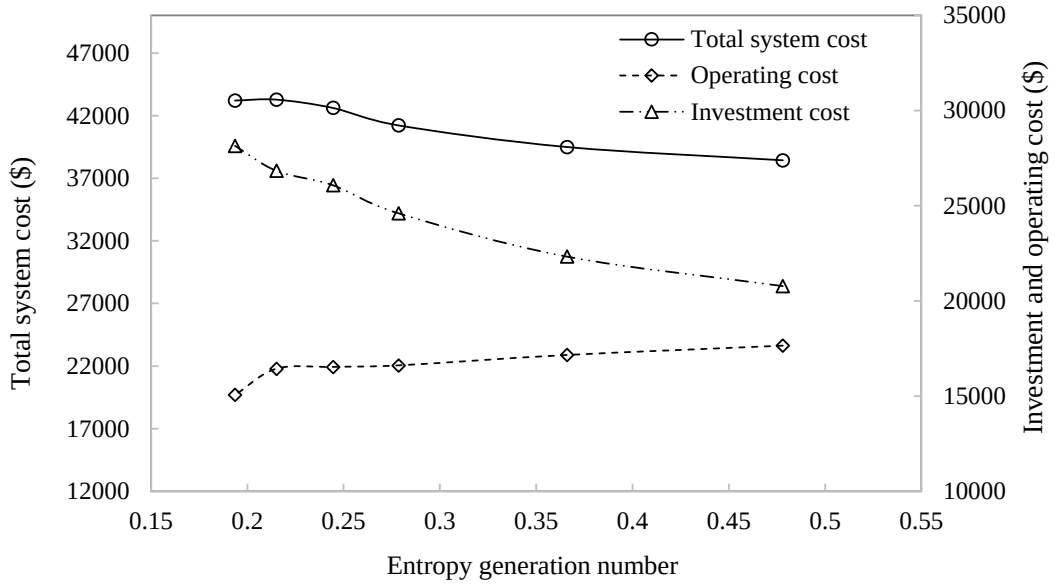

Fig. 6.10 Variations of the entropy generation number with respect to the total system cost, upfront cost and operating cost of the vertical GSHP.

6.4 Summary

In this chapter, a new method for optimal design of vertical U-tube ground heat exchangers was proposed. In this method, the entropy generation number was used as the objective function, and a genetic algorithm optimisation technique was applied to solve the optimisation problems and identify the globally optimal design settings.

The performance of the proposed design method was evaluated through simulations. Five key design variables, including number of boreholes, borehole depth, outer pipe diameter, borehole radius, and circulating fluid mass flow rate per pipe, were identified by the global sensitivity analysis. The entropy generation minimisation (EGM)-based optimisation was used to globally optimise the key design variables. The results showed that the total system cost (i.e. the upfront cost and 20 years operation cost) of the system studied with the decision parameters optimised by the EGM optimisation was 3.5% lower than that of using the original design parameters. The results also demonstrated the effectiveness of integrating the entropy generation minimisation method with economic analysis for optimal design of vertical ground heat exchanger.

Chapter 7

Multi-Objective Design Optimisation of Vertical Ground Heat Exchangers

A single-objective design optimisation methodology based on entropy generation minimisation was presented in Chapter 6. However, decision making process requires more than the simply minimising the entropy generation rate, due to the fact that, the system with a higher thermodynamic perfection may result in a higher system upfront cost, despite that the operating cost may be reduced. This chapter presents a multi-objective design optimisation strategy for vertical U-tube ground heat exchangers (GHEs) to find solutions that can simultaneously satisfy the economic objective (i.e. system upfront cost) and thermodynamic objective (i.e. entropy generation number). The optimisation process is the search for a range of Pareto optimal solutions with the consideration of two competing objective functions. The same design variables of vertical U-tube GHEs as identified in Chapter 6 are used and optimised by a genetic algorithm (GA) optimiser implemented in MATLAB. Based on the Pareto frontier obtained from the GA optimisation, a decision-making strategy is then used to determine a final solution. Two case studies are presented to validate the effectiveness of the proposed strategy. The first case study is a small scale GSHP system in Australia which was presented in Chapter 6. The second case study is a relatively large scale GSHP system implemented in China.

This chapter is organised as follows: Section 7.1 overviews the application of multi-objective optimisation in thermodynamic system analysis. Section 7.2 outlines the proposed multi-objective design optimisation methodology for vertical GHEs. Two case studies to validate the proposed design optimisation methodology are presented in Section 7.3. Section 7.4 summaries the main findings of this study.

7.1 Introduction

In general, the design optimisation of a thermal energy system is a process which includes

the modification of the system component structure and design parameters based on single or multiple specified design objectives (Bejan 1996). The design optimisation requires specific design objectives, which can be classified into three groups, including thermodynamic objective (i.e. maximum thermal efficiency), economic objective (i.e. minimum unit cost) and environmental objective (i.e. minimum GHG gas emissions) (Peters *et al*. 1991).

In the design optimisation of GSHP systems, as reviewed in Chapter 2, most studies conducted considered one objective function, either the economic objective or the thermodynamic objective. In the economic optimisation, the objective function is normally derived based on life cycle cost analysis (Kreith *et al.* 2008, Peterson *et al*. 2012), while in the thermodynamic performance optimisation, entropy generation number (EGN) often serves as the objective function in the entropy generation minimisation (EGM) method (Maheshkumar *et al*. 2011, Li *et al*. 2013). For a single-objective optimisation method, it considers one objective function, either the economic objective (i.e. minimisation of cost) or the thermodynamic objective (i.e. minimisation of thermodynamic irreversibility), the limited consideration of the objective function would lead to the search of possible extreme points (Toffolo *et al*. 2002, Ndao *et al*. 2009, Sayyaadi *et al*. 2009).

In order to overcome the disadvantage of single-objective design optimisation, the theory of multi-objective optimisation has been proposed. Various approaches have been used to formulate the multi-objective optimisation methodologies (Frangopoulos 1987, Von Spakovsky *et al*. 1990). As reviewed in Chapter 2, multi-objective optimisation has been used to facilitate the optimal design of various thermodynamic systems and exhibited better performance than that of single-objective optimisation.

In this chapter, a multi-objective design optimisation strategy for vertical U-tube ground heat exchangers is first developed by considering entropy generation number (EGN) and system upfront cost as two conflicting objective functions. The design variables identified by a global sensitivity analysis method in Chapter 6 are then used as the decision variables. Finally, two case studies are presented to validate the effectiveness of the proposed multi-objective design optimisation strategy.

7.2 Development and formulation of the design optimisation strategy

7.2.1 Outline of the multi-objective design optimisation strategy

The multi-objective design optimisation strategy for vertical U-tube GHEs proposed is outlined in Fig. 7.1, which mainly consists of three steps. The first step is to use a global sensitivity analysis method to reduce the size of the optimisation problem by identifying the high sensitive design parameters. The high sensitive design parameters identified are then globally optimised in the second step through a multi-objective genetic algorithm optimiser, to search for a set of Pareto optimal solutions based on the two objective functions defined and the mathematic model of the vertical U-tube heat exchanger as well as the constraints defined for each key design variable. The third step is the decision-making process to determine the desired optimal solution among a set of Pareto optimal points.

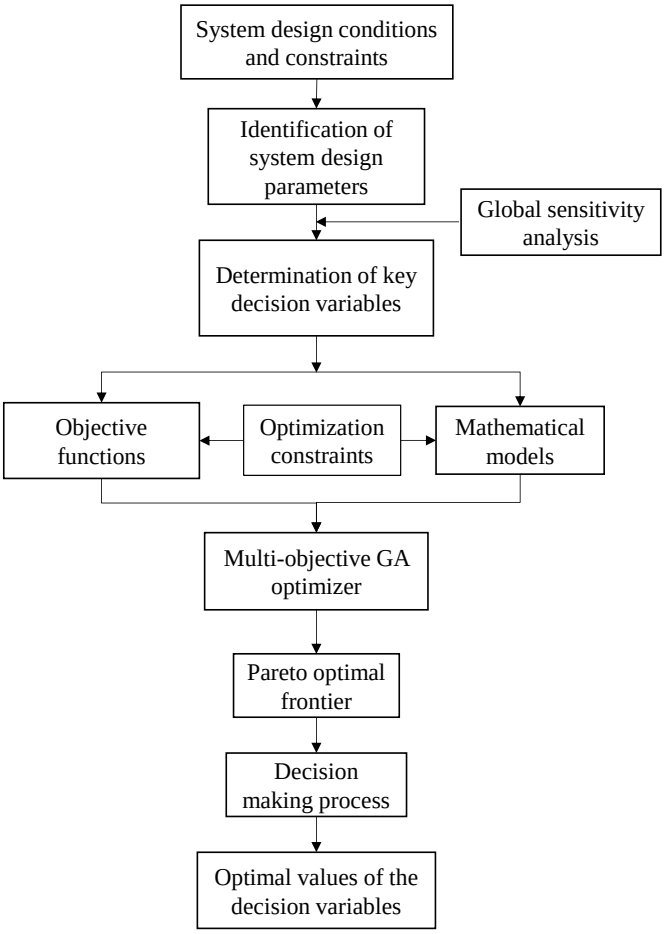

Fig. 7.1 Outline of the design optimisation strategy.

MATLAB's multi-objective genetic algorithm solver, namely *gamultiobj* (Mathworks 2004), is used to solve the optimisation problem and identify a set of Pareto optimal solutions. The *gamultiobj* genetic algorithm solver consists of the objective functions and the parameter space along with some genetic algorithm options, and the results of the function are a set of non-inferior solutions (Mathworks 2004).

In this study, the same design variables and their constraints, and the same mathematical models as that used in Chapter 6 were used to formulate the multi-objective optimisation strategy. The formulation of the objective functions and the decision-making in the multi-objective design optimisation are described below.

7.2.2 Formulation of the objective functions

There are two different objective functions used to formulate the design optimisation strategy. One is the entropy generation number (i.e. EGN) and the other is the system upfront cost. EGN is used to represent thermodynamic irreversibility due to the friction fluid flow and heat transfer driven by the finite temperature difference in the vertical GHEs (Bejan 1996). It is represented based on the entropy generation rate (S_{gen}) expressed in Equation (7.1) (Bejan 1996).

$$N_s = \frac{S_{gen} \cdot T_{f,m}}{Q} \tag{7.1}$$

where, N_s is the dimensionless entropy generation number, S_{gen} is the entropy generation rate, $T_{f,m}$ is the mean fluid temperature, and Q is the heat transfer rate.

The system upfront cost (UC) is the sum of the capital costs of major components in the vertical GSHP system, as expressed in Equation (7.2). As the upfront costs of the water pumps and valves in the pipelines are relatively small when compared to the costs of the water-water heat pumps and ground heat exchangers, their upfront costs are not considered in this study. The upfront costs of the U-tube ground heat exchangers (UC_{GHE}) and water-water heat pumps (UC_{HP}) are determined by Equation (7.3) and Equation (7.4), respectively.

$$UC = UC_{GHE} + UC_{HP} \tag{7.2}$$

$$UC_{GHE} = C_p L_p + C_b L_{tot} \tag{7.3}$$

$$UC_{HP} = \sum_{i=1}^{n} C_{HP,i} \tag{7.4}$$

where, C_p is the cost of the U-tube per meter, C_b is the drilling and grouting costs of per borehole per meter, C_{HP} is the cost of per water-water heat pump, L_{tot} is the total borehole length which is calculated by multiplying the borehole number and borehole depth, L_p is the total U-tube length within the boreholes, and n is the total number of the water-water heat pumps.

7.2.3 Decision-making in multi-objective design optimisation

Generally, the purpose of the multi-objective optimisation is to obtain the sound trad-off solutions by analysing the multiple conflicting objective functions (Asadi *et al*. 2014). As the multiple objective functions are conflicting, it is not possible to find a single solution that is optimal for all the objective functions simultaneously, but a set of Pareto optimal solutions (Giagkiozis *et al*. 2015). The Pareto frontier is one of the key concepts and can be used to establish a hierarchy among the solutions of a multi-objective optimisation problem to determine whether a solution is one of the best possible trades-offs (Najafi *et al*. 2011, Giagkiozis *et al*. 2015, Sreepathi *et al*. 2015).

In multi-objective design optimisation, decision-making is essential for the selection of the final solution among a set of optimum points on the Pareto frontier. The decision-making process is generally performed based on the engineering experience and the importance of each objective for decision-makers (Sayyaadi *et al*. 2009, Najafi *et al*. 2011). In this study, a hypothetical point, named as ideal point (Navidbakhsh *et al*. 2013), is used to assist in determining the final optimal solution in the decision-making process. In the Pareto frontier, both objectives have their optimum values and are independent with each other in the ideal point. The ideal point cannot be located on the Pareto frontier as it is impossible to have both objectives at their optimum values simultaneously. Therefore, the closest point of the Pareto frontier to the ideal point can be considered as a desired final solution (Ghanadi *et al*. 2012). The dimension of various objectives in a multi-objective optimisation problem might be different. For instance, in this study, the EGN is a dimensionless objective while

the system upfront cost is a dimensional objective. It is therefore necessary to non-dimensionalise the objective vectors prior to the decision-making process (Navidbakhsh *et al*. 2013, Ahmadi *et al*. 2013).

In this study, the solutions on the Pareto frontier are normalised using a fuzzy non-dimensionalisation method, which is capable of handling the ambiguity associated with the relative importance of objective functions (i.e. objective space) (Perera *et al*. 2013). The normalised values for each objective vary between 0 and 1.

In a fuzzy non-dimensionalisation method, the non-dimensional objective function (F_{ij}^{n}), is defined by Equation (7.5) for minimising objectives or Equation (7.6) for maximising objectives (Koski 1984, Koski *et al*. 1987, Marler *et al*. 2004)

$$\min F_{ij}^{n} = \frac{\max(F_{ij}) - F_{ij}}{\max(F_{ij}) - \min(F_{ij})} \tag{7.5}$$

$$\max F_{ij}^{n} = \frac{F_{ij} - \min(F_{ij})}{\max(F_{ij}) - \min(F_{ij})} \tag{7.6}$$

where *ij* is an index for each individual solution on the Pareto frontier, *min* and *max* represent the minimum and maximum values of each objective among the corresponding values for all solutions on the Pareto frontier.

7.3 Performance tests and evaluation

7.3.1 Description of two case studies

In this study, two case studies are used to validate the effectiveness of the proposed multi-objective design optimisation strategy for vertical U-tube GHEs. *Case I* uses the same GSHP system used in Chapter 6, which is based on the GSHP system implemented in the Sustainable Buildings Research Centre (SBRC), University of Wollongong, Australia, as introduced in Chapter 3.

Case II is based on a relatively large scale GSHP system designed for a three story dining hall, as illustrated in Fig. 7.2, at Xi'an Jiaotong University, China. Xi'an is in the sub-humid warm temperate continental monsoon climate, with hot and rainy summer and cold

winter. The total floor area of the building is 15,528 m^2, and the total design cooling load and heating load of the building are 1871 kW and 1451 kW, respectively. The GSHP system in this building consists of 270 vertical U-tube GHEs with a 100 m borehole depth each, a 90 mm borehole radius and a 4 m borehole distance. The total required installation area is 4320 m^2. In order to simplify the simulation process, a water-to-water heat pump with a cooling capacity of 937 kW is assumed to connect with the 270 vertical boreholes to supply the heating and cooling for the cooking area and student dining area, which accounts for approximately 50% of the total building heating and cooling demand. The rest of the heating and cooling demand of the building is supplied by the conventional air-conditioning systems.

The specifications and design conditions of the above two GSHP systems are summarized in Table 7.1. The indicative installation costs for vertical U-tube GHEs in Australia and in China are presented in Table 7.2.

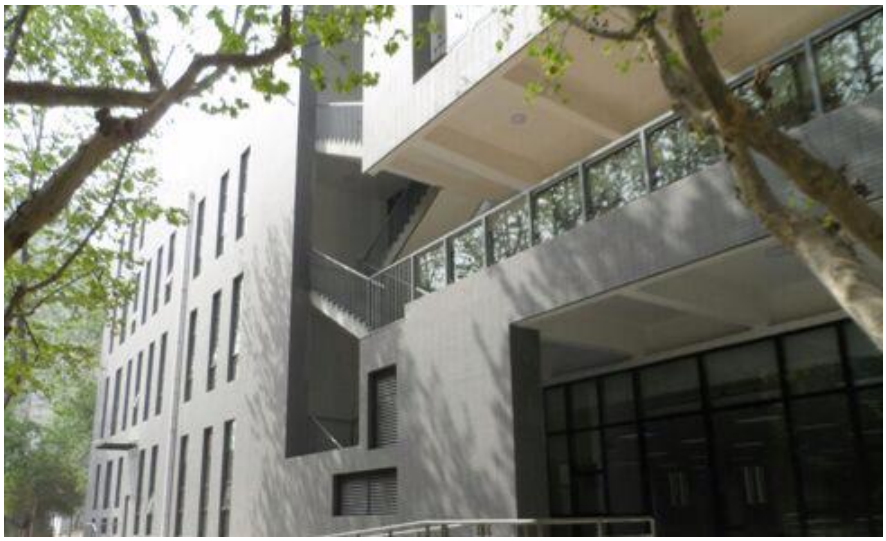

Fig. 7.2 Render of the building concerned in *Case II*.

Table 7.1 Design specifications and design conditions of the two GSHP systems concerned

Parameters		*Case I*	*Case II*
Pipe material conductivity k_p (W/m·K)		0.5	0.5
Borehole distance B (m)		8	4
Half shank space D (m)		r_b-2r_o	r_b-2r_o
Soil material conductivity k_s (W/m·K)		2.0	2.0
Grout material thermal conductivity k_b (W/m·K)		2.42	2.42
Undisturbed soil temperature $T_{s,0}$ (°C)		20	18
Design condition	Design cooling load (kW)	15	927
	Indoor design temperature for cooling (°C)	24	25
	Outdoor design temperature (°C)	31	33
	Mean undisturbed soil temperature (°C)	20	18
Water-water heat pump	Rated cooling capacity/power (kW/kW)	16.4/4.1	937/209
	Rated heating capacity/power (kW/kW)	20.5/5.5	1024/231

Table 7.2 Installation costs for vertical U-tube heat exchangers

Component	Cost (Australia)	Cost (China)
U-shaped polyethylene pipe	2.5* ($/m)	10 (¥/m)
Drilling cost	75 ($/m)	110 (¥/m)
Grouting cost	8 ($/m)	
Water-water heat pump	6000 ($/unit)	749,600 (¥/unit)
Electricity price	0.25 ($/kWh)	0.79 (¥/kWh)

* Mean cost determined based on the installation costs for 40 mm and 32 mm outer diameters of the U-shaped polyethylene pipes

7.3.2 Setup of the tests

The same simulation platform, as illustrated in Fig. 6.7 of Chapter 6, is applied to facilitate the system performance evaluation and economic analysis. The heating and cooling loads associated to the vertical GSHP system in *Case I* were estimated based on the total building loads simulated in Chapter 4 and the load ratio of the vertical system at the design

condition. The estimated building load profiles and Sydney weather conditions are illustrated in Fig.4.2, Chapter 4**.**

Fig. 7.3 (a) shows the total heating and cooling loads of the three story dining hall (*Case II*) with the floor areas supplied by the GSHP system, based on the Chinese Standard Weather Data (CSWD) for Xi'an, China, as shown in Fig. 7.3(b), which was also simulated using DesignBuilder.

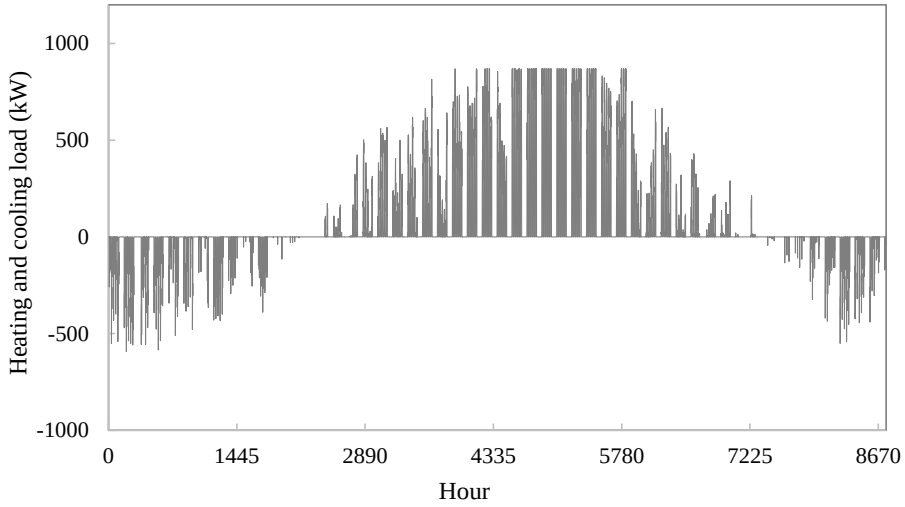

a) Load profile of the areas supplied by the GSHP - *Case II*

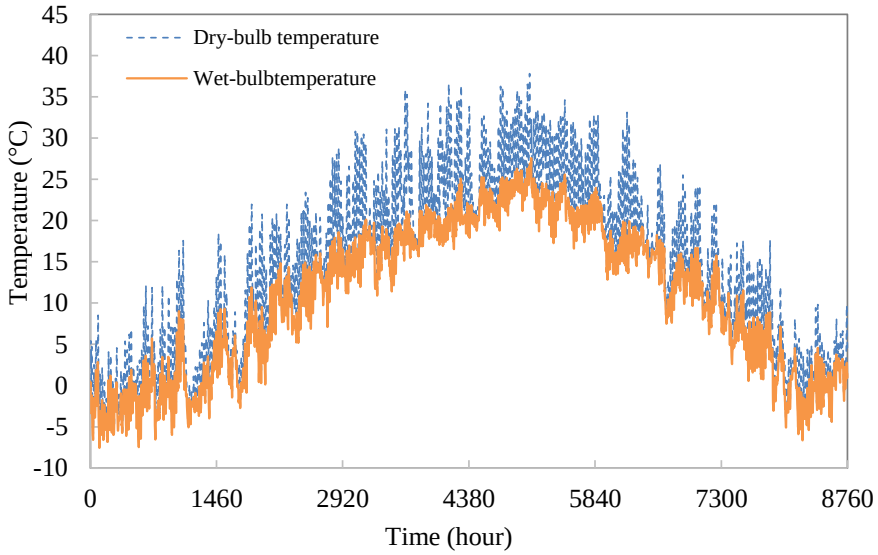

b) Xi'an weather condition - *Case II*

Fig. 7.3 Building heating and cooling load profiles and weather conditions - *Case II*.

7.3.3 Test results from *Case I*

7.3.3.1 Determination of the final optimal solution in the multi-objective design optimisation

Fig. 7.4 presents the Pareto optimum frontier obtained by using the proposed multi-objective design optimisation strategy, which was generated based on the design conditions described in Table 7.1 and the cost data presented in Table 7.2. It can be found that the system upfront cost decreased with the increase of the EGN, which indicates that the optimal solutions are the trade-off between the two competing objective functions. Theoretically, each point on the Pareto frontier could be the optimal solution for a specific project dependent on the preference of the decision makers and the project limits.

Fig. 7.5 shows the approach employed to determining the final optimal solution, and the normalized Pareto frontier based on the method introduced in Section 7.2.3. The closest point in the normalized Pareto frontier to the ideal unreachable point (e.g. hypothetical point) was selected as the desired final optimal solution. This solution is considered as a trade-off between the system upfront cost and EGN. It is worthy to note that the final solution determined by this approach might not be the globally optimised solution but it can be considered as one of the best solutions.

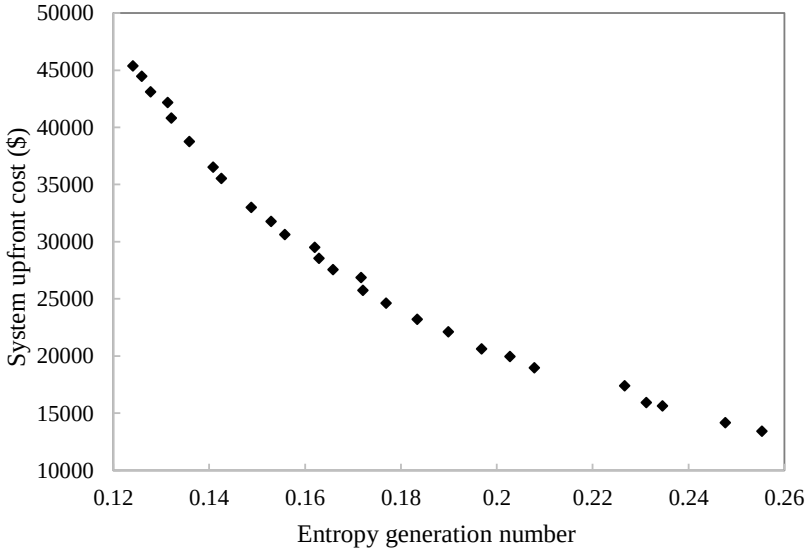

Fig. 7.4 Illustration of the Pareto optimal frontier identified - *Case I*.

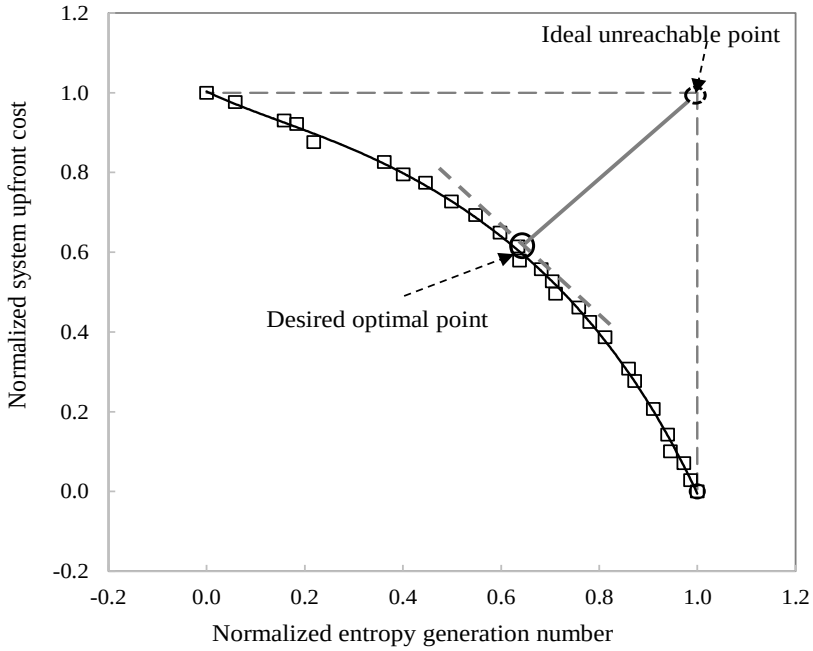

Fig. 7.5 Normalized Pareto frontier and determination of the final solution - *Case I*.

7.3.3.2 Comparison among the results using different design strategies

In this section, a comparison among the results by using the proposed multi-objective design optimisation strategy and an entropy generation minimisation (EGM)-based single-objective design optimisation strategy as well as the original design is provided. The EGM-based single-objective design optimisation strategy employed the EGN as the objective function, and used the same mathematic models and optimisation constraints as those used in the proposed multi-objective design optimisation strategy. The details on the EGM single-objective design optimisation strategy used can be found in Chapter 6.

Table 7.3 summaries the results obtained by using the three different design strategies. It can be observed that the EGNs by using the original design, EGM-based single-objective design optimisation and multi-objective design optimisation were 0.2180, 0.1913 and 0.1929, respectively. The higher EGN represents the larger thermal irreversibility and the lower thermal performance of the vertical U-tube GHEs. Compared to the original design, a 12.2% reduction in the EGN was achieved by using the EGM-based single-objective design optimisation, and an 11.5% reduction was achieved by using the proposed multi-objective

design optimisation. Compared with the EGM-based single-objective design optimisation, the use of the multi-objective design optimisation resulted in a larger EGN. The larger EGN may deteriorate the thermal performance of the vertical U-tube GHEs, but it will help reduce the system upfront cost, which will be demonstrated in Section 7.3.3.3.

Table 7.3 Comparison among three different designs - *Case I*

Design optimisation strategy	r_b (m)	m_f (kg/s)	L_b (m)	N (-)	r_o (m)	EGN (-)	EGN reduction (%)
Original	0.075	0.4	91	3	0.020	0.2180	-
EGM-based single-objective	0.06	0.595	126	2	0.016	0.1913	12.2
Multi-objective	0.085	0.75	110	2	0.020	0.1929	11.5

7.3.3.3 Economic analysis

An economic analysis was also performed to validate the effectiveness of the proposed multi-objective design optimisation strategy for the vertical U-tube GHEs. In this study, the total system cost, including the upfront cost and 20 years' operating cost of the concerned GSHP system, is used as the performance indicator. The analysis was performed based on the simulation platform presented in Fig. 6.7 of Chapter 6, and the cost data presented in Table 7.2.

The annual maximum entering water temperature to the water-water heat pump and the variation of the annual energy consumption of the GSHP system with the vertical U-tube GHEs in 20 years of operation are shown in Fig. 7.6 and Fig. 7.7, respectively. As mentioned earlier, the energy consumption did not include the energy consumption of the water pump in the system. It is worthwhile to note that including the energy consumption of the water pump will affect the overall optimisation results, but the impact on the total system cost is less than 1.0% in this case.

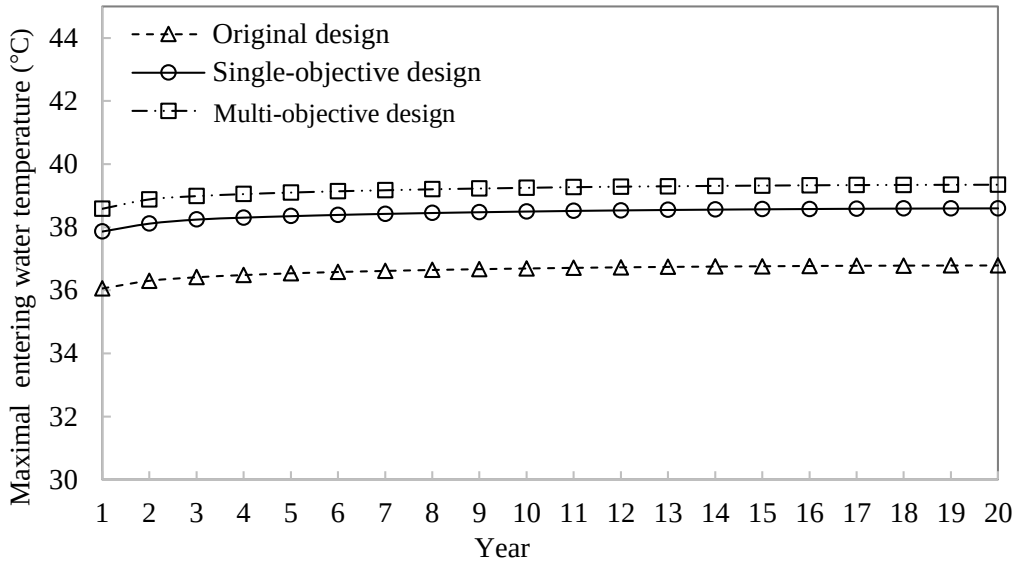

Fig. 7.6 Annual maximum entering water temperature to the water-water heat pump - *Case I.*

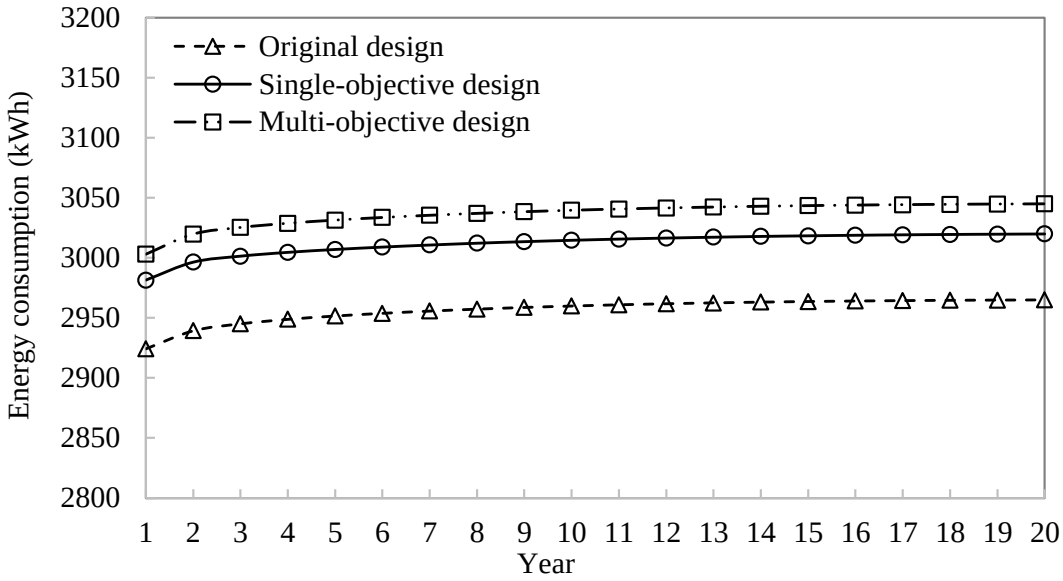

Fig. 7.7 Annual energy consumption of the GSHP concerned - *Case I.*

It is shown that the annual maximum entering water temperature to the water-water heat pump and the annual energy consumption of the system concerned by using the proposed multi-objective design optimisation strategy were higher than that using the EGM-based single-objective design optimisation and the original design. This is mainly due to the reduction of the total borehole length when the proposed strategy was used. The shorter

total borehole length resulted in an increase in the heat flux per meter per borehole, which increased the mean circulating fluid temperature in the vertical U-tube GHEs. The increase of the entering water temperature will lead to an increase of the energy consumption of the water-water heat pump for this cooling-dominated building. Compared to the original design and the EGM-based single-objective design optimisation, the use of the proposed strategy can result in a reduction of the total borehole length by 19.4% and 12.7%, respectively. The use of the EGM-based single-objective design optimisation also led to a higher annual energy consumption and a larger annual maximum entering water temperature to the water-water heat pump, as compared to the original design. From Fig. 7.7, it can also be found that the annual energy consumption of the GSHP system increased with the increase of the operating years due to the performance degradation of the vertical U-tube GHEs resulted by the unbalanced heat rejection and extraction.

Table 7.4 summarises the results from the economic analysis by using the three different designs. It is clearly shown that the total system costs (i.e. the upfront cost and 20 years' operating cost) by using the proposed multi-objective design optimisation and EGM-based single-objective design optimisation were 9.5% and 3.5% lower than those by using the original design, respectively.

Table 7. 4 Economic analysis of the system by using three different designs - *Case I*

	Original design	Single-objective design	Multi-objective design
Number of boreholes	3	2	2
Borehole depth (m)	91	126	110
Energy consumption in 20 years operation (kWh)	59,128	60,233	60,724
20 years' operating cost ($)	14,782	15,058	15,181
Total upfront cost ($)	30,024	28,176	25,360
Total system cost (i.e. upfront cost and 20 years' operating cost) ($)	44,806	43,234	40,541
Total cost savings (%)	-	3.5	9.5

It can also be found in Table 7.4 that the system operating costs by using the multi-objective design optimisation and EGM-based single-objective design optimisation were $15,181 and $15,058 respectively, where were 2.7% and 1.9% higher than those of using the original design, while the system upfront costs by using the two design optimisation strategies were $25,360 and $28,176, respectively, where were 15.5% and 6.2% lower than those using the original design.

7.3.4 Test results from *Case II*

7.3.4.1 Determination of the final optimal solution in the multi-objective design optimisation

Fig. 7.8 shows the desired optimal point and normalized Pareto frontier of the two objective functions, which was determined based on the cost data in China presented in Table 7.2. The normalization of the original Pareto frontier was carried out using the same method as that used in *Case I*.

The optimal values of the decision variables obtained by using the proposed multi-objective design optimisation strategy are compared with that of the original design and are summarised in Table 7.5. The optimised borehole number and the total area required for installation of the vertical U-tube GHEs by using the proposed strategy were 164 and 2624 m^2, respectively. Compared to the original design which required a land area of 4320 m^2, a 39.3% reduction in the installation area was achieved by using the proposed design optimisation strategy when the same borehole distance of 4 m was used. The shortage of available land source is always a common problem in metropolises. The minimisation of the usage of the land area for installation of vertical U-tube GHEs is therefore important. The results also show that the EGNs of using the original design and multi-objective design optimisation were 0.2125 and 0.1885, respectively. Compared to the original design, around 11.3% decrease in the EGN was achieved by using the multi-objective design optimisation strategy.

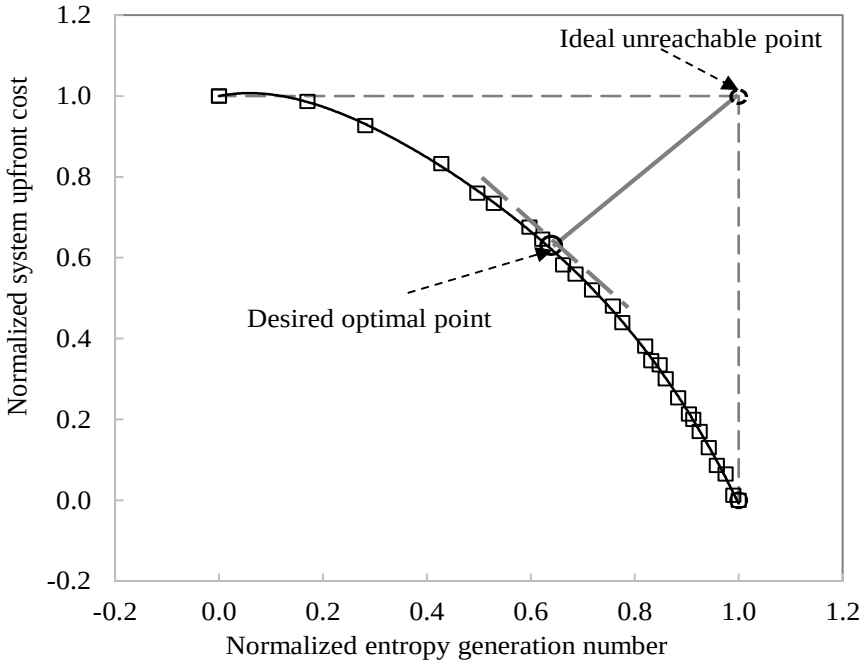

Fig. 7.8 Normalized Pareto frontier and determination of the final solution - *Case II*

Table 7.5 Comparison between the two different designs - *Case II*

Design optimisation strategy	r_b (m)	m_f (kg/s)	L_b (m)	N	r_o (m)	Installation area (m^2)	EGN	EGN reduction (%)
Original	0.09	0.37	100	270	0.017	4320	0.2125	-
Multi-objective	0.095	0.55	132	164	0.022	2624*	0.1885	11.3

* The installation area was estimated based on the assumption of the squared configuration of the boreholes.

7.3.4.2 Economic analysis

An economic analysis was also performed for validating the effectiveness of the multi-objective design optimisation strategy for this case. Fig. 7.9 and Fig. 7.10 illustrate the annual maximum entering water temperature to the water-water heat pumps and annual energy consumption of the GSHP system under the two different designs, respectively. Similar conclusions as that from *Case I* can be drawn, i.e. that the annual maximum

entering water temperature to the water-water heat pumps using the multi-objective design optimisation strategy was larger than that using the original design.

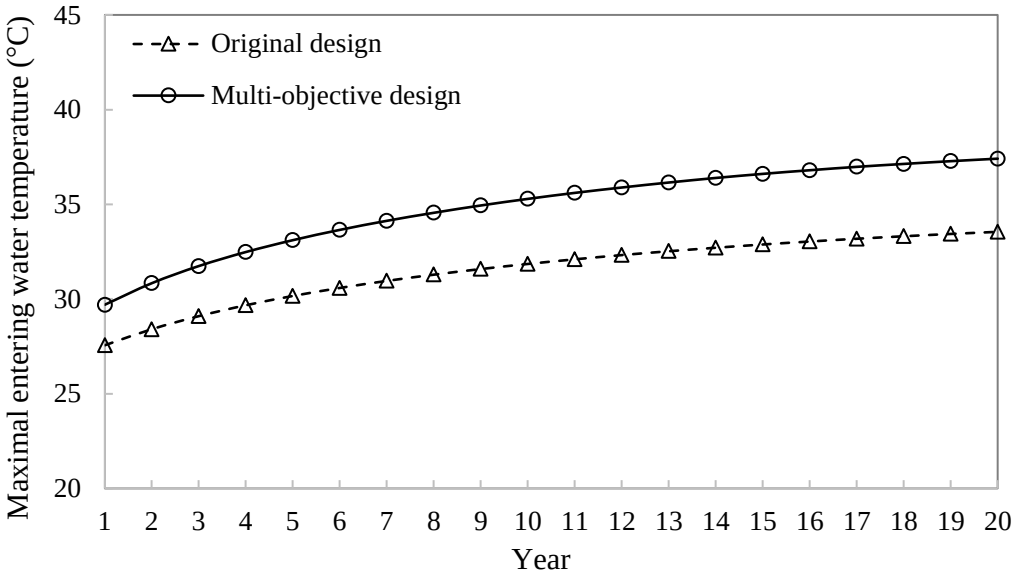

Fig. 7.9 Annual maximum entering water temperature to the water-water heat pumps - *Case II*.

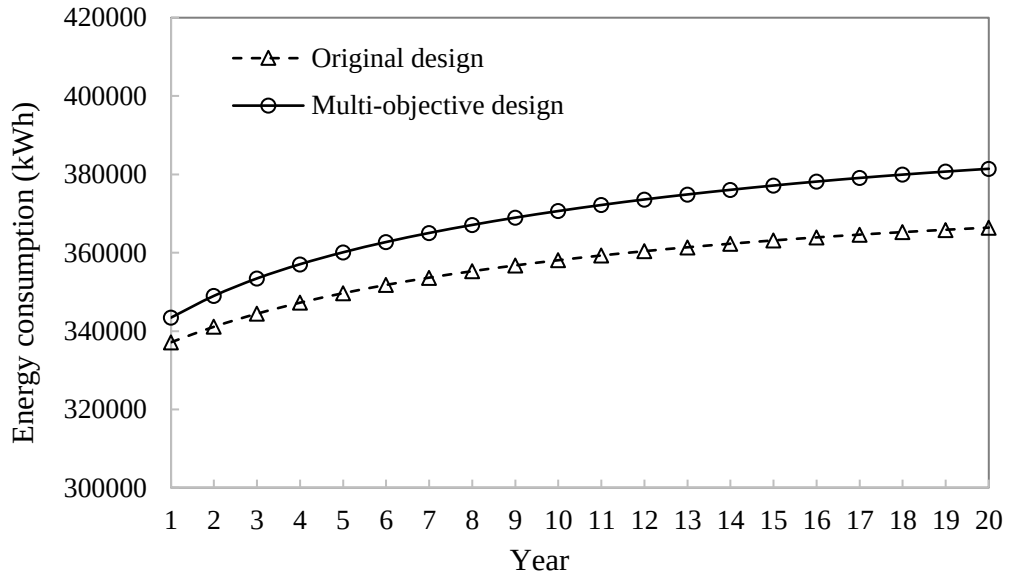

Fig. 7.10 Annual energy consumption of the GSHP concerned - *Case II*.

Table 7.6 summarises the results from the economic analysis by using the original design and the multi-objective design optimisation. It is clearly shown that the total system cost

(i.e. the upfront cost and 20-year operating cost) by using the multi-objective design optimisation strategy was ¥ 9,371,595, which was 5.2% lower than that of using the original design. The 20-year operating cost of the system by using the multi-objective design optimisation strategy was ¥ 5,807,755, which was 3.1% higher than that of using the original design, while the system upfront cost using the multi-objective design optimisation was ¥ 3,563,840, where was 16.3% lower than that of the original design.

Table 7.6 Economic cost analysis of the system using two different design strategies - *Case II*

	Original design	Multi-objective design
Number of boreholes	270	164
Borehole depth (m)	100	132
Energy consumption in 20 years operation (kWh)	7,128,020	7,351,588
20 years' operating cost (¥)	5,631,136	5,807,755
Total system upfront cost (¥)	4,259,600	3,563,840
Total system cost (i.e. upfront cost and 20 years' operating cost) (¥)	9,890,736	9,371,595
Total cost savings (%)	-	5.2

7.4 Summary

This chapter presented a multi-objective design optimisation strategy for vertical U-tube ground heat exchangers used in GSHP systems. A multi-objective genetic algorithm implemented in MATLAB was used to search for a set of Pareto optimal solutions, which were presented in the Pareto frontier. A decision-making strategy based on an ideal point was used to determine a final optimal solution.

The performance of the proposed multi-objective design optimisation strategy was validated based on a small scale GSHP system in Australia (*Case I*) and a relatively large scale GSHP system in China (*Case II*), respectively. The results from *Case I* showed that the use of the proposed strategy can achieve around 9.5% total system cost savings (i.e. the

upfront cost and 20 years' operating cost) of the GSHP system concerned, as compared to the use of the original design. Compared to the single-objective design optimisation with the entropy generation number (EGN) as the objective function, 6.2% more total system cost can be saved by using the multi-objective design optimisation, based on the same mathematic models and optimisation constraints. The results from *Case II* showed that the use of the multi-objective design optimisation can result in a 5.2% reduction in the total system cost, when compared with the results of using the original design. The results from both case studies also demonstrated that the proposed multi-objective design optimisation strategy taking into consideration both thermodynamic and economical aspects is technically feasible and effective in facilitating the design of vertical U-tube ground heat exchangers.

Chapter 8

Optimal Control of Ground Source-Air Source Combined Heat Pump Systems

Besides design optimisation, control optimisation is another essential step to maximising the system operating efficiency in order to further offset the high installation cost of a GSHP system. This chapter presents a strategy for optimal control of ground source-air source combined heat pump systems to determine the optimal sequence of the heat pumps and optimal water flow rate in the ground loop in order to minimise the power consumption of both heat pumps and water pumps. Ground source-air source combined heat pump systems have been used in some projects where the ground source heat pumps were used to provide part of building heating and cooling demands while the rest of the heating and cooling demands of the building were provided by the air source heat pumps.

This chapter is organised as follows. Section 8.1 briefly introduces the research background of control optimisation of GSHP systems. Section 8.2 describes the development and formulation of the optimal control strategy. The performance test and evaluation of the control strategy is presented in Section 8.3. Section 8.4 summarises the main findings of this study.

8.1 Introduction

In the past few decades, there has been a growing interest in energy saving concepts and thermal comfort analysis within the building sector due to continuous increase in power consumption and higher demands on quality of life as well as environmental related impacts (Ardakani *et al*. 2008, Lee *et al*. 2011, Broin *et al*. 2013, Mandley *et al*. 2015). Efficient control of air conditioning systems has a great influence on the thermal comfort sensation of the residents along with the energy efficiency (Fan *et al*. 2011, Tahersima *et al*. 2011, Azar *et al*. 2014). A well-designed control strategy can enhance the system operating efficiency while providing satisfactory indoor thermal comfort.

Compared with conventional HVAC systems, e.g. air source heat pumps, a ground source heat pump system will require extra water pumps to circulate the fluid flowing through the ground heat exchangers (GHEs), which will increase the system's power consumption. An inappropriate control of the water flow rate through the GHEs might lead to considerable power consumption of the water pumps which will impair the overall energy efficiency of a GSHP system. Furthermore, when the heat pump becomes more and more efficient, it will be more and more important to optimise the operation of the system in order to minimise power consumption (Cervera-Vázquez *et al*. 2015).

Differential pressure control and differential temperature control are commonly used to control the water flow rate in a water loop through varying the running speed of water pumps (Lian 2011). In the differential pressure control, the water pump is controlled to maintain the pressure difference across a system or a subsystem (e.g. main pipelines of the water supply and return) at a desired set-point. However, for GSHP systems, once the ground heat exchangers have been installed, the hydronic system resistance characteristics of the ground loop is relatively stable and the pressure difference between the main pipelines of the supply and return of the ground loop is only related to the water flow rate in the ground loop, which is different from the load side commonly equipped with modulating control valves for air-handling units. In the differential temperature control, temperature sensors are required to be installed to measure the temperature difference of a system or a subsystem (e.g. the temperature difference between the supply and return water). However, the temperature response to the variation of the working conditions is usually slower than that of the water flow rate. For GSHP systems, an inappropriate temperature set-point may lead to a low fluid flow rate in the GHEs, in particular when the building load is small, which will impair the heat transfer coefficient of the GHEs and lead to the low performance of the GSHP system (Cervera-Vázquez *et al*. 2015).

In this chapter, a strategy for optimal control of the ground source-air source combined heat pump systems is presented in order to minimise the total power consumption of both water pumps and heat pumps without sacrificing indoor thermal comfort and violating the relevant operating constraints. This strategy consists of the sequence control of heat pumps and optimisation of the circulating water flow rate in ground heat exchangers (GHEs). The proposed optimal control strategy was simulated and evaluated based on the system

implemented in the SBRC building presented in Chapter 3.

8.2 Development and formulation of the optimal control strategy

8.2.1 Outline of the optimal control strategy

The proposed optimal control strategy for the ground source-air source combined heat pump systems is illustrated in Fig. 8.1. The overall optimisation process consists of two steps.

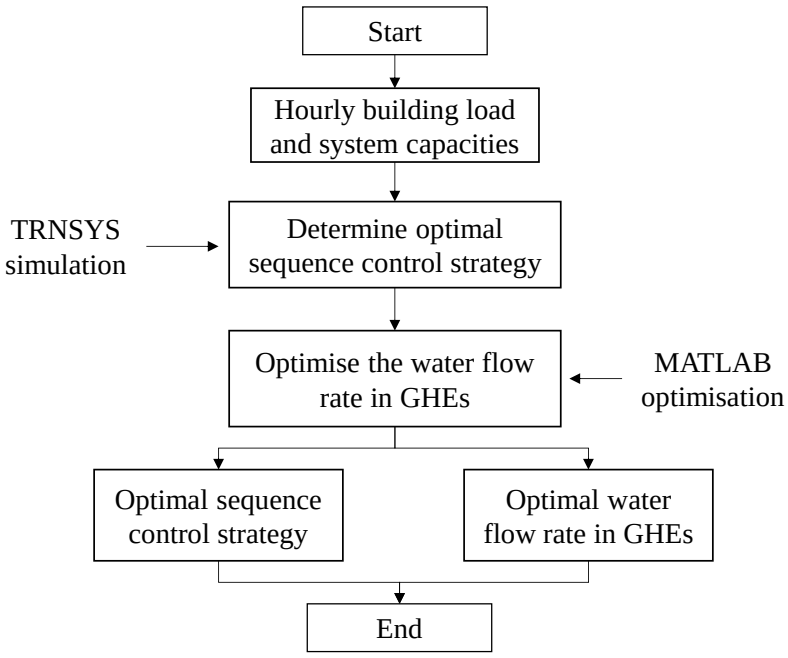

Fig. 8.1 Outline of the two-step control optimisation.

The first step is to determine the optimal sequence control of the air source heat pumps and water source heat pumps based on the building load distribution characteristics and the heat pump capacities. This is achieved based on the TRNSYS simulation through comparing the performance of several candidate sequence control strategies in order to identify the best strategy with minimal power consumption. The second step is to determine the optimal water flow rate in the ground heat exchangers (GHEs) to minimise the power consumption of both water pumps and water-to-water heat pumps. This is achieved through a model-based approach, in which simplified component models were used to formulate a nonlinear programming problem with operating constraints for optimisation. MATLAB was chosen

as the optimisation engine due to the convenience provided by its optimisation toolboxes.

8.2.2 Determination of optimal sequence control strategy for heat pumps

The ground source-air source combined heat pump system normally consists of air-to-water heat pumps and water-to-water heat pumps. Therefore, the first step in optimising such systems is to identify the optimal sequence control for the air-to-water heat pumps and water-to-water heat pumps. The overall strategy used to determine the optimal sequence of the heat pumps is shown in Fig. 8.2, which was achieved through the TRNSYS simulation.

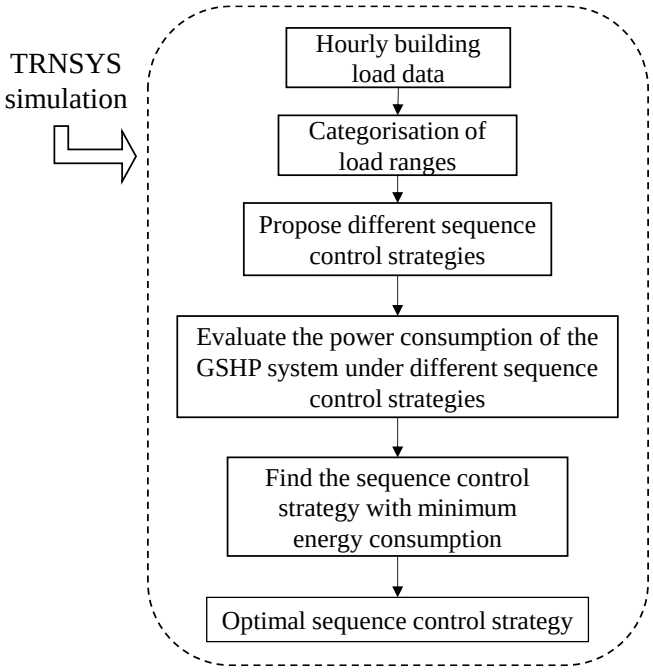

Fig. 8.2 Method to determine the optimal sequence control strategy.

The simulated building loads from DesignBuilder were first categorised into a number of ranges based on the load distribution and the capacities of the heat pumps. Based on the categorised load ranges, several candidate sequence control strategies can be proposed based on the capacities of each heat pump and then simulated in the TRNSYS simulation system. The annual power consumptions of the ground source-air source combined heat pump system with different sequence control strategies can be evaluated and compared with each other. The sequence control strategy with the least power consumption can be identified, which will be used in the next level optimisation. For the combined heat pump

systems with multiple water-to-water heat pumps, a multi-stage control can be used to control the operation of the boost water pump(s) (if any) in the ground loop. For instance, a two-stage control can be used for the system presented in Chapter 3. When the two water-to-water heat pumps are in operation, the boost water pump can operate at its rated frequency (i.e. 50 Hz), whereas when there is only one water-to-water heat pump in operation, the boost water pump can reduce to a low frequency (i.e. 30 Hz).

8.2.3 Optimisation of the water flow rate in the ground loop

The second step optimisation is the optimisation of the water flow rate in the ground heat exchangers (GHEs). In this level optimisation, the optimal sequence control strategy identified in the first step was used to control the operation of the air-to-water heat pumps and water-to-water heat pumps. The output of the optimisation is the optimal water flow rate in the GHEs which can be used as a set-point to control the boost water pumps in the ground loop. It should be noted that the control optimisation of air source heat pumps is not a focus of this study and their operation are therefore not optimised in this study.

The overall process for the water flow rate optimisation is illustrated in Fig. 8.3. It mainly consists of the objective function, performance models and optimisation techniques as well as the operating constraints. MATLAB *fminbnd* (find minimum of single-variable function on fixed interval), which is based on the polynomial interpolation and the golden section search (Mathworks 2010), was used as the optimisation technique to search for the optimal water flow rate for the optimisation problem. The formulation of the objective function and description of the simplified component models are presented in the following sections.

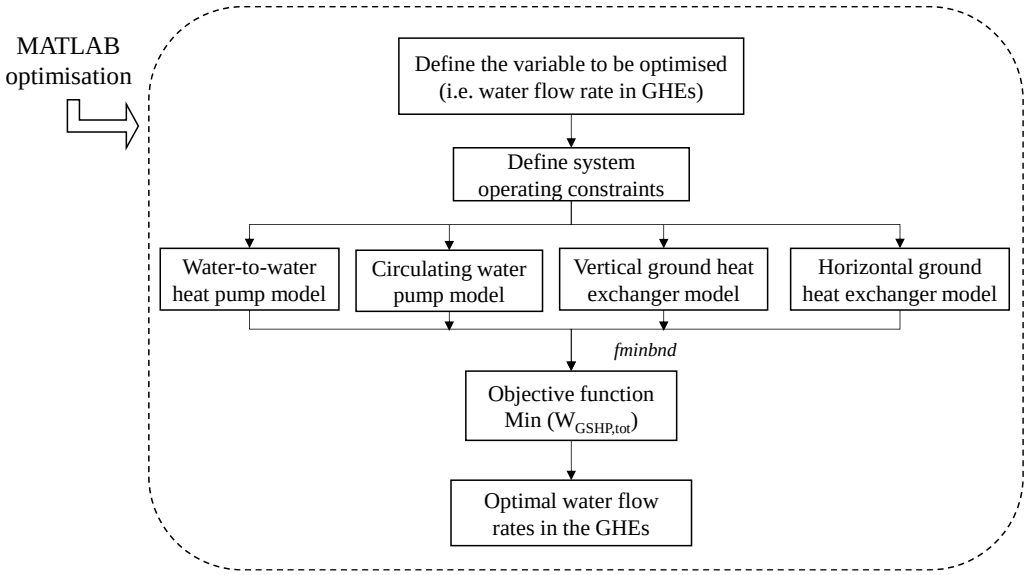

Fig. 8.3 Optimisation of the water flow rate in the ground loop.

8.2.3.1 Objective function

The objective function of the optimisation problem is expressed in Equation (8.1).

$$W_{GSHP,tot} = \sum W_{WWHP} + \sum W_{pump} \tag{8.1}$$

where, $W_{GSHP,tot}$ is the total power consumption of the ground source heat pump system except the power consumption of the water pumps in the load side, W_{WWHP} and W_{pump} are the power consumptions of the water-to-water heat pumps and all water pumps in the source side of the water-to-water heat pumps, respectively.

The parameter to be optimised is the total water flow rate ($m_{f,tot}$) circulating through the ground heat exchangers.

8.2.3.2 Mathematical modelling

Water-to-water heat pump model

The water-to-water heat pump unit was simulated based on Gordon's method (Gordon *et al*. 1995). The water-to-water heat pump can be modelled using the indicative relationship of the chiller. The power consumption can be calculated based on the specific source inlet temperature, load outlet temperature and load fraction.

Equation (8.2) and (8.3) represent the water-to-water heat pump model for cooling mode operation and heating mode operation, respectively (Gang *et al*. 2013, 2014).

$$W_{WWHP} = Q_{c,r} \times ((L_d + C_1) \times \frac{T_{source,in} + 273}{T_{load,out} + 273} - K_1(L_d + C_2)) \quad (8.2)$$

$$W_{WWHP} = Q_{h,r} \times ((L_d + C_3) \times \frac{T_{load,out} + 273}{T_{source,in} + 273} - K_2(L_d + C_4)) \quad (8.3)$$

where, $Q_{c,r}$ and $Q_{h,r}$ are the rated cooling capacity and heating capacity of the water-to-water heat pump respectively, L_d is the part load ratio, $T_{source,in}$ and $T_{load,out}$ are the inlet water temperature of the source side of the water-to-water heat pump and outlet water temperature of the load side of the water-to-water heat pump respectively, C_1, C_2 and K_1 are the coefficients determined based on the cooling performance data of the heat pump provided by the manufacturer, and C_3, C_4 and K_2 are the coefficients determined based on the heating performance data of the heat pump.

It is worthwhile to note that this simplified model assumed a constant water temperature supply at the load side of the water-to-water heat pumps, i.e. 7°C in the cooling mode operation and 45°C in the heating mode operation.

Water pump model

The constant speed water pumps were simulated by using Equation (3.6) described in Chapter 3. For variable speed water pumps, due to the insufficient pump performance data provided by the manufacturer, the pump affinity laws as presented in Equations (3.7) - (3.9) in Chapter 3, were used to predict the power consumption of the water pump under different operating speeds.

Ground heat exchanger model

For vertical ground heat exchangers, the infinite line source model (LSM) as shown in Equation (8.4), developed based on Kelvin's line source theory (Yang *et al*. 2010), was used to analyse the heat transfer process.

$$T_b = T_s(r_b, \tau) = T_{s,0} + \frac{q}{4\pi k_s} \int_{\frac{r_b^2}{4\alpha_s \tau}}^{\infty} \frac{e^{-u}}{u} du \cong T_{s,0} + \frac{q}{4\pi k_s} E_1(\frac{r_b^2 \rho_s c_s}{4k_s \tau}) \quad (8.4)$$

More detailed of this model can be found in Section 6.3.1, Chapter 6.

For horizontal ground heat exchangers, the plane source heat transfer model as expressed in Equation (8.5) was used to analyse the heat transfer phenomenon (Lin *et al*. 2010).

$$T_p = T_{s,0} + q_{hori}\sqrt{\frac{\tau}{\pi\rho_s c_s k_s}} \tag{8.5}$$

where, q_{hori} is the plane heating rate, T_p is the plane source temperature, $T_{s,0}$ is the undisturbed soil temperature, k_s is the soil thermal conductivity, ρ_s is the soil density, and c_s is the specific heat of the soil.

Similar with the borehole heat exchanger, the horizontal ground heat exchanger thermal resistance (R_h) was computed based on Equation (8.6) and the average fluid temperature (T_f) is calculated in Equation (8.7) (Lin *et al*. 2010, Sanaye *et al*. 2010)

$$\begin{aligned} R_h &= R_g + R_p \\ &= \frac{1}{2\pi k_s}\ln(\frac{\Delta d}{d_o}) + \frac{1}{2\pi k_p}\ln\frac{d_o}{d_i} + \frac{1}{\pi d_i h_f} \end{aligned} \tag{8.6}$$

where R_g is the thermal resistance of soil adjacent to the horizontal heat exchanger pipe, R_p is the thermal resistance of pipe, d_o and d_i are the outer and inner diameter of the heat exchanger pipe, Δd is the distance between two adjacent heat exchanger pipes.

$$T_f = T_p + \frac{q_{hori}}{L_{pn}}R_h \tag{8.7}$$where L_{pn} is the horizontal ground heat exchanger length per square meter.

8.3 Results and discussions

8.3.1 Results of testing sequence control strategies

8.3.1.1 Analysis of building load distribution characteristics

The performance of the optimal control strategy proposed was validated and evaluated based on the system implemented in the SBRC building. As the SBRC building was still under the commissioning stage at the time of writing, the hourly heating and cooling loads of the building were therefore simulated using DesignBuilder based on the hourly RMY

weather data for the typical year in Sydney. The simulated hourly building heating and cooling load profiles and ambient air conditions have been presented in Fig. 4.2, Chapter 4. As the building is a cooling dominated building and more than 80% of the heating demand of the building can be satisfied by the two water-to-water heat pumps, the sequence control strategies presented below were therefore developed based on the cooling demand, which can also be applied to control the operation of the heat pumps in the heating mode operation.

Based on the cooling capacities of the water-to-water heat pumps and air-to-water heat pump specified in Table 3.1, Chapter 3, the cooling load of the SBRC building can be divided into five ranges, as shown in Table 8.1. *Range I* was less than 16.4 kW, which is the cooling capacity of one water-to-water heat pump. *Range II* was between 16.4 kW and 32.8 kW, the upper limit was the total cooling capacities of the two water-to-water heat pumps. In *Range III*, the cooling capacity of the air-to-water heat pump (109.4 kW) was set as the upper limit and in *Range IV*, the upper limit of 125.8 kW was determined as the sum of the cooling capacities of one water-to-water heat pump and the air-to-water heat pump. The cooling load larger than 125.8 kW was categorised as *Range V*.

Table 8.1 The cooling load range categorisation

Range	Cooling load (kW)				
	I	*II*	*III*	*IV*	*V*
	< 16.4	16.4 - 32.8	32.8 -109.4	109.4 -125.8	> 125.8

In order to analyse the building cooling load distribution characteristics within each divided load ranges, the probability distribution function was applied. The building cooling load was first represented in terms of the cooling load ratio (CLR) and was then statistically analysed by the probability density distribution (Fan *et al*. 2011). The CLR is defined as below.

$$\mathrm{CLR} = \frac{Q_c}{Q_{c,\max}} \tag{8.6}$$

where, Q_c is the cooling load, and $Q_{c,\max}$ is the maximum cooling load.

The probability density distribution was realised by using Parzen-window density estimation. The Parzen-window an effective and convenient data interpolation method (Parzen 1962, Duda *et al*. 1973). The Parzen-window estimation was defined in Equation (8.7).

$$P(x) = \frac{1}{n}\sum_{i=1}^{n}\frac{1}{h^d}K(\frac{x - x_i}{h}) \tag{8.7}$$

where h is the window width parameter, d is the d-dimensional, x is a random sample with the dimension of d, x_i is the d-dimensional i^{th} observation, and $K(u)$ is the kernel function satisfying Equation (8.8).

$$\int K(u)du = 1 \tag{8.8}$$

In general, the Gaussian function can be used to represent the kernel function, therefore, the final expression of Parzen-window estimation can be found in Equation (8.9).

$$P(x) = \frac{1}{n}\sum_{i=1}^{n}\frac{1}{(\delta\sqrt{2\pi})^d}\exp(-\frac{1}{2}(\frac{\| x - x_i \|}{\delta})^2) \tag{8.9}$$

where, σ is the standard deviation of the Gaussian probability density function along each dimension.

The probability density distribution of the SBRC building cooling load ratio with the cooling load ranges divided is shown in Fig. 8.4.

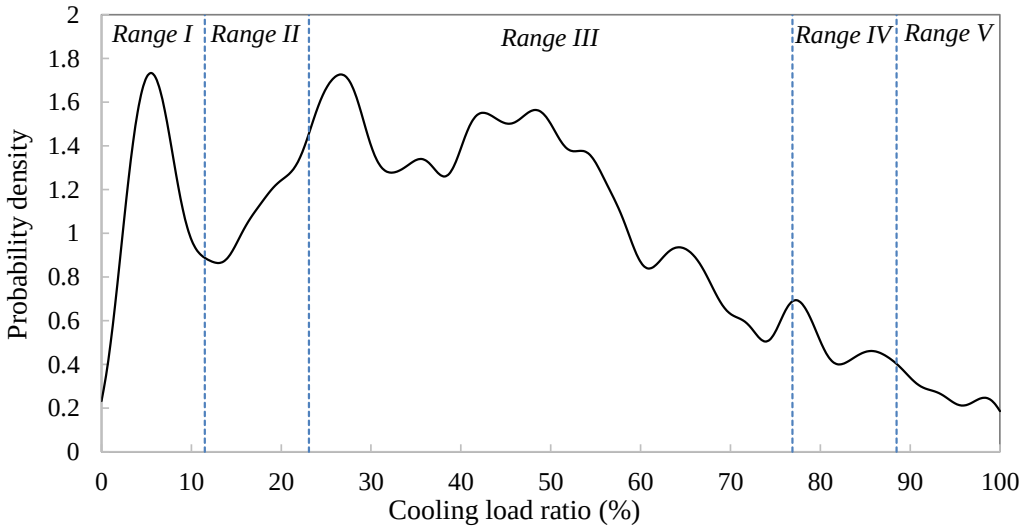

Fig. 8.4 Cooling load time frequency profile of the SBRC building.

It can be seen that most cooling demands of the building were less than 70% of the maximum cooling demand. The majority of the cooling load probability density profile was in load *Range III*, which suggested that the sequence control strategies of the heat pumps under *Range III* have a significant influence on the annual power consumption of the ground source-air source combined heat pump system. While in *Ranges I*, *II*, *VI* and *V*, the change of sequence control strategies of the heat pumps will have limited effects on the annual power consumption of the ground source-air source combined heat pump system.

8.3.1.2 Proposed sequence control strategies

A total of four sequence control strategies were considered in this study. The sequence control strategy implemented in the SBRC building to control the on/off of the heat pumps is denoted as the *original* strategy and is presented below.

1) If the building load is less than the rated capacity of one water-to-water heat pump, then only one water-to-water heat pump is in operation;
2) If the building load is larger than the rated capacity of one water-to-water heat pump and less than the rated capacity of the two water-to-water heat pumps, then the two water-to-water heat pumps are in operation;
3) If the load is larger than the sum of the rated capacity of the two water-to-water heat pumps, then the air source heat pump is also put into operation.

Three sequence control strategies (named as *SI*, *SII* and *SIII*) are proposed based on the analysis above, and these control strategies are presented in Fig. 8.5 along with the *original* strategy.

Due to the relatively small designed capacity and higher efficiency of the GSHP in this case study system, the operation priority will also be given to the two water-to-water heat pumps for the other three proposed sequence control strategies. For instance, in Range *I*, only one water-to-water heat pump is in operation, and in Range *II*, the two water-to-water heat pumps are in operation. In *Range V*, all three heat pumps should operate in order to satisfy the high cooling demand of the building. Thus, as shown in Fig. 8.5, the differences among the four strategies (*Original*, *SI*, *SII* and *SIII*) are mainly in the *Range III* and *Range IV*. The difference between the *original* strategy and *SI* is in the *Range III* and *Range IV*. The difference between *SI* and *SII* is in the *Range III*, and the difference between *SII* and *SIII* is in the *Range IV*.

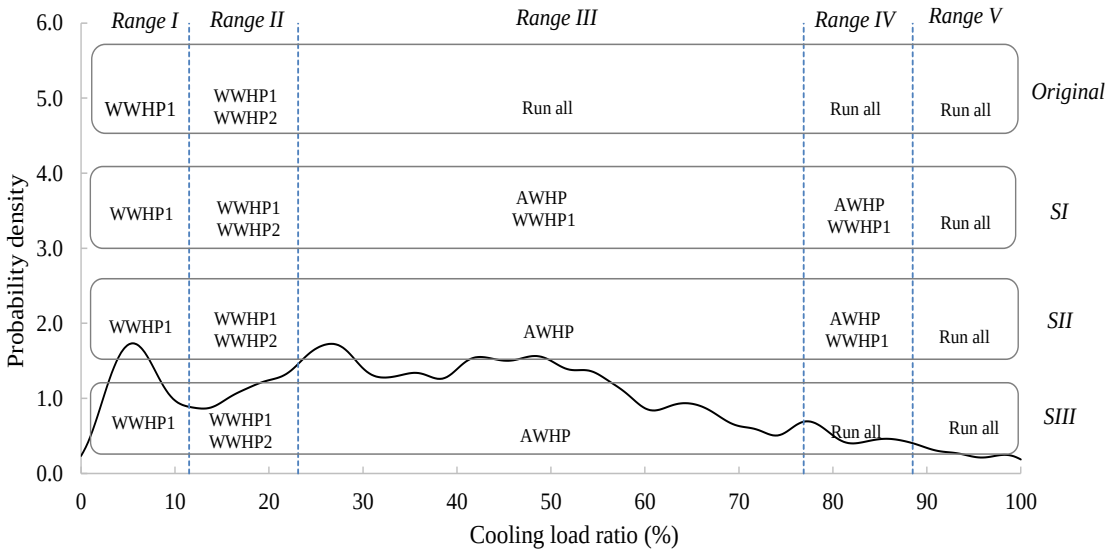

Fig. 8.5 Sequence control strategies for the three heat pumps based on the probability density distribution profile of cooling load ratio of the SBRC building.

Based on the developed simulation system as presented in Chapter 4, the annual power consumption of the ground source-air source combined heat pump system using the *original* sequence control strategy and the three proposed sequence control strategies (*SI*, *SII* and *SIII*) were simulated and the results are summarised in Table 8.2. As mentioned in

section 8.2.2, a two-stage control was used to control the boost pump in the ground loop. When one water-to-water heat pump is in operation, the boost pump operates at a low frequency (i.e. 30 Hz). When the two water-to-water heat pumps are in operation, the boost pump operates at a high frequency of 50 Hz.

From Table 8.2, it can be seen that the ground source-air source combined heat pump system consumed about 5.0%, 10.4% and 11.3% less power when using the strategies of *SI*, *SII* and *SIII*, as compared with the use of the *original* sequence control strategy, respectively. The strategy *SIII* provided the best performance among the four strategies simulated. Strategy *SIII* was therefore deemed as the optimal sequence control strategy and was employed to control the on/off of the heat pumps in the next level optimisation of the water flow rate in the ground loop.

Table 8.2 Annual power consumption of the system using different sequence control strategies

Sequence control strategies	Annual power consumption (kWh)	Power difference (kWh)	Savings (%)
Original	18,108	-	-
SI	17,210	898	5.0
SII	16,227	1,881	10.4
SIII	16,065	2,043	11.3

8.3.2 Results of optimisation of the water flow rate in the ground heat exchangers

The coefficients of the simplified water-to-water heat pump model and water pump model can be identified based on their performance data provided by the manufacturers. Table 8.3 and Table 8.4 present the coefficients of the water-to-water heat pump model and the constant speed water pump model used in this study, respectively. The previously determined optimal sequence control strategy (*SIII*) was used to control the on/off of the three heat pumps.

Table 8.3 Coefficients of the water-to-water heat pump model

Coefficients	C_1	C_2	K_1	C_3	C_4	K_2
Values	2.7440	3.0075	0.9486	0.5219	0.4824	0.9816

Table 8.4 Coefficients of the constant speed water pump model

Coefficients	$W_{p,rated}$	β_0	β_1	β_2	β_3
Source side water pumps	1.6	0.4199	0.5914	0.2976	-0.306

Fig. 8.6 shows the water flow rates in the ground loop optimised when using the proposed control strategy and the two-stage control for the boost water pump in the ground loop, respectively. It can be seen that there is an obvious difference between the two sets of water flow rates determined by the two control strategies. The water flow rates optimised by the proposed control strategy in general were less than that of using the two-stage control. The less flow rate in the ground loop means less power consumption of the source side water pumps in the ground loop.

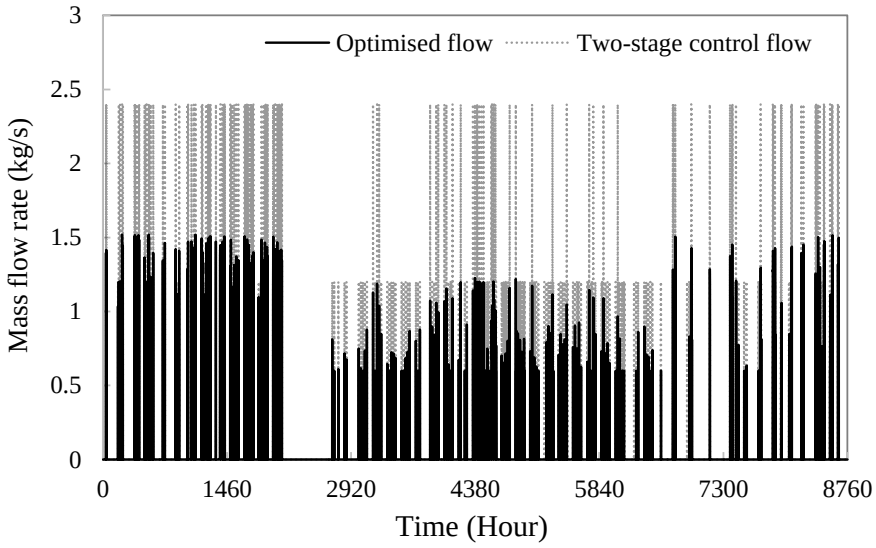

Fig. 8.6 Water flow rates in GHEs when using the two different control strategies.

Fig. 8.7 presents the difference between the water temperature at the inlet and outlet of the GHEs when using the proposed control strategy. It can be seen that the maximum temperature difference in the cooling mode operation was around 5.9°C, while the

maximum temperature difference in the heating mode operation was 4.7°C. In general, the temperature difference in the heating mode operation is smaller than that in the cooling mode operation because the heating demand of the building is smaller than the cooling demand.

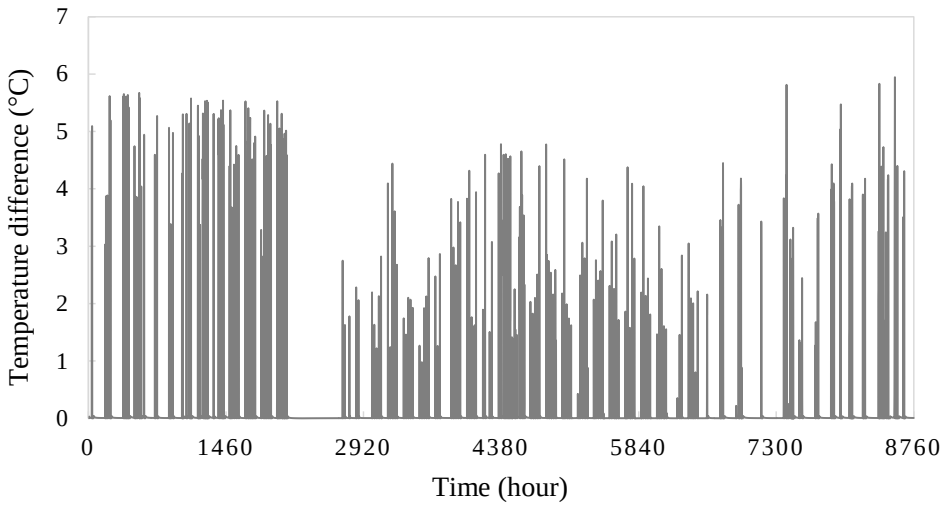

Fig. 8.7 Water temperature difference between the inlet and outlet of GHEs when using the proposed control strategy.

Fig 8.8 shows the difference between the water temperature at the inlet and outlet of the GHEs when using the two-stage control for the boost water pump. The maximum temperature difference was 4.0 °C in the cooling mode operation and it was 2.8°C in the heating mode operation. Compared to the temperature difference when using the proposed control strategy, the temperature difference using the two-stage control is smaller due to larger water flow rates in the GHEs determined by the two-stage control, as shown in Fig. 8.6.

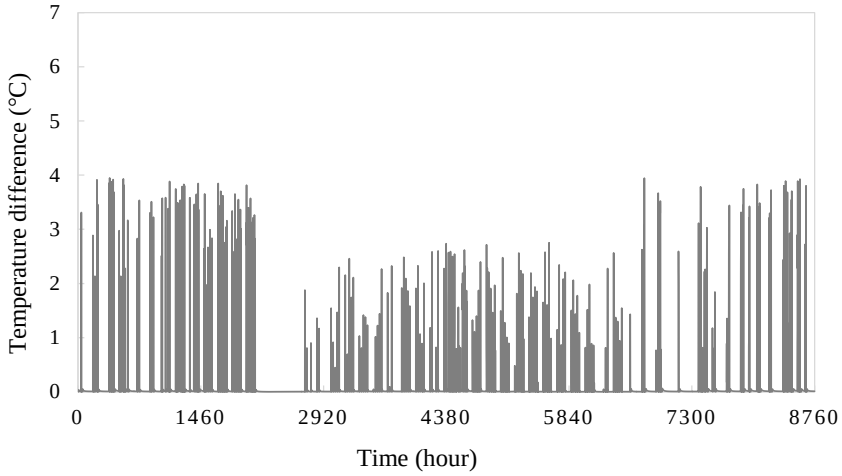

Fig. 8.8 Water temperature difference between the inlet and outlet of GHEs when using the two-stage control strategy.

Table 8.5 summarises the annual power consumptions of the source side water pumps, water-to-water heat pumps and the GSHP system when using the proposed control strategy and the two-stage control for the boost pump in the ground loop. The source side water pumps include the two water pumps dedicated with the two water-to-water heat pumps and one boost water pump. The total GSHP system power consumption includes the power consumption of the water-to-water heat pumps and the source side water pumps. It can be seen that, when the proposed control strategy was used, the power consumption of the source side water pumps reduced by 363 kWh while the power consumption of the water-to-water heat pumps increased by 92 kWh, as compared to that of using the two stage control for the boost pump. The savings of the total power consumption of the GSHP system related to the use of the proposed control is 9.3 %, compared to the use of the two-staged control.

Table 8.5 Annual power consumption of the source side water pumps, water-to-water heat pumps using the two-stage control and optimal control

Control strategy	Source side water pumps (kWh)	Water-to-water heat pumps (kWh)	Total GSHP system (kWh)	Savings (%)
Two-stage control	970	1,937	2,907	-
Proposed control	607	2,029	2,636	9.3

The integrated effects of using the sequence control for the heat pumps and optimisation of the water flow rate in the ground loop system were also simulated and analysed. The three integrated control strategies investigated are presented below.

- *Strategy A: Original* sequence control and two-stage control for the boost water pump. The operation of the three heat pumps is controlled using the *original* sequence control strategy, while the boost pump is controlled using the two-stage control.
- *Strategy B: SIII* sequence control and two-stage control for the boost pump. The operation of the three heat pumps is controlled using the *SIII* sequence control strategy, while the operation of the boost pump is controlled using the two-stage control.
- *Strategy C*: *SIII* sequence control and optimal control proposed for the water flow rate optimisation. The operation of the three heat pumps is controlled using the *SIII* sequence control strategy, while the water flow rate in the ground loop is optimised by the proposed model-based control strategy.

20 years simulations were performed in order to analyse the power consumption of the system using each control strategy based on the established simplified ground source-air source heat pump system in the TRNSYS simulation platform. Table 8.6 shows the total system power consumption when using the three different control strategies for 20 years' operation. The total system power consumption is the sum of the power consumptions of the air-to-water heat pump, two water-to-water heat pumps and all source side water pumps. It can be seen that the ground source-air source combined heat pump system using *Strategy B* and *Strategy C* consumed 9.4% and 12.0% less power respectively, when compared to that of using *Strategy A* (the *original* sequence control for the heat pumps and two-stage control for the boost water pump). The comparison between *Strategy B* and *Strategy C* showed that the optimisation of the water flow rate in the ground heat exchangers further saved 2.9% of the total system power consumption. However, the savings achieved by optimising the water flow rate in the GHEs is not significant as compared with the savings (i.e. 9.4%) achieved by using optimal sequence control. This is mainly due to the fact that the power consumption of the water pumps is relatively small in

comparison with that of the two water-to-water heat pumps and one air-to-water heat pump implemented in the system studied.

Table 8.6 Power consumption of the system using three control strategies for 20 years operation

Control methods		Total power consumption (kWh)	Savings (%)
Strategy A	*Original* sequence control and two-stage control for the boost water pump	298,890	-
Strategy B	*SIII* sequence control and two-stage control for the boost pump	268,297	10.2
Strategy C	*SIII* sequence control and optimal control proposed for the water flow rate optimisation	262,955	12.0

8.4 Summary

A strategy for optimal control of ground source-air source combined heat pump systems was proposed in this chapter. The effectiveness of the proposed optimal control strategy was validated against the ground source-air source combined heat pump system implemented in the UOW Sustainable Buildings Research Centre. This strategy can be easily extended to deal with more complex GSHP systems. The main conclusions of this chapter are as follows.

1) The use of the proposed optimal control strategy (i.e. *Strategy C*) in the ground source-air source combined heat pump system studied can save 12.0% of total power consumptions of three heat pumps (i.e. two water-to-water heat pumps and one air-to-water heat pump) and all the source side water pumps, when compared to that of using *Strategy A* (*original* sequence control for heat pumps and two-stage control for the boost water pump).

2) Properly designed sequence control strategies for the heat pumps can bring certain amount of energy savings. The results from the case study showed that 2,043 kWh power can be saved during the course of one year of operation through the use of the

optimal sequence control strategy for the water-to-water heat pumps and the air-to-water heat pump, when compared to the use of the *original* sequence control strategy.

3) The optimisation of the water flow rate in the ground heat exchangers is also of great importance to achieve better performance of the GSHP systems. In the case studied, the system using the proposed optimal control strategy for the boost pump reduced 9.3% total power consumption of the two water-to-water heat pumps and the source side water pumps when compared with the system using the two-stage control for the boost pump with one year operation.

4) The comparison among *Strategy A* (*original* sequence control for heat pumps and two-stage control for the boost water pump), *Strategy B* (*SIII* sequence control and two-stage control for the boost water pump) and *Strategy C* (proposed optimal control strategy) showed that the optimisation of the water flow rate in the ground heat exchangers have limited effects on the total ground source-air source heat pump system power consumption. This may be due to the fact that the power consumption of the water pumps in the system studied was relatively small compared with the power consumption of the heat pumps.

It is worthwhile to mention that the control settings identified by the proposed control strategy might not be the global optimal settings. To date, it seems that there are no good models for horizontal heat exchanges suitable for control applications and efforts are therefore needed to develop an appropriate control model for horizontal heat exchangers.

Chapter 9

Conclusions and Recommendations

This thesis presents an energy performance evaluation and optimisation of ground source heat pump (GSHP) systems. Simulation and experimental analysis were first performed to provide a better understanding of the dynamic characteristics and energy performance of GSHP systems. A feasibility study was then carried out to evaluate the economic and environmental feasibility of using GSHP systems in the main Australian climate zones. Single-objective and multi-objective design optimisation methods were then developed to facilitate the optimal sizing and design of vertical ground heat exchangers (GHEs) commonly used in GSHP systems. The dimensionless entropy generation number was employed as the objective function in the single-objective design optimisation, while both the system upfront cost and entropy generation number were used as the objective functions in the multi-objective design optimisation. An optimal control strategy was also developed to maximise the operating efficiency of the ground source-air source combined heat pump systems without sacrificing indoor thermal comfort and violating the system operating constraints. Major findings from this study are summarised as follows.

9.1 Summary of the main findings

9.1.1 Dynamic characteristics and energy performance analysis of GSHP systems

Experimental tests and detailed computer simulations were carried out in order to understand the dynamic characteristics and energy performance of GSHP systems. Experimental tests were conducted based on the ground source-air source combined heat pump system implemented in the Sustainable Building Research Centre (SBRC) building at the University of Wollongong to investigate the effects of the parallel and series operation of GHEs and the water flow rate in GHEs on the performance of the GSHP system. Simulation analyses were performed on a numerical representation of the real ground source-air source combined heat pump system implemented in the SBRC building using the TRNSYS simulation platform. The effects of different design variables of vertical GHEs

and horizontal GHEs on the system energy performance were examined. The main conclusions from the numerical and experimental analyses are presented below:

- Parallel operation of the GHEs is better than series operation in respect of overall performance of the water-to-water heat pumps. The average coefficient of performance (COP) of the water-to-water heat pumps with GHEs in parallel configurations in cooling mode was 19.5±2.5% higher than that with GHEs in series.
- A larger water flow rate in the ground loop can improve the performance of the water-to-water heat pumps. However, it will also increase the power consumption of the water pumps in the source side of the water-to-water heat pumps. The experimental results showed that, for the system with GHEs in both parallel and series configurations, an increase in the source flow rates from low to high resulted in an average increase in the COP of the water-to-water heat pump system of 7.1% and 2.6%, respectively.
- The simulation results for typical working conditions showed that for both vertical and horizontal GHEs, the length of the GHEs is the main design parameter influencing performance, while other parameters such as the thermal conductivity of the grout/soil and the borehole/pipe separation spacing also have an important effect on the overall energy efficiency of GSHP systems.

9.1.2 Feasibility analysis of GSHP systems for different Australian climate zones

To provide a better understanding of the effects of local climate on the performance of GSHP systems, a feasibility study was carried out to evaluate the economic and environmental benefits of GSHP systems for several Australian climate zones. The specific conclusions obtained from this study are presented below.

- GSHP systems are economically feasible for all the Australian climate zones studied. For Sydney, Alice Springs, Brisbane and Hobart, the net present values (NPV) of using GSHP systems can be reduced by modest values 3.22%, 1.09%, 1.44% and 2.73%, respectively, as compared to the use of air source heat pump systems for the reference system studied. The improvements of NPV by using

GSHP systems achieved in this study were relatively small due to the high drilling costs of vertical GHEs. Thus the design optimisation of vertical GHEs is important in the enhancement of the economic feasibility of GSHP systems.

- An economic sensitivity analysis showed that drilling costs for vertical GHEs were found to have a modest influence on the NPV of GSHP systems. With ±5.0% variations in the drilling cost, electricity price and discount rate, the resultant changes in NPV were found to be 3.0%, 1.5% and 1.0%, respectively. These results further indicated the importance of optimal sizing of vertical GHEs to reduce the drilling cost to enhance the economic benefits of using GSHP systems.
- An environmental analysis showed that GSHP systems are environmentally feasible with a 33.0±4.0% reduction in 20 years CO_2 emissions for the main Australian climate zones when compared with conventional air source heat pump systems.

9.1.3 Design optimisation of GSHP systems

Vertical GHEs are commonly used in GSHP systems due to their high energy efficiency and less land area required. A global sensitivity analysis based on Sobol's method was first used to identify the key design variables of vertical GHEs. An entropy generation minimisation (EGM) single-objective design optimisation method for vertical GHEs was then developed to optimise the key design variables identified for vertical GHEs. The vertical GSHP system, which was part of the ground source-air source heat pump system implemented in the UOW SBRC building, was used as a case study to demonstrate the effectiveness of the proposed design optimisation strategy. The case study showed the effectiveness and efficiency of applying the second-law of thermodynamic analysis for the optimisation of vertical GHEs. The major findings were as follows.

- The results from the case study showed that the total system cost (i.e. the upfront cost of the vertical GHEs and water-to-water heat pumps and the operating cost of the water-to-water heat pumps over 20 years) of the GSHP system designed using the proposed optimisation strategy was 3.5% lower than that of the original design.

In order to further facilitate the design optimisation of vertical GHEs, a multi-objective design optimisation strategy was proposed and evaluated. The multi-objective optimisation

method has been studied for many years, yet has not been widely used in facilitating the optimal design of vertical GHEs. The multi-objective design optimisation method provides rich and useful information regarding the conflicting effects of the economic objective (i.e. system upfront cost) and thermodynamic objective (i.e. represented by the entropy generation number, EGN) enabling designers to determine one or more suitable solutions from the obtained Pareto-solutions. A decision-making strategy based on the fuzzy non-dimensionalisation method was used to help identify the near-optimal solution from a set of Pareto optimal solutions obtained with respect to the two competing objectives. The effectiveness and efficiency of this multi-objective design optimisation strategy was trialled against a small scale GSHP system in Australia and a relatively large scale GSHP system in China, respectively. The major findings are summarised below.

- The multi-objective design optimisation method was found to be better than the single-objective design optimisation method. The total system cost was demonstrated to be reduced by 6.2% or more using multi-objective design optimisation as compared to single-objective design optimisation.
- The results from a small scale GSHP system in Australia and a relatively large scale GSHP system in China showed that the use of the proposed optimisation method can achieve around 9.5% and 5.2% total system cost savings of the GSHP systems, respectively, as compared to their original designs based on commercial design tools, i.e. GLD (ground loop design).

9.1.4 Optimisation of the control of GSHP systems

Control optimisation is also essential in the maximisation of the system operating efficiency to further offset the high investment costs of GSHP systems. A strategy for optimal control of ground source-air source combined heat pump systems was developed in this study. This methodology consisted of the optimal sequence control of heat pumps and optimisation of the circulating water flow rate in the GHEs. The performance of this proposed methodology was simulated and verified against the system implemented in the SBRC building. This methodology can be easily extended to deal with other types of GSHP systems. The main findings are summarised below.

- Optimal sequence control of the air-to-water heat pumps and water-to-water heat pumps can realise energy savings of around 11.3% per year, as compared to the use of the *original* sequence control strategy implemented in the BMS (building management system) of the building.
- Optimisation of the water flow rate in the ground loop can reduce total GSHP system power consumption by 9.3% as compared with the system using the two-stage control for the boost pump in the source side of the water-to-water heat pumps with one year operation.
- The use of optimal sequence control for the heat pumps and the optimisation of the water flow rate in the GHEs can save 12.0 % of total system energy consumption, which includes the power consumption of one air-to-water heat pump, two-water-to-water heat pumps and all source side water pumps of the case studied system, as compared to that of using the *original* sequence control strategy for heat pumps and two-stage control for the boost water pump in the ground loop over 20 years of operation.

9.2 Recommendations for future work

Firstly, the design optimisation carried out in this study was focused on vertical ground heat exchangers (GHEs) as vertical GHEs are commonly used in GSHP systems and associated with high drilling costs. It is also suggested that it would be worthwhile to develop appropriate design optimisation methods for horizontal GHEs, as well as for other types of ground heat exchangers such as foundation pile heat exchangers and standing column wells.

Secondly, the control optimisation for ground source-air source heat pump systems developed in this study was mainly focused on the GHE side of the GSHP system (i.e. ground loop). It would be beneficial to develop dynamic control optimisation methodologies for the whole GSHP system, including the load distribution side.

Furthermore, seasonal load imbalance is a critical issue in the design and operation of GSHP systems with vertical GHEs. However, the investigation of potential solutions to effectively alleviate seasonal load imbalance issue was not a focus of this study.

Development of cost-effective solutions to solve seasonal load imbalance in the ground loop would be a fruitful area worthwhile of future research.

References

1. Ahmadi MH, Hosseinzade H, Sayyaadi H, Mohammadi AH, Kimiaghalam F. 2013. Application of the multi-objective optimisation method for designing a powered Stirling heat engine: design with maximized power, thermal efficiency and minimised pressure loss. Renewable Energy, vol. 60, pp. 313-322.
2. Ahn BC, Mitchell JW. 2001. Optimal control development for chilled water plants using a quadratic representation. Energy and Buildings, vol. 33, no. 4, pp. 371–378.
3. Alavy M, Nguyen Hiep V, Leong HW, Dworkin SB. 2013. A methodology and computerized approach for optimizing hybrid ground source heat pump system design. Renewable Energy, vol. 57, pp. 404-412.
4. Allaerts K, Coomans M, Salenbien R. 2015. Hybrid ground-source heat pump system with active air source regeneration. Energy Conversion and Management, vol. 90, pp. 230-237.
5. Ally MR, Munk JD, Baxter VD, Gehl AC. 2012. Exergy analysis and operational efficiency of a horizontal ground source heat pump system operated in a low-energy test house under simulated occupancy conditions. International Journal of Refrigeration, vol. 35, no. 4, pp. 1092–1103.
6. ANSI/AHRI 210/240-2008: 2008 Standard for Performance Rating of Unitary Air-Conditioning & Air-Source Heat Pump Equipment. Air Conditioning, Heating and Refrigeration Institute. 2008.
7. APVA, 2011. Modelling of PV and electricity prices in the Australian Commercial Sector, 2011.
8. Aravelli A. 2014. Multi-objective Design Optimization of Engineering Systems: Uncertainty Approach and Practical Applications. Open Access Dissertations.
9. Ardakani AJ, Ardakani FF, Hosseinian SH. 2008. A novel approach for optimal chiller loading using particle swarm optimization. Energy and Buildings, vol. 40, no. 12, pp. 2177-2187.

10. Asadi E, da Silva MG, Antunes CH, Dias L. 2012. A multi-objective optimization model for building retrofit strategies using TRNSYS simulations, GenOpt and MATLAB. Building and Environment, vol. 56, pp. 370-378.

11. Asadi E, da Silva MG, Antunes CH, Dias L, Glicksman L. 2014. Multi-objective optimization for building retrofit: A model using genetic algorithm and artificial neural network and an application. Energy and Buildings, vol. 81, pp. 444-456.

12. ASHRAE. 2011, HVAC APP SI HDBK. "HVAC Applications Handbook." SI Edition.

13. Aste N, Adhikari RS, Manfren M. 2013. Cost optimal analysis of heat pump technology adoption in residential reference buildings. Renewable Energy, vol. 60, pp. 615-624.

14. Australian Bureau of Statistics. 2012. Year Book Australia, 2012.

15. Australian Climate Average - Climate Classifications. April 10, 2012. http://www.bom.gov.au/jsp/ncc/climate_averages/climate-classifications/index.jsp (accessed Feb 12, 2015).

16. Azar E, Menassa CC. 2014. A comprehensive framework to quantify energy savings potential from improved operations of commercial building stocks. Energy Policy, vol. 67, pp. 459-472.

17. Bakirci K, 2010. Evaluation of the performance of a ground-source heat-pump system with series GHE (ground heat exchanger) in the cold climate region. Energy, vol. 35, no. 7, pp. 3088 – 3096.

18. Ball DA, Fischer RD, Hodgett DL. 1983. Design methods for ground-source heat pumps. ASHRAE Trans, vol. 89, no. 2B, pp. 416–40.

19. Bandos TV, Montero Á, de Córdoba PF, Urchueguía JF. 2011. Improving parameter estimates obtained from thermal response tests: Effect of ambient air temperature variations. Geothermics, vol. 40, no. 2, pp. 136-143.

20. Banks D. 2012. An introduction to thermogeology: ground source heating and cooling. 2nd ed. John Wiley & Sons, Inc.; 2012.

21. Bazkiaei AR, Niri ED, Kolahdouz EM, Weber AS, Dargush GF. 2013. A passive design

strategy for a horizontal ground source heat pump pipe operation optimization with a non-homogeneous soil profile. Energy and Buildings, vol. 61, pp. 39–50.

22. Bejan A, Tsatsaronis G, Moran M, 1996. Thermal design and optimization. J. Wiley.
23. Bejan A. 1996. Entropy generation minimization: the method of thermodynamic optimization of finite-size systems and finite-time processes. Boca Raton: CRC Press Inc.; 1996.
24. Bejan A. 2006. Advanced engineering thermodynamics. 3rd ed. Hoboken: John Wiley & Sons, Inc.
25. Bejan A. 2004. Convective heat transfer. 3rd ed. Hoboken: John Wiley & Sons, Inc.; 2004.
26. Benli H. 2013. A performance comparison between a horizontal source and a vertical source heat pump systems for a greenhouse heating in the mild climate Elaziğ, Turkey. Applied Thermal Engineering, vol. 50, no. 1, pp. 197-206.
27. Benli H, Durmuş. A. 2009. Evaluation of ground-source heat pump combined latent heat storage system performance in greenhouse heating. Energy and Buildings, vol. 41, no. 2, pp. 220-228.
28. Bertagnolio S, Bernier M, Kummert M. 2012. Comparing vertical ground heat exchanger models. Journal of Building Performance Simulation, vol. 5, no. 6, pp. 369-383.
29. Bi Y, Wang X, Liu Y, Zhang H, Chen L. 2009. Comprehensive exergy analysis of a ground-source heat pump system for both building heating and cooling modes. Applied Energy, vol. 86, no. 12, pp. 2560–2565.
30. Bose JE. 1984. Closed Loop Ground Coupled Heat Pump Design Manual, Engineering Technology Extension Oklahoma State University.
31. Branan CR. 2012. Rules of thumb for chemical engineers. Butterworth-Heinemann.
32. Broin EÓ, Mata É, Göransson A, Johnsson F. 2013. The effect of improved efficiency on energy savings in EU-27 buildings. Energy, vol. 57, pp. 134-148.
33. Cabeza L, Rincon L, Vilarino V, Perez G, Castell A. 2014 Life cycle assessment (LCA)

and life cycle energy analysis (LCEA) of buildings and the building sector: A review. Renewable and Sustainable Energy Reviews, vol. 29, pp. 394–416.

34. Cane RLD, Forgas DA, 1991. Modeling of Ground Source Heat Pump Performance, ASHRAE Transactions, vol. 97, no. 1, pp. 909-925.

35. Cannavó F. 2012. Sensitivity analysis for volcanic source modelling quality assessment and model selection. Computers & Geoscience, vol. 44, pp. 52-59.

36. Capozza A, De Carli M, Zarrella A. 2012. Design of borehole heat exchangers for ground-source heat pumps: a literature review, methodology comparison and analysis on the penalty temperature. Energy and Buildings, vol. 55, pp. 369-379.

37. Carslaw HS, Jaeger JC, 1959. Conduction of heat in solids. (2nd ed.) Oxford University Press, London.

38. Casasso A, Sethi R. 2014. Sensitivity analysis on the performance of a ground source heat pump equipped with a double U-pipe borehole heat exchanger. Energy Procedia, vol 59, pp. 301-308.

39. CEC. 2011. California's Customer Energy Centre, www.consumerenergycenter.org, Sacramento: California Energy Commission.

40. Cervera-Vázquez J, Montagud C, Corberán JM. 2015. In situ optimization methodology for the water circulation pumps frequency of ground source heat pump systems: Analysis for multistage heat pump units. Energy and Buildings, vol. 88, pp. 238-247.

41. Chachuata B, Srinivasanb B, Bonvin D. 2008. Model parameterization tailored to real-time optimization. Compute & Chemical Engineering, vol. 25, pp. 1-13.

42. Chai L, Ma C, Ni JQ. 2012. Performance evaluation of ground source heat pump system for greenhouse heating in northern China. Biosystems Engineering, vol. 111, no. 1, pp. 107-117.

43. Chen X, Lu. L, Yang. HX. 2011. Long term operation of a solar assisted ground coupled heat pump system for space heating and domestic hot water. Energy and Buildings. Vol. 43, no. 8, pp. 1835-1844.

44. Cheng XT, Liang XG. 2014. Discussion on the applicability of entropy generation minimization and entransy theory to the evaluation of thermodynamic performance for heat pump systems. Energy Conversion and Management, vol. 80, pp. 238-42.

45. Chiasson, AD, Yavuzturk. C, 2003. Assessment of the viability of hybrid geothermal heat pump system with solar thermal collector. ASHRAE Transactions: Symposia KC-03-3-3, pp.487-499.

46. Chiasson, AD. 2006. Final report: Lift cycle cost study of a geothermal heat pump system, BIA office building, Winnebago, NE, Geo-heat centre, Oregon Institute of Technology, February 2006.

47. Chiasson AD. 2007. Simulation and design of hybrid geothermal heat pump systems. ProQuest.

48. Cho H, Choi JM, 2014. The quantitative evaluation of design parameter's effects on a ground source heat pump system. Renewable Energy, vol. 65, pp. 2-6.

49. Chong. CSA, Gan. G, Verhoef. A, Garcia. RG, Vidale. PL. 2013. Simulation of thermal performance of horizontal slinky-loop heat exchangers for ground source heat pumps. Applied Energy, vol. 104, pp. 603-610.

50. Chung JT, Choi. JM. 2012. Design and performance study of the ground-coupled heat pump system with an operating parameter, Renewable Energy, vol. 42, pp. 118–124.

51. Claesson J., Dunard A. 1983. Heat extraction from the ground by horizontal pipes: a mathematical analysis. Documet DI: 183, Stockholm: Swedish Council for Building Research.

52. Congedo PM, Colangelo G, Statace G. 2012. CFD simulations of horizontal ground heat exchangers: A comparison among different configurations. Applied Thermal Engineering, vol. 33-34, pp. 24-32.

53. Council of Australian Governments (COAG) National Strategy on Energy Efficiency. 2012. Guide to best practice maintenance & operation of HVAC systems for energy efficiency. Commonwealth of Australia 2012.

54. Dai L, Li S, Lin DM, Shang Y, Dong M. 2015. Experimental performance analysis of a

solar assisted ground source heat pump system under different heating operation modes. Applied Thermal Engineering, vol. 75, pp. 325-333.

55. DCCEE. 2013. National greenhouse accounts (NGA) factors (pp. 19–20) Department of Climate Change and Energy Efficiency, Canberra, Australia (2013).

56. Deerman JD, Kavanaugh SP, 1991. Simulation of vertical U-tube ground-coupled heat pump systems using the cylindrical heat source solution. ASHRAE Trans, vol. 97, pp. 287–294.

57. Diao NR, Zeng HY, Fang ZH, 2004. Improvement in modeling of heat transfer in vertical ground heat exchangers. HVAC&R Research, vol.10, no.4, pp. 459-470.

58. Dincer I, 2002. On energetic, exergetic and environmental aspects of drying systems. International Journal of Energy Research, vol. 26, no. 8, pp. 717–727.

59. Duda RO, Hart PE. 1973. Pattern Classification and Scene Analysis, John Wiley &Sons, New York, 1973.Parzen. E. 1962. On the estimation of a probability density function and the mode, Annals of Math Statistics, vol. 33, pp. 1065–1076.

60. Esen H, Inalli M, Esen M. 2006. Techno-economic appraisal of a ground source heat pump system for a heating season in eastern Turkey. Energy Conversion and Management, vol. 47, pp. 1281-97.

61. Eskilson P. 1987. Thermal analysis of heat extraction boreholes. PhD thesis. Sweden: University of Lund; 1987.

62. Fan B, Jin XQ, Du ZM. 2011. Optimal control strategies for multi-chiller system based on probability density distribution of cooling load ratio. Energy and Buildings, vol 4, no. 10, pp. 2813-2821.

63. Fan D, Rees S, Spitler J. 2013. A dynamic thermal network approach to the modelling of Foundation Heat Exchangers. Journal of Building Performance Simulation, vol. 6, no. 2, pp. 81-97.

64. Fesangharya M, Damangira E, 2009. Soleimani I. Design optimization of shell and tube heat exchangers using global sensitivity analysis and harmony search algorithm. Applied Thermal Engineering, vol. 29, pp. 1026-31.

65. Florides G, Kalogirou S 2007. Ground heat exchangers – a review of systems, models and applications Renewable Energy, vol. 32, pp. 2461–2478.

66. Florides G, Pouloupatisa PD, Kalogiroua S, Messaritisa V, Panayidesb I, Zomenib Z, Partasidesc G, Lizidesc A, Sophocleousd E, Koutsoumpase K. 2013. Geothermal properties of the ground in Cyprus and their effect on the efficiency of ground couple heat pumps. Renewable Energy, vol. 49, pp. 85 – 89.

67. Frangopoulos CA, 1987. Thermoeconomic functional analysis and optimization. Energy, vol. 7, pp. 563–571.

68. Fujii H, Nishi L, Komaniwa Y, Chou N. 2012. Numerical modeling of slinky-coil horizontal ground heat exchangers. Geothermics, vol. 41, pp. 55-62.

69. Gang W, Wang J, Wang S. 2014. Performance analysis of hybrid ground source heat pump systems based on ANN predictive control. Applied Energy, vol. 136, pp. 1138–1144.

70. Gang W, Wang J. 2013. Predictive ANN models of ground heat exchanger for the control of hybrid ground source heat pump systems. Applied Energy, vol. 112, pp. 1146–1153.

71. Garber D, Choudhary R, Kenichi S, 2013. Risk based lifetime costs assessment of a ground source heat pump (GSHP) system design: methodology and case study. Building and Environment, vol. 60, pp. 66-80.

72. Gehlin S, 2002. Thermal response test: method development and evaluation. Doctoral thesis, Luleå University of Technology, Sweden.

73. Genetic Algorithm and Direct Search Toolbox for use with MATLAB, User's Guide, Version 1, Release 13SP1+, The Mathworks Inc., 2004.

74. Ghanadi AMM, Hajabdollahi M, Hajabdollahi H. 2012. Multi-objective optimisation of a fin with two-dimensional heat transfer using NSGA-II and ANN, Journal of Applied Mechanic Engineering, vol. 2, no. 2, pp. 1-7.

75. Gholap AK, Khan JA. 2007 Design and multi objective optimisation of heat exchangers for refrigerators. Applied Energy, vol. 84, pp. 1226-1239.

76. Giagkiozis I, Fleming PJ. 2015. Methods for multi-objective optimization: An analysis. Information Sciences, vol. 293, pp. 338-350.

77. Goetzler W, Guernsey M, Kar R. 2012. Research and development roadmap: Geothermal (ground-source) heat pumps. U.S. Department of Energy, Energy Efficiency and Renewable Energy, October 2012.

78. Gordon JM, Ng KC, Chua HT. 1995. Centrifugal chillers: thermodynamic modeling and a diagnostic case study. International Journal of Refrigeration, vol 18, no. 4, pp. 253-257.

79. Group ASBEC Climate Change Task, 2007. Capitalising on the building sector's potential to lessen the costs of a broad based GHG emissions cut.

80. Gutiérrez F, Méndez F. 2012 Entropy generation minimization for the thermal decomposition of methane gas in hydrogen using genetic algorithms. Energy Conversion and Management, vol. 55, pp. 1-13.

81. Haaker MPR, Verheijen PJT. 2004. Local and global sensitivity analysis for a reactor design with parameter uncertainty. Chemical Engineering Research and Design, vol. 82, pp. 591-598.

82. Hackel S, Nellis G, Klein S. 2008. Optimization of hybrid geothermal heat pump systems. In: 9th International IEA Heat Pump Conference, Zurich, Switzerland, May 20 – 22, 2008.

83. Hamada Y, Nakamura M, Kubota H. 2007. Field measurements and analyses for a hybrid system for snow storage/melting and air conditioning by using renewable energy. Applied energy, vol. 84, no.2, pp. 117-134.

84. Hellstrom G. 1991. Ground heat storage. PhD thesis. Sweden: University of Lund; 1991.

85. Hepbasli A, Akdemir O. 2004. Energy and exergy analysis of a ground source (geothermal) heat pump system. Energy Conversion and Management, vol. 45, no. 5, pp. 737-753.

86. Houck CR, Joines J, Key M. 1996. A genetic algorithm for function optimization: a

Matlab implementation. ACM Transactions on Mathematical Software, 1996. http://scholarlyrepository.miami.edu/oa_dissertations/1156

87. Hwang YJ, Lee JK, Jeong YM, Koo KM, Lee DH, Kim IK, Jin SW, Kim SH 2009. Cooling performance of a vertical ground-coupled heat pump system installed in a school building. Renewable Energy, vol. 34, no. 3, pp. 578-582.

88. IGSHPA, 1998. Closed-loop/ground-source heat pump systems – installation guide. National Rural Electric Cooperative Association Research (NRECA) project 86-1, prepared by the University of Oklahoma and published by the International Ground Source Heat Pump Association (IGSHPA), 236 pp.

89. İnallı M, Esenb H. 2004. Experimental thermal performance evaluation of a horizontal ground source heat pump system. Applied Thermal Engineering, vol. 24, no. 14-15, pp. 2219-2232.

90. İnallı M, Esenb H. 2005. Seasonal cooling performance of a ground-coupled heat pump system in a hot and arid climate. Renewable Energy, vol. 30, no. 9, pp. 1411-1424.

91. Ingersoll LR, Plass HJ. 1948. Theory of the ground pipe heat source for the heat pump. ASHVE Trans, vol. 47, pp. 339–348.

92. Ingersoll. LR, Zobel. OJ. 1954. Heat conduction with engineering, geological and other applications. McGraw-Hill, New York.

93. Iranmanesh A, Mehrabian MA. 2014. Optimization of a lithium bromide-water solar absorption cooling system with evacuated tube collectors using genetic algorithm. Energy and Buildings, vol. 85, pp. 427-435.

94. Jiang Y, Xie X. 2010. Theoretical and testing performance of an innovative indirect evaporative chiller. Solar Energy, vol. 84, pp. 12, pp. 2041-2055.

95. Jin X. 2008. A simulation study of using low-grade waste heat to save electricity consumption in compression type refrigeration plant. M.Sc. Thesis. Huazhong University of Science and Technology, Wuhan, P.R. China.

96. Jin X, Ren H, Xiao X. 2005. Prediction-based online optimal control of outdoor air of

multi-zone VAV air conditioning systems. Energy and Buildings, vol. 37, no. 9, pp. 939–944.

97. Junghans L. 2015. Evaluation of the economic and environmental feasibility of heat pump systems in residential buildings, with varying qualities of the building envelope. Renewable Energy, vol. 76, pp. 699-705.

98. Kalinci Y, Hepbasli A, Tavman I. 2008. Determination of optimum pipe diameter along with energetic and exergetic evaluation of geothermal district heating systems: modeling and application. Energy and Building, vol. 40, no. 5, pp. 742–55.

99. Karabacak. R, Acar. SG, Kumsar. H, Gökgöz. A, Kaya. M, Tülek, Y 2011. Experimental investigation of the cooling performance of a ground source heat pump system in Denizli, Turkey. International Journal of Refrigeration, vol. 34, no. 2, pp. 454–465.

100. Kavanaugh SP, Rafferty KD. 1997. Ground-source heat pumps: design of geothermal systems for commercial and institutional buildings. American Society of Heating, Refrigerating and Air-Conditioning Engineers.

101. Kent B, Philip E. 2011. Capital budgeting valuation-financial analysis for today's investment projects. New Jersey: John Wiley & Sons, Inc; 2011.

102. Khan MH, Spitler JD. 2004. Performance Analysis of a Residential Ground Source Heat Pump Systemwith Antifreeze Solution. Proceedings of SimBuild 2004, Boulder, Colorado August 4-6.

103. Kharseha M, Altorkmanyb L, Al-Khawaja M, Hassanic F. 2014. Warming impact on energy use of HVAC system in buildings of different thermal qualities and in different climates. Energy Conversion and Management, vol. 81, pp. 106-11.

104. Khorasaninejad E, Hajabdollahi H. 2014. Thermo-economic and environmental optimization of solar assisted heat pump by using multi-objective particle swarm algorithm. Energy, vol. 71, pp. 680-690.

105. Kjellsson E, Hellstrom. G, Perers. B. 2010. Optimization of systems with the combination of ground-source heat pump and solar collectors in dwellings. Energy, vol. 35, pp. 2667–2673.

106. Klein SA. 2010. A Transient System Simulation Program (TRNSYS 17) Manual. Thermal Energy System Specialists. Madison, USA, (2010).

107. Koski J. 1984. Multicriterion optimization in structural design. In: Atrek, E.; Gallagher, R.H.; Ragsdell, K.M.; Zienkiewicz, O.C. (eds.) New Directions in Optimum Structural Design, pp. 483–503. New York: John Wiley and Sons.

108. Koski J, Silvennoinen R. 1987: Norm methods and partial weighting in multicriterion optimization of structures. International Journal for Numerical Methods in Engineering, vol. 24, pp. 1101–1121.

109. Kreith F, Goswami. DY. 2008. Energy Management and Conservation Handbook. CRC Press, Taylor & Francis Group, Boca Raton, Florida, USA.

110. Lamarche L, Kajl S, Beauchamp B, 2010. A review of methods to evaluate borehole thermal resistances in geothermal heat-pump systems. Geothermics, vol. 39, no. 2, pp. 187-200.

111. Lee CK, Lam HN. 2008. Computer simulation of borehole ground heat exchangers for geothermal heat pump systems. Renewable Energy, vol 33, pp. 6, pp. 1286-1296.

112. Lee D, Jin S, Lee J, Jeong Y. 2008. Cooling performance of a water-to-refrigerant type ground source heat pump system installed in the building. International Refrigeration and Air Conditioning Conference. Paper 873. http://docs.lib.purdue.edu/iracc/873

113. Lee JU, Kim Y, Leigh SB. 2013. Thermal performance analysis of a ground-coupled heat pump integrated with building foundation in summer. Energy and Building, vol. 59, pp. 37–43.

114. Lee WS, Chen YT, Kao Y. 2011. Optimal chiller loading by differential evolution algorithm for reducing energy consumption. Energy and Buildings, vol. 43, no. 2, pp. 599-604.

115. Leong WH, Tarnawski VR, Aittomäki A, 1998. "Effect of soil type and moisture content on ground heat pump performance: Effet du type et de l'humidité du sol sur la performance des pompes à chaleur à capteurs enterrés." International Journal of Refrigeration, vol. 21, no.8, pp. 595-606.

116. Lhendup T, Aye L, Fuller RJ. 2014. In-situ measurement of borehole thermal properties in Melbourne. Applied Thermal Engineering, vol. 73, no. 1, pp. 287-295.

117. Li M, Lai AKC. 2013. Thermodynamic optimization of ground heat exchangers with single U-tube by entropy generation minimization method. Energy Conversion and Management, vol. 65, pp. 133-139.

118. Li X, Li Y, Seem JE, Li P. 2013. Dynamic modelling and self-optimizing operation of chilled water systems using extremum seeking control. Energy and Buildings, vol. 58, pp. 172-182.

119. Li XG, Chen ZH, Zhao J. 2006. Simulation and experiment on the thermal performance of U-vertical ground coupled heat exchanger. Applied Thermal Engineering, vol. 26, no. 14-15, pp. 1564-1571.

120. Lian, Xu. 2011. Optimized control strategies for a typical water loop heat pump system. Architectural Engineering -- Dissertations and Student Research. Paper 12. http://digitalcommons.unl.edu/archengdiss/12

121. Lin Y, Zhao Q, Fang ZH, 2010. Study on ground-source heat pump systems with slinky ground heat exchangers. Journal of HV&AC, vol. 4, pp.141-145.

122. Liu Y. 2012. A study of control strategy for hybrid ground-source heat pump based on load characteristics. M.Sc. Thesis. Huazhong University of Science and Technology, Wuhan, P.R. China.

123. Lohani SP, Schmidt D. 2010. Comparison of energy and exergy analysis of fossil plant, ground and air source heat pump building heating system. Renewable Energy, vol. 35, no. 6, pp. 1275-1282.

124. Lu Y, Wang S, Zhao Y, Yan C. 2015. Renewable energy system optimization of low/zero energy buildings using single-objective and multi-objective optimization methods. Energy and Buildings, vol. 89, pp. 61-75.

125. Lucich SM, Smith AD. 2014. Estimating CO2 Emissions Reductions With EnergyPlus for an Office Building in Salt Lake City. In ASME 2014 8th International Conference on Energy Sustainability collocated with the ASME 2014 12th International Conference on Fuel Cell Science, Engineering and Technology (pp. V002T11A005-

V002T11A005). American Society of Mechanical Engineers.

126. Luo J, Rohn J, Bayer M, Priess A, Wilkmann L, Xiang, W. 2015. Heating and cooling performance analysis of a ground source heat pump system in Southern Germany. Geothermics, vol. 53, pp. 57-66.

127. Ma Z, Wang S. 2011. Testing and evaluation of energy saving potentials in a complex building central chilling system using genetic algorithm. Building Services and Engineering Research and Technology, vol. 32, pp. 109-26.

128. Ma Z, Wang S. 2009. An optimal control strategy for complex building central chilled water systems for practical and real-time applications. Building and Environment, vol. 44, no. 6, pp. 1188–1198.

129. Madani H, Claesson J, Lundqvist P. 2011. Capacity control in ground source heat pump systems part II: Comparative analysis between on/off controlled and variable capacity systems. International Journal of Refrigeration, vol, 34, no. 8, pp. 1934-1942.

130. Maehara N, Shimoda Y. 2013. Application of the genetic algorithm and downhill simplex methods (Nelder-Mead methods) in the search for the optimum chiller. Applied Thermal Engineering, vol. 61, no. 2, pp. 433-442.

131. Maheshkumar P, Muraleedharan. C. 2011. Minimization of entropy generation in flat heat pipe. International Journal of Heat and Mass Transfer, vol. 54, pp. 645-648.

132. Man Y, Yang HX, Spitler JD, Fang ZH. 2011. Feasibility study on novel hybrid ground coupled heat pump system with nocturnal cooling radiator for cooling load dominated buildings. Applied Energy, vol. 88, no. 11, pp. 4160–4171.

133. Mandley S, Harmsen R, Worrell E. 2015. Identifying the potential for resource and embodied energy savings within the UK building sector. Energy and Buildings, vol. 86, pp. 841-851.

134. Marcotte D, Pasquier P, 2008. On the estimation of thermal resistance in borehole thermal conductivity test. Renewable Energy, vol. 33, pp.2407-15.

135. Marler RT, Arora J S. 2004. Survey of multi-objective optimization methods for engineering. Structural and multidisciplinary optimization, vol. 26, no. 6, pp. 369-395.

136. Mei VC. 1986. Horizontal ground-coil heat exchanger theoretical and experimental analysis. No. ORNL/CON-193. Oak Ridge National Lab., TN (USA), 1986.

137. Michopoulos A, Zachariadis. T, Kyriakis. N. 2013. Operation characteristics and experience of a ground source heat pump system with a vertical ground heat exchanger, Energy, vol. 51, pp. 349–357.

138. Mihalakakou G, Santamouris M, Asimakopoulos D. 1994. Modelling the thermal performance of earth-to-air heat exchangers. Sol Energy, vol. 53, no.3, pp. 301–305.

139. Moffat RJ. 1988. Describing the uncertainties in experimental results. Experimental Thermal Fluid Science, vol. 1, no. 1, pp. 3–17.

140. Moon C E, Choi J M. 2014. Heating performance characteristics of the ground source heat pump system with energy-piles and energy-slabs. Energy, vol. 81, pp. 27-32.

141. Morrone B, Coppola G, Raucci V. 2014. Energy and economic savings using geothermal heat pumps in different climates. Energy Conversion and Management, vol. 88, pp. 189-198.

142. Nam Y, Ooka R, Shiba Y. 2010. Development of dual-source hybrid heat pump system using groundwater and air. Energy and Buildings, vol. 42, no. 6, pp. 909-916.

143. Najafi H, Najafi B, Hoseinpoori P. 2011. Energy and cost optimisation of a plate and fin heat exchanger using genetic algorithm. Applied Thermal Engineering, vol. 31, pp. 1839-1847.

144. Navidbakhsh M, Shirazi A, Sanaye S. 2013. Four E analysis and multi-objective optimisation of an ice storage system incorporating PCM as the partial cold storage for air-conditioning applications, Applied Thermal Engineering, vol. 58, pp. 30-41.

145. Ndao S, Peles Y, Jensen MK. 2009. Multi-objective thermal design optimisation and comparative analysis of electronic cooling technologies. International Journal of Heat Mass Transfer, vol. 52, pp. 4317-4326.

146. Nguyen HV, Law Y LE, Alavy M, Walsh PR, Leong WH, Dworkin SB. 2014. An analysis of the factors affecting hybrid ground-source heat pump installation potential in North America. Applied Energy, vol. 125, pp. 28-38.

147. Nikolaidis Y, Pilavachi PA, Chletsis A. 2009. Economic evaluation of energy saving measures in a common type of Greek building. Applied Energy, vol. 86, pp. 2550–2559.

148. Omer AM. 2008. Ground-source heat pumps systems and applications. Renewable and Sustainable Energy Reviews, vol. 12, no. 2, pp.344-371.

149. Ouyang ZW, Xu LH, Xu SS, Hu PF. 2012. Study of optimal operating for hybrid ground source heat pump system in Wuhan. Acta Energiae Solaris Sinica, vol. 5, pp. 832–837.

150. Ozgener O, Hepbasli A. 2007. Modeling and performance evaluation of ground source (geothermal) heat pump systems. Energy and Buildings, vol. 39, no. 1, pp. 66-75.

151. Pahud O, Hellström G, Mazzarella L. 1996. Heat Storage in the Ground. Duct Ground Heat Storage Model for TRNSYS (TRNVDST). User Manual for the October 1996 Version. Laboratoire des systèmes énergétiques, Département de Génie Civil, Ecole Polytechnique Fédérale de Lausanne (Lasen/DGC/EPFL), Lausanne, Switzerland.

152. Pardo N, Montero Á, Martos J, Urchueguía JF. 2010. Optimization of hybrid-ground coupled and air source–heat pump systems in combination with thermal storage. Applied Thermal Engineering, vol. 30, no. 8, pp. 1073-1077.

153. Park H, Lee JS, Kim W, Kim. Y. 2012. Performance optimization of a hybrid ground source heat pump with the parallel configuration of a ground heat exchanger and a supplemental heat rejecter in the cooling mode. International Journal of Refrigeration, vol. 35, pp. 1537–1546.

154. Paul ND. 1996. The effect of grout thermal conductivity on vertical geothermal heat exchanger design and performance. M.Sc. Thesis. South Dakota University, Vermillion, SD, USA.

155. Perera ATD, Attalage RA, Perera KKCK, Dassanayake VPC. 2013. A hybrid tool to combine multi-objective optimization and multi-criterion decision making in designing standalone hybrid energy systems. Applied Energy, vol. 107, pp. 412-425.

156. Peters MS. Timmerhaus KD. 1991. Plant design and economics for chemical engineers, McGraw-Hill, New York.

157. Peterson S, Svendsen S. 2012. Method for component-based economical optimisation for use in design of new low–energy buildings. Renewable Energy, vol. 38, pp. 173–180.

158. Philippe M, Bernier M, Marchio D, Lopez S. 2011. A semi-analytical model for serpentine horizontal ground heat exchangers, HVAC&R Research, vol.17, no.6, pp. 1044-1058.

159. Piechowski M A. 1996. Ground coupled heat pump system with energy storage. PhD thesis, University of Melbourne, Australia, 1996.

160. Pulat E, Coskun S, Unlu K, Yamankaradeniz N. 2009. Experimental study of horizontal ground source heat pump performance for mild climate in Turkey. Energy, vol. 34, pp. 1284-95.

161. Pussoli BF, Barbosa Jr. JR, Silva LW, Kaviany M. 2012. Optimization of peripheral finned-tube evaporators using entropy generation minimization. International Journal of Heat Transfer, vol. 55, pp. 7838-7846.

162. Qi Z, Gao Q, Liu Y, Yan YY, Spitler JD. 2014. Status and development of hybrid energy systems from hybrid ground source heat pump in China and other countries. Renewable and Sustainable Energy Reviews, vol. 29, pp. 37-51.

163. Rad FM, Fung AS, Leong WH. 2013. Feasibility of combined solar thermal and ground source heat pump systems in cold climate, Canada. Energy and Buildings, vol. 61, pp. 224-232.

164. Rees S, Curtis R. 2014. National deployment of domestic geothermal heat pump technology: Observations on the UK experience 1995–2013. Energies, vol. 7, no. 8, pp. 5460-5499.

165. Retkowski W, Thöming J. 2014. Thermoeconomic optimization of vertical ground-source heat pump systems through nonlinear integer programming. Applied Energy, vol. 114, pp. 492-503.

166. Rice K, Baxter V, Hern S, McDowell T, Munk J, Shen B. 2013. Development of a residential ground source integrated heat pump. ASHRAE Trans, vol. 119, no. 1, pp. DD1.

167. Robert F, Gosselin L. 2014. New methodology to design ground coupled heat pump systems based on total cost minimization. Applied Thermal Engineering, vol. 62, no. 2, pp. 481–491.

168. Rosen B, Gabrielsson A, Fallsvik J, Hellstrom G, Nilsson G. 2001. System for ground source heating and cooling – A status report. vol. 511, Statens Geotekniska Institute, Linkoping, Sweden.

169. Roth P, Georgiev A, Busso A, Barraza E, 2004. First in situ determination of ground and borehole thermal properties in Latin America. Renewable Energy, vol. 29, pp.1947-1963.

170. Ruan W. 2012. Modelling vertical U-tube ground heat exchangers for ground-coupled heat pump applications, PhD Thesis, Purdue University, USA.

171. Russo SL, Taddia G, Verda V. 2012. Development of the thermally affected zone (TAZ) around a groundwater heat pump (GWHP) system: A sensitivity analysis. Geothermics, vol. 43, pp. 66-74.

172. Sadeghzadeh H, Ehyaei MA, Rosen MA. 2015. Techno-economic optimization of a shell and tube heat exchanger by genetic algorithm and particle swarm algorithms. Energy Conversion and Management, vol. 93, pp. 84-91.

173. Sanaye S, Niroomand B. 2009. Thermal-economic modelling and optimization of vertical ground-coupled heat pump. Energy Conversion and Management, vol. 50, pp. 1136–1147.

174. Sanaye S, Niroomand B. 2010. Horizontal ground coupled heat pump: Thermal economic modeling and optimization. Energy Conversion and Management, vol. 51, no. 21, pp. 2600-2612.

175. Sanner B, Mands E, Sauer MK. 2003. Larger geothermal heat pump plants in the central region of Germany. Geothermics, vol. 32, no. 4–6, pp. 589–602.

176. Sarbu I, Sebarchievici C. 2014. General review of ground-source heat pump systems for heating and cooling of buildings. Energy and Building, vol. 70, no. 2, pp. 441–454.

177. Sayyaadi H, Nejatolahi M. 2011. Thermodynamic and thermoeconomic optimization

of a cooling tower-assisted ground source heat pump. Geothermics 2011, vol. 40, no. 3, pp. 221-32.

178. Sayyaadi H, Hadaddi E, Amidpour M. 2009. Multi-objective optimization of a vertical ground source heat pump using evolutionary algorithm, Energy Conversion and Management. Vol. 50, pp. 2035-2046.

179. Self SJ, Reddy BV, Rosen MA. 2013. Geothermal heat pump systems: Status reviews and comparison with other heating options. Applied Energy, vol. 101, pp. 341-348.

180. Shan K. 2013. Sensitivity and uncertainty analysis, and robust optimal control strategies for air-conditioning systems with low quality measurements. Doctoral dissertation, The Hong Kong Polytechnic University.

181. Shi ZG, Li Z. 2012. Thermoeconomic Optimization of a Seawater Source Heat Pump System for Residential Buildings. Advanced Materials Research, vol. 354, pp. 794-797.

182. Shonder JA, Baxter VD, Hughes PJ, Thornton JW, 2000. A comparison of vertical ground heat exchanger design software for commercial applications. Oak Ridge National Lab., TN (US).

183. Shyr WJ. 2010. Parameters determination for optimum design by evolutionary algorithm. Convergence and Hybrid Information Technologies, Marius Crisan (Ed.), ISBN: 978-953-307-068-1, InTech, DOI: 10.5772/9638.

184. Si Q, Okumiya M, Zhang X. 2014. Performance evaluation and optimization of a novel solar-ground source heat pump system. Energy and Buildings, vol. 70, pp. 237-245.

185. Sichilalu S, Xia X, Zhang J. 2014. Optimal scheduling strategy for a grid-connected photovoltaic system for heat pump water heater. Energy Procedia, vol. 61, pp. 1511-1514.

186. Simms RB, Haslam SR, Craig JR. 2014. Impact of soil heterogeneity of horizontal ground heat exchangers. Geothermics, vol. 50, pp. 35-43.

187. Sobol′ IM. 2011. Global sensitivity indices for nonlinear mathematical models and their Monte Carlo estimates. Mathematics and Computers in Simulation, vol.55, no.1-

3, pp. 271-280.

188. Spitler JD, X Liu, SJ Rees, C Yavuzturk. 2005. Simulation and Optimization of Ground Source Heat Pump Systems. 8th International Energy Agency Heat Pump Conference. Las Vegas. May 30-June 2.

189. Sreepathi BK, Rangaiah GP. 2015. Retrofitting of heat exchanger networks involving streams with variable heat capacity: Application of single and multi-objective optimization. Applied Thermal Engineering, vol. 75, pp. 677-684.

190. Tahersima F, Stoustrup J, Rasmussen H. 2011. Optimal power consumption in a central heating system with geothermal heat pump. In The 18th World Congress of the International Federation of Automatic Control (IFAC 2011).

191. Tang Y, Reed P, Wagener T, Werkhoven K. 2007. Comparing sensitivity analysis methods to advance lumped watershed model identification and evaluation. Hydrology and Earth System Science, vol. 11, pp. 793–817.

192. Tindale A. 2004. Designbuilder and energyplus, The Building Energy Simulation User News, vol. 25, pp. 2-5.

193. Toffolo A, Lazzaretto A. 2002. Evolutionary algorithms for multi-objective energetic and economic optimization in thermal system design. Energy, vol. 27, no. 6, pp. 549-567.

194. Trillat-Berdal V, Souyri B, Achard G. 2007. Coupling of geothermal heat pumps with solar collectors. Applied Thermal Engineering, vol. 27, no. 10, pp.1750-1755.

195. Urchueguía JF, Zacarés M, Corberán JM, Montero Á, Martos J, Witte H. 2008. Comparison between the energy performance of a ground coupled water to water heat pump system and an air to water heat pump system for heating and cooling in typical conditions of the European Mediterranean coast. Energy Conversion and Management, vol. 49, no. 10, pp. 2917-2923.

196. Vakiloroaya V, Samali B, Fakhar A, Pishghadam K. 2014. A review of different strategies for HVAC energy saving. Energy Conversion and Management, vol. 77, pp. 738-754.

197. Verhelst C 2012. Model Predictive Control of Ground Coupled Heat Pump System for Office Buildings. PhD thesis, Faculty of Engineering, Katholieke Universiteit Leuven.

198. Von Spakovsky MR, Evans. RB. 1990. The design and performance optimization of thermal systems. Journal of engineering for gas turbines and power, vol. 112, no. 1, pp. 86-93.

199. Wall G. 1985. Thermoeconomic optimisation of a heat pump system. Chalmers University of Technology and University of Göteborg; pp. 1–17.

200. Wan K, Li DH, Pan W, Lam JC. 2012. Impact of climate change on building energy use in different climate zones and mitigation and adaptation implications. Applied Energy, vol. 97, pp. 274-282.

201. Wang H, Qi C, Du H, Gu J. 2010. Improved method and case study of thermal response test for borehole heat exchangers of ground source heat pump system. Renewable Energy, vol. 35, pp.727-733.

202. Wark KJ. 1995. Advanced Thermodynamics for Engineers. McGraw-Hill, New York.

203. West SR, Ward JK, Wall J. 2014. Trial results from a model predictive control and optimization system for commercial building HVAC. Energy and Buildings, vol. 72, pp. 271-279.

204. Witte HJ. 2013. Error analysis of thermal response tests. Applied Energy, vol. 109, pp. 302-311.

205. Woloszyn J, Gołaś A. 2014. Sensitivity analysis of efficiency thermal energy storage on selected rock mass and grout parameters using design of experiment method. Energy Conversion and Management, vol. 87, pp. 1297-1304.

206. Wu W, Wang B, You T, Shi W, Li X. 2013. A potential solution for thermal imbalance of ground source heat pump systems in cold regions: Ground source absorption heat pump. Renewable Energy, vol. 59, pp. 39-48.

207. Wu W, Wang B, Shi W, Li X. 2014. Techno-economic analysis of air source absorption heat pump: Improving economy from a design perspective. Energy and Buildings, vol. 81, pp. 200-210.

208. Wu Y, Gan G, Verhoef A, Vidale PL, Gonzalez RG. 2010. Experimental measurement and numerical simulation of horizontal-coupled slinky ground source heat exchangers, Applied Thermal Engineering, vol. 30, pp. 2574–2583.

209. Xu J, Li J. 2002. A class of stochastic optimization problems with one quadratic & several linear objective functions and extended portfolio selection model. Journal of Computational and Applied Mathematics, vol. 146, no. 1, pp. 99-113.

210. Yang W, Zhou J, Xu W, Zhang G. 2010. Current status of ground-source heat pumps in China. Energy Policy, vol. 38, no. 1, pp. 323-332.

211. Yang H, Cui P, Fang ZH, 2010, Vertical-borehole ground-coupled heat pumps: A review of models and systems, Applied Energy, vol.87, no. 1, pp. 16-27.

212. Yang J, Xu L, Hu P, Zhu N, Chen X. 2014. Study on the intermittent operation strategies of a hybrid ground-source heat pump system with double-cooling towers for hotel buildings. Energy and Buildings, vol. 76, pp. 506-512.

213. Yang W, Sun L, Chen Y, 2015. Experimental investigations of the performance of a solar-ground source heat pump system operated in heating modes. Energy and Buildings, vol. 89, pp. 97-111.

214. Yau YH, Rismanchi B. 2012. A review on cool thermal storage technologies and operating strategies. Renewable and Sustainable Energy Reviews, vol. 16, no. 1, pp. 787-797.

215. Yavuzturk C, Spitler JD. 2000. Comparative study of operating and control strategies for hybrid ground-source heat pump systems using a short time step simulation model. ASHRAE Transactions, vol. 106, no. 2, pp. 192–209.

216. Yekoladio PJ, Bello-Ochende T, Meyer JP. 2013. Design and optimization of a downhole coaxial heat exchanger for an enhanced geothermal system (EGS). Renewable Energy, vol. 55, pp. 128-137.

217. You T, Wang B, Wu W, Shi W, Li X. 2014. A new solution for underground thermal imbalance of ground-coupled heat pump systems in cold regions: Heat compensation unit with thermosyphon. Applied Thermal Engineering, vol. 64, no. 1-2, pp. 283-292.

218. Yuan Y, Cao X, Sun L, Lei B, Yu N. 2012. Ground source heat pump system: A review of simulation in China. Renewable and Sustainable Energy Reviews, vol. 16, no. 9, pp. 6814-6822.

219. Zeng H, Diao N. 2003. Heat transfer analysis of boreholes in vertical ground heat exchangers. International Journal Heat and Mass Transfer, vol 46, no.23, pp. 4467-4481.

220. Zhai XQ, Qu M, Yu X, Yang Y, Wang RZ. 2011. Review for the applications and integrated approaches of ground-coupled heat pump systems, Renewable and Sustainable Energy Reviews, vol. 15, pp. 3133–3140.

221. Zhai XQ, Wang XL, Pei HT, Yang Y, Wang RZ. 2012. Experimental investigation and optimization of a ground source heat pump system under different indoor set temperatures. Applied Thermal Engineering, vol. 48, pp. 105–116.

222. Zhang X, Wang F. 2015. Life-cycle assessment and control measures for carbon emissions of typical buildings in China. Building and Environment, vol. 86, pp. 89-97.

223. Zhao Y, Shigang Z, Xun L. 2003. Cost-effective optimal design of groundwater source heat pumps. Applied Thermal Engineering, vol. 23, pp. 1595–1603.

224. Zhao L, Yuan C. 2014. Exergy Analysis of a Ground Source Heat Pump System Under Cooling and Heating Conditions. In Proceedings of the 8th International Symposium on Heating, Ventilation and Air Conditioning (pp. 799-806). Springer Berlin Heidelberg. 2014, January.

225. Zhu N, Hu P, Xu L, Jiang Z, Lei F. 2014. Recent research and applications of ground source heat pump integrated with thermal energy storage systems: A review. Applied Thermal Engineering, vol. 71, no. 1, pp. 142-151.

226. Zogou O, Stamatelos A. 1998. Effect of climatic conditions on the design optimization of heat pump systems for space heating and cooling. Energy Conversion and Management, vol. 39, pp. 609–622.

Appendix A - SBRC ground loop design

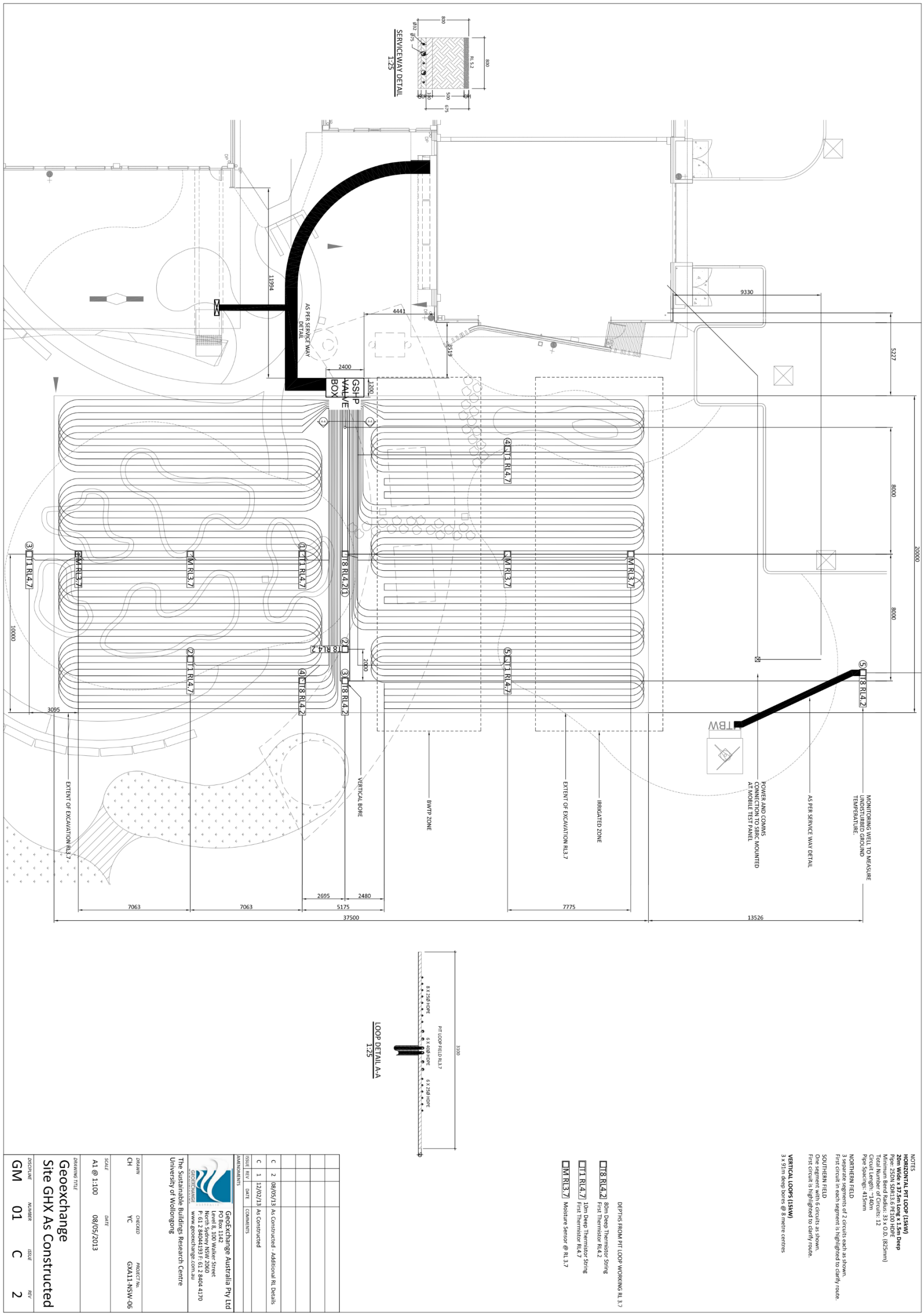

Appendix B - SBRC hydronic loop system